# KHAZAR JOURNAL
# OF
# SCIENCE AND TECHNOLOGY
# (KJSAT)

**Hamlet Isayev/Isaxanli[1] \***
Editor-in-Chief
Khazar University, Azerbaijan

[1] Also H. Issakhanly, H. Isakhanly, H. Isakhanli, H.A.Isayev, G.A.Isayev, or G.A.Isaev due to differences in transliteration. I use Hamlet Isayev in mathematics and science fields and Hamlet Isakhanli/Isaxanli in humanities.

Managing Editors
Khazar University, Azerbaijan

| | |
|---|---|
| Oktay Gasymov | Karim Gasymov |
| Ilham Shahmuradov | Irada Khalilova |
| Javid Ojaghi | Seyyed Abolghasem Mohammadi |
| Saida Sharifova | Jamala Eldarova |
| Rasul Moradi | Muhammad Irfan Maqsudi |
| Mehdi Kiyasatfar | |

**KHAZAR UNIVERSITY PRESS**

# CONTENTS

# A Retrospective Analysis of a Feline Rabies Case in Baku, Azerbaijan

## Chichak Aliyeva

*Azerbaijan Food Safety Institute, Baku, Azerbaijan*
*ciceksuleymanova3@gmail.com*

**Abstract**

Rabies is a mandatory reportable disease in Azerbaijan and is endemic throughout the country. Wild carnivores, roaming dogs, and cats are considered the main sources of rabies and the natural reservoir. The characteristics of the populations of these animals, such as density and growth dynamics, are unknown, necessitating scientific and epidemiological research. In recent years, there has been an increasing focus on rabies cases, especially among domestic pets. The main objective of this research study is to retrospectively analyze cases of domestic cats presenting with symptoms of lethargy and vomiting, which may resemble rabies in the form of an agonal state, without a suspicion of rabies. The aim is to identify cases of rabies and raise awareness about the clinical manifestations of the disease. Additionally, this highlights the need for strengthening vaccination efforts among pet animals. Epidemiological investigations and research in this area are crucial to gain a better understanding of rabies dynamics in Azerbaijan and implementing effective preventive measures.

**Keywords:** rabies, retrospective, Azerbaijan, cat, disease, virus

**Introduction**

Viruses like Rabies (Lyssavirus, Family Rhabdoviridae) have the capability to infect humans and animals intensively and fatally. As a neurotropic virus, it binds to cell receptors, cytoplasm and transports across synapses in interneurons. In addition to causing fatal encephalitis, the rabies virus also affects other organs (Ichhpujani et al., 2008; Abubakar and Bakari, 2012). It usually takes 3-6 weeks for rabies to incubate, although it can take up to a year. Animal type, age, immune status, virulence, proximity to the brain, and characteristics of the wound determine the amount and duration of the infection (Rodney and Charles, 2020). There are usually three phases to rabies in animals: the prodromal phase, the excitation, and the paralysis phase:

The prodromal period lasts for 2-3 days. The bite area is licked frequently, exhibiting behavioural disorder, and feverish symptoms (Dietzschold, et al., 2000; Sarah et al., 2008; Nigar et al., 2016).

Period of excitation - lasts 2-4 days. In animals, timidity and cowardice appear first, followed by aggression. It is observed that the dog becomes more interested in foreign objects, less hungry, afraid of light and water, loses his memory, and disobeys his owner.

There is a period of paralysis that lasts 2-4 days. The bitten area first shows signs of paralysis, then all tissues. There are several symptoms that suggest rabies in general:

General sickness, swallowing difficulties, excessive saliva or drool, animals that are aggressive, animals that bite imaginary objects (sometimes called fly biting), animals that appear tamer than you'd expect, animals that are unable to move or may even be paralyzed, etc (McQuiston et al., 2016).

This study was designed to increase veterinarians' awareness of the degree of rabies symptoms in cats that had no rabies symptoms before and were rabies positive after retrospective analysis

**Material and Methods**

A cat named Winston was admitted to the Veterinary Clinic with symptoms of weakness, immobility, loss of appetite, persistent vomiting for several days, and excessive salivation. According to the owner, these symptoms began to occur after the cat was seen wandering around an area where rat poison had been placed. The owner reported losing the cat's passport and was unsure whether vaccinations had been administered.

Based on the examinations and analyses conducted, the cat was diagnosed with acute gastritis and treatment was initiated. After two weeks of treatment, a slight improvement in the cat's condition was observed. The cat started to move slowly and showed a decrease in salivation. However, despite the initial progress, 21 days after the initial examination, the cat was brought back to the clinic due to sudden respiratory distress and, despite the necessary resuscitation efforts, unfortunately, passed away. The cat had no contact with other animals during outpatient treatment and had not caused any harm to its owners. During its demise, the cat exhibited signs of bradycardia, tachycardia, visible cyanosis in the gums, excessive drooling from the mouth, muscle weakness, and paralysis.

The animal's agonal state raised suspicions of rabies, so after the animal's death, its body was sent to the Veterinary Laboratory of the Azerbaijan Food Safety Institute, which is the only rabies laboratory in the country, for rabies analysis. The head of the carcass was separated following biosecurity protocols, and relevant brain samples were taken for rabies analysis using Immunofluorescence Assay (IFA) and Polymerase Chain Reaction (PCR) methods.

**Result and discussion**

In the initial examination, no signs of injury were observed in the affected animal, which was a pet cat with no contact with other animals. Also, the cat had moved residence a few days before vomiting, loss of appetite, and weakness started, according to the owner's history. The cat was found in a dark area where rat poison had been thrown. Vitamin K was administered to the cat immediately due to the lethal effects of rat poison. A number of medications were administered due to the persistent vomiting, including Metoclopramide, Maropitant citrate, Omeprazole, and Almagel Plus, along with Metronidazole and other appropriate infusions. An abdominal examination was performed using ultrasound, contrast-enhanced X-rays, and non-contrast X-rays, and treatment was initiated. Inflammation and immune system stress usually cause leukopenia and neutropenia in the blood (Figure 1, 2, and 3).

A high temperature (40°C) on the 15th day of treatment was the only significant observation during the 21-day treatment period. The cat's general condition did not change on other days, and his temperature returned to normal. Having been unable to eat, the cat was given nasal feedings with a feeding tube. During this period, no signs of aggression or abnormal behavior were observed. The initial X-ray images with contrast and without contrast showed an image resembling a foreign object in the intestines, which initially suggested the need for bowel cleansing, and an enema was administered promptly. As a result of the enema, the cat produced greenish, unformed faeces, raising the possibility of poisoning from a foreign object. In the following days, the cat had diarrhoea, but towards the end of the treatment, the faecal consistency began to normalize.

On the 22nd day of treatment, a sudden change in the cat's condition occurred, and severe respiratory distress was observed. When brought to the clinic, the cat exhibited aggression, biting the veterinarian, and subsequently died of paralysis. It was precisely during the suspicion of rabies that the cat's death occurred, manifested by the immediate constriction of the pupils and third eyelids, as well as rapid dehydration. The body of the cat was sent to the laboratory for analysis, and upon retrospective evaluation, the cat's condition was assessed.

The laboratory examinations revealed the presence of Negri bodies and the virus in the brain tissues of the cat, indicating a diagnosis of rabies.
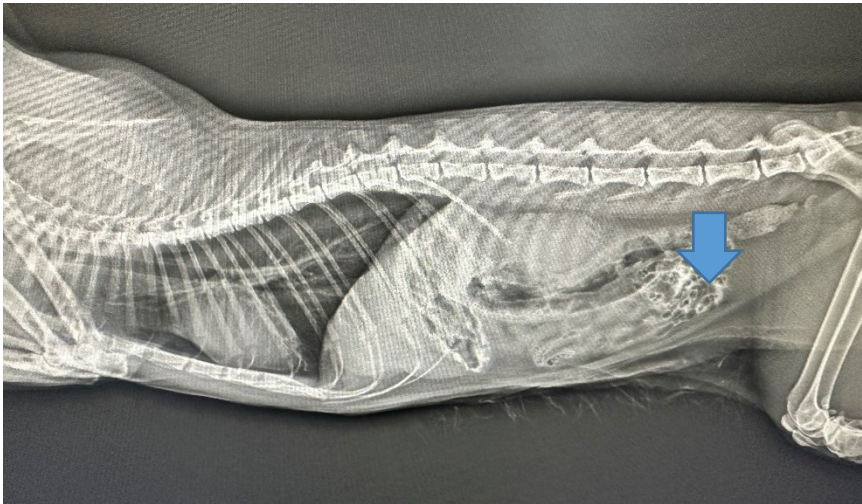


**Figure 1.** X-ray imaging with contrast
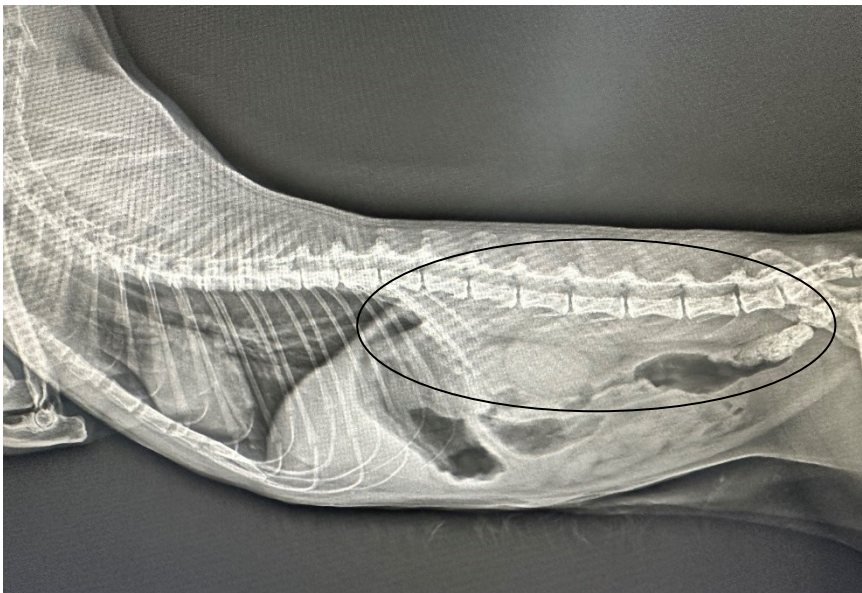


**Figure 2.** X-ray imaging without contrast
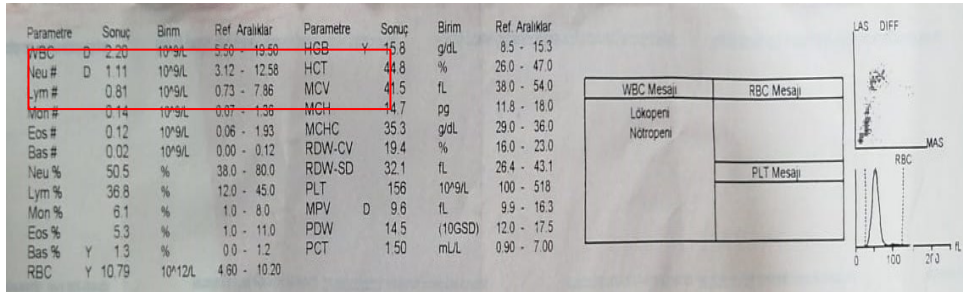
**Figure 3.** The result of the full blood count

## Conclusion

The signs that were present during the period from Winston's admission to the clinic until the occurrence of his death, which did not initially raise suspicion of rabies but resembled it in retrospect, were as follows:

Upon admission, the cat remained immobile in one place, drooled from the mouth, and opening the cat's mouth was impossible. The brightness of the cat's eyes was reduced and dull. Throughout the day, the cat vomited 7-8 times. Later, stiffness was observed during movement, but no aggression or abnormal behavior was observed until the cat's final day. However, at the moment of death, abnormal aggression, attacking the veterinarian, and rapid dehydration significantly increased suspicion of rabies. The results of laboratory analysis confirmed this suspicion.

In retrospect, it can be determined that the fact that the cat was not found for a day and the uncertainty regarding vaccination had actually contributed to the suspicion of rabies. Furthermore, it was noted that not all of the signs mentioned in the literature were standard, including their appearance duration.

Therefore, veterinary professionals in this field should approach with greater caution and evaluate all suspicions without ignoring them for proper diagnosis. Additionally, veterinarians should emphasize the importance of vaccination against rabies for animals. Considering such real threats, rabies should be considered as an occupational disease for veterinarians, and proactive and protective vaccination measures should be taken regularly.

## References

**Abubakar S.A, Bakari A.G:** (2012). Incidence of dog bite injuries and clinical rabies in a tertiary health care institution: a 10-year retrospective study. Ann Afr Med. 11 (2): 108–111.

**Dietzschold B., Morimoto K., Hooper D.C.** (2000). Genotypic and phenotypic diversity of rabies virus variants involved in human rabies: Implications for postexposure prophylaxis. J Hum Virol. 3(1): 50–7.

**Ichhpujani RL, Mala C, Veena M, Singh J, Bhardwaj M, Bhattacharya D, et al.** (2008). Epidemiology of animal bites and rabies cases in India. A multicentric study. J Commun Dis. 40 (1) :27-36.

**Mc Quiston J.H, Yager P.A, Smith J.S.** (2001). Epidemiologic characteristics of rabies virus variants in dogs and cats in the United States. J Am Vet Med Assoc. 218:1939.

**Nigar Safi, Kliment Asadov, Shalala K. Zeynalova, Eldar Gasanov, Natig Javadov.** (2016).

The prevalence of rabies cases in the territory of Azerbaijan, January 2015-June 2016

**Rodney E Rohde., Charles E Rupprecht.** (2020). Update on lyssaviruses and rabies: will past progress play as prologue in the near term towards future elimination? Fac Rev. 16 (9).

**Sarah N. Lackay, Yi Kuang, and Zhen F. Fu.** (2008). Rabies in small animals. Vet Clin North Am Small Anim Pract. 38 (4): 851-61.

# Collection of Azerbaijan Tea (*Camellia sinensis* (L.) *Kuntze*) Varieties Belonged the Lankaran-Astara Region and using their Valuable in Breeding Program

## Afsana Abdullayeva

*Department of Life Sciences, Khazar University, Baku, Azerbaijan*
[afsana.abdullayeva@khazar.org](mailto:afsana.abdullayeva@khazar.org)

**Abstract**

Research was focused on selecting newly created tea samples that were high yielding, high quality, and drought-resistant. For this purpose, genetic diversity of tea samples from plantations of Lankaran-Astara region was studied by morphological traits. From the tea plantations in Lankaran-Astara, potential clones were selected based on parameters affecting the industry. A number of morphological traits were studied, including yield, shooting intensity, leaves quality, and other characteristics. As a result of this study, the selection of the best clones for the creation of improved tea populations was ensured using the clone selection method on tea plantations operating in Lankaran-Astara for many years, which were each investigated and studied separately in order to obtain the best results. According to the results of this study, the clones placed in the garden of the collection gene pool have greater shooting intensity, leaf blade, flash weight, mechanical composition, and biochemical qualities than the control variety Azerbaijan-2. This research led to identification of form-clones with valuable economic characteristics.

**Keywords**: tea, clone, collection, morphological traits

**Introduction**

Tea plant (*Camellia sinensis* (L.) *Kuntze*) is known as one of the popular non-alcoholic beverages worldwide and is used by about 70% of the world's population due to its refreshing taste, attractive aroma, and medicinal benefits (Karunarathna et.al., 2018). Tea is an economically important product grown in more than 52 countries in Asia, Africa and South America (Wambulwa et.al., 2017). The tea plant of the southern region of the Republic of Azerbaijan is considered one of its important products and plays an important role in the regional economy (Huseynov et al., 2020). The Chinese variety of tea is cultivated in the humid subtropics of

Azerbaijan. The prospective varieties and forms of the tea plant adapted to local soil conditions have been recommended for production purposes (Babayev, 2018).

One of the primary focuses of economic policy carried out in our republic in the modern era is thought to be the development of traditional agricultural sectors, improvement of the social well-being of the nation's population, particularly those engaged in this activity, and decrease in unemployment. In addition to the growth in many economic sectors, this strategic framework's actions contributed to an increase in the non-oil sector's share of the gross domestic product. (Gurbanov et.al., 2016).

A number of significant steps have been taken, and positive outcomes have been obtained, in order to increase state support for the growth of the production of citrus fruits and tea, meet the population's demand for these products, enhance the supply of raw materials for processing enterprises, and increase the variety of finished products. Ensuring sustainable development in this area, meeting demand through local production, as well as increasing cropland and productivity, developing seed and nursery farms, strengthening information and advisory services, human resources, promoting investments and exports, necessary infrastructure and financial resources for the expansion of clone opportunities, improvement of the level of provision requires acceleration of the measure (Guliyev F.A and others, 2012).

In light of this, on February 12, 2018, the President of the Republic of Azerbaijan issued an order approving the "State Program for the Development of Tea Cultivation in the Republic of Azerbaijan for 2018-2027"(Gurbanov et.al., 2016).

In the subtropical Lankaran-Astara region, in the existing tea plantations established since the 1930s - in the Hirkan and Haftoni regions of the Lankaran region, in Kijaba, Lovain of Astara and Kolatansin in the Masalli region discovered tea plantations and determined by long-term observation, and according to about 50 different economic indicators, more than 50 clones of different forms of tea have been cut and rooted and introduced into the harvesting area of the Lankaran tea industry for comparative research (Guliyev et al., 2014).

The main goal is to improve the productivity and product quality of tea plantations in Azerbaijan, create new varieties and strains of tea on the unique soil and climatic conditions of the Lankaran-Astara region and introduce them to the farm.

Research and scientific work was first started in 1948 by M.A. Mammadov at the Lankaran Tea Branch of the Az ETB and SB Institute with the aim of obtaining locally selected Azerbaijani tea varieties (Guliyev et al., 2012; Mammadov, 1965). Using the convetional breeding method, the author obtained 9 Azerbaijani tea varieties (Guliyev et al., 2014; Babayev 1986; Bakhtadze, 1948).

The selection of tea in Azerbaijan is aimed at obtaining the following local varieties. Azerbaijan №1 - a hybrid of large-leaved Chinese tea; Azerbaijan № 2 - half-leaf Chinese tea; Azerbaijan №3 - mid-leaved tea of the southern group intersort hybrid; Azerbaijan №4 - intersort hybrid of broad-leaved tea and Azerbaijan №6 - "Kimin" hybrid, etc (Guliyev F.A and others, 2012).

When testing the obtained tea varieties, special attention was paid to their productivity, product quality and resistance to the unfavorable climate of the Lankaran-Astara region.

Thus, 7 of the 9 selection varieties of tea obtained in the Lankaran-Astara region of Azerbaijan (Azerbaijan №1, №2, №3, №4, №5, №6, and №9) were submitted to the State Variety Trial, and 2 selection varieties from them - Azerbaijan №2 was regionalized in 1977 and Azerbaijan №4 (Talish) in 1979 (Guliyev et al., 2014; Mammadov, 1965).

The productivity, longevity, and quality of the tea plantations are highly dependent on the variety composition of the tea plant. Tea populations and varieties vary significantly in yield, harvest time and leaf quality indicators. At the same time, the characteristics of the tea plant and its response to the growing conditions play an important role. Each variety is adapted to certain natural climatic conditions and differs in giving the highest quality products in those conditions. Tea plants respond best to soil conditions. The variety with the same name differs in productivity and quality of the product in one massif, but in different soil conditions (Guliyev et al., 2014; Babayev and d., 1986; Bakhtadze, 1948; Dzhakeli, 1988).

 In 1980, research work on clone selection of tea at Lankaran Chay branch of Az.ETB and SB Institute was carried out. For this purpose, the method of propagation of tea by vegetative method under the conditions of Lankaran-Astara region under polyethylene cork curtains was developed (F.A. Guliyev and M.M. Babayev, 1986).

**Materials and methods**

The research were carried out in 2022-2023 on different varieties and forms of the tea plant (*Camellia sinensis* (L.) *Kuntze*) cultivated in the experimental area of the Lankaran tea branch of the Scientific Research Institute of Fruit and Tea Cultivation.

The biomorphological description of tea varieties and forms is given based on the instructions of M.I. Dashkevich (1963) and the method of P.J. Lapin (1986).

Phenological observations cover the period from March to October during the active vegetation period of the plant. At this time, the beginning of height and development

of the variety, form or clone, depending on the external environmental conditions of the phenophases, depending on the external harsh environmental conditions of the plant, the reaction of the plant to external harsh environmental conditions was studied. Phenological observations were carried out every 5 days from the beginning of "Painting" to the end of vegetation. Phenological observations are recorded according to the scheme given in the journal. Tea variety, form and clone weight were studied according to the specified procedure. The morphological characteristics of the flashes are determined according to the order shown in the relevant table (Table 1). Productivity indicators of tea bushes are shown in table1.

The plant height and plant width are measured at the beginning of vegetation and also at the end of vegetation.

The yielding biology and intensity of tea bushes are studied separately for each sample in 0.0625 m$^2$ area (0.25m x 0.25m= 0.0625m$^2$) in four replicates.

 For this purpose, in the spring, after pruning the wallpaper, certain stumps are separated and labeled.

 Observations on the growth of crows are made every 5 days. To find the volume of the tea bush, the formula presented by O.A. Kovalyov (Guliyev et al., 2014) was used:

$$V = \frac{3,14 * D^2 * H}{4}$$

Here,

H- bush height

D- bush diameter (cm)

V- bush volume (cm$^3$)

The leaf blade of the tea plant was studied by the method of D.A. Vardikadze, A.S. Sanikidze (1973). At this time, 25 leaf blades characteristic for each variant were determined.

The obtained numbers are mathematically calculated by the dispersion method (Dospexov V.A. 1973).

According to its signs, the delicacy, shine, color and curl of the leaf are recorded, and an assessment is made for all three types (strong, medium, weak).

During the vegetation period, the symptoms of the leaves are observed twice in spring and summer.

Winter damage, percentage of shoots, leaves, annual shoots, perennial branch, whole aboveground part and whole plant are recorded as a percentage of the whole bush from the beginning of spring growth. Damages in the summer, damages observed in the plant until May-August due to drought are recorded.

A number of additional indicators for the selection of the tea bush according to its productivity: the nature of the tea bush development, the size of the leaf blade, buds, the buds ripening at the same time for harvesting, strong dyeing energy and good development of the buds, the plant during the season - more than 4-5 during the leaf collection period the formation of graded ridges has been taken into account.

To obtain tea variety-clones, the following scheme was used: selection of mother plants, analysis of their morphological and biological characteristics, yield rate and product quality, their selection based on the obtained data, and then creation of varieties by multiplying the best clones.

**Results and discussion**

In addition to the tea bush's yield, other morphological characteristics like leaf blade's high shooting intensity, seasonally high shooting intensity, flash weight, growing intensity, and shoot development were examined in our investigation.

**Table 1. Volume measurements and yield of studied tea samples**

| Samples | 1 clone | | | Node distance (cm) | Total leaves Per bush (gr) | Yied kg/ha | Comparison among varities ( %) |
|---|---|---|---|---|---|---|---|
| | Height (cm) | Diameter (cm) | Volume, $(cm^3)$ | | | | |
| FAQ-12 | 70,0 | 110,0 | 664,89 | 3,0 | 232,0 | 5104 | 163 |
| FAQ-13 | 50,0 | 110,0 | 474,92 | 4,5 | 249,0 | 5346 | 171 |
| FAQ-15 | 70,0 | 125,0 | 858,69 | 4,5 | 389,0 | 7238 | 232 |
| FAQ-16 | 50,0 | 110,0 | 474,92 | 4,0 | 202,0 | 4444 | 142 |
| FAQ-17 | - | - | - | - | - | - | - |
| FAQ-18 | 65,0 | 95,0 | 460,50 | 3,0 | 173,0 | 3806 | 122 |
| FAQ-19 | 50,0 | 115,0 | 519,08 | 4,0 | 503,0 | 1106 | 354 |
| FAQ-20 | 80,0 | 135,0 | 1.144,53 | 5,0 | 268,0 | 5896 | 188 |
| FAQ-21 | 75,0 | 100,0 | 588,75 | 5,0 | 295,0 | 6490 | 207 |
| FAQ-22 | 80,0 | 130,0 | 1.061,32 | 4,0 | 550,0 | 12100 | 387 |
| Control | 45,0 | 95,0 | 318,80 | 2,5 | 142,0 | 3124 | 100 |

More than 50 forms were gathered, and some clones were taken for comparative analysis. In addition to several of their morphological and biological traits that give

them farm values, the quality indicators of the green leaf product (flashes) are also carefully examined in parallel.

Using the collection garden established at the Lankaran Tea Branch, form-clones of the tea plant were compared with the "Azerbaijan 2" tea variety as a control.

As shown in tables, research was conducted on a collection of form-clones. Table 1 shows the volume size and node distances of the compared form-clones.

It is evident from the table that the form-clones differ as much as possible from the control variety (Azerbaijan 2). Therefore, the comparable clones had an average bush volume of 460.5-1144.5 cm3, compared to 318.8 cm3 for the control variant. That is, the volume size was relatively large in form-clones compared to the control, and FAQ-20 and 22 had the largest volume size.

| Forms № | Start of the Spring vegetation | End | Start of the Summer vegetation | End | Start of the Fall vegetation. | End | Start of the buttons | End | Start of the flowering |
|---|---|---|---|---|---|---|---|---|---|
| FAQ-12 | 1/IV | 4/VI | 14/VI | 3/IX | 10/IX | | 17/VII | | 14/IX |
| FAQ-13 | 31/III | 4/VI | 13/VI | 2/IX | 12/IX | | 15VII | | 13/IX |
| FAQ-15 | 31/III | 4/VI | 13/VI | 3/IX | 11/IX | | 17/VII | | 11/IX |
| FAQ-16 | 1/IV | 4/VI | 14/VI | 2/IX | 12/IX | | 16/VII | | 12/IX |
| FAQ-17 | - | heavy | pruning | - | - | - | - | - | - |
| FAQ-18 | 31/III | 4/VI | 13/VI | 3/IX | 10/IX | | 15/VII | | 11/IX |
| FAQ-19 | 1/IV | 4/VI | 14/VI | 5/IX | 8/IX | | 18/VII | | 13/IX |
| FAQ-20 | 30/III | 4/VI | 14/VI | 1/IX | 10/IX | | 17/VII | | 12/IX |
| FAQ-21 | 1/IV | 4/VI | 13/VI | 2/IX | 12/IX | | 16/VII | | 11/IX |
| FAQ-22 | 29/III | 4/VI | 14/VI | 3/IX | 11/IX | | 18/VI | | 14/IX |
| Control | 2/IV | 4/VI | 17/VI | 1/IX | 13/IX | | 14/VII | | 8/IX |

The result of observations on vegetative and generative organs in Table2 show that the beginning of spring vegetation in the control option 2.IV, in some of the comparatively studied FAQs (FAQ-12,16,19,21) 1 day earlier, the remaining form - clones started earlier, which had its effect on the start of summer and autumn vegetation.

Regarding the development of generative organs, it has been known that compared to the control variant, form-clones are different to one degree or another.

The study of the leaf surface is of particular importance in tea bushes. Thus, the surface area of the leaves has an important effect on the synthesis of organic substances. From this point of view, the study of the surface of the leaf blade in tea bushes shows its effect on the growth and development of the plant, the realization of its photosynthesis process and the formation of organic substances. The study of the leaf surface was carried out in 3 stages of the leaf harvesting season. While the largest leaf area vegetation is observed in spring (May) and relatively small in summer (July), it appears to be larger in autumn (September) than in summer. So, in the control option, this number is 24.4 in May, July, and September, respectively; In case of 22.0 and 23.1 $cm^2$ involved forms-clones this comparative degree in spring (May) -27.5-36.0; in summer (July)-24.6-27.2; in autumn (September) it was 25.6-29 $cm^2$.

It was determined that the tea form-clones included in the comparison are superior in comparison with the control variant in terms of leaf surface. This situation was observed in green tea leaf harvested seasonally.

As the flash intensity of tea bushes is the basis of high productivity, the application of complex agrotechnical measures to plants for this purpose plays an important role.

The correct mode of cultivation, cultivation, fertilizing, pruning, harvesting, etc. by applying it has a positive effect on the flash intensity due to the collection of tea bushes during the season. It was determined that in this case, the difference between tea flash ripening in the studied tea form-clones and control variants is almost the same, that is, the intensity of flash ripening during the season occurs almost 7-9 times. Here, the main difference is observed in the size and development of the flashes, mainly in the mass and quality indicators of the collected flashes.

The scientific-research works conducted on the various tea forms-clones collected in this way show that they differ with positive signs according to economic and quality indicators.

As a result of the research, form-clones with valuable economic characteristics were identified.

In the scientific investigation, it was determined that FAQ-20, FAQ-22, FAQ-18 are superior to regionalized "Azerbaijan-2" tea variety (control) and at the same time compared to clones with selection number studied in terms of both sizes of tea bushes. Observations made on vegetative and generative organs show that the form-clones with the selection number FAQ-22, FAQ-20 start vegetation earlier than the control and mature relatively late. At the same time, in the comparison of yield and

variants from Hk, form-clones show higher results than "Azerbaijan-2" tea variety (control). Similar differences were also found in other biometric measures.

## References

**Babaev M. M., Guliev F. A.** (1986). Results of studying vegetative propagation of tea in the conditions of the Lankaran zone. Journal Subtropical Crops, 3, 178–186.

**Bakhtadze K.E.** (1948). Biology, selection and seed production of tea plant. M., Pischepromizdat. 210 p.

**Dzhakeli V.E.** (1986). Towards further development of tea growing in Azerbaijan . Journal Subtropical Crops. 5(3), 120-128.

**Guliyev F.A. et al.** (2012). Tea in Azerbaijan (*Teasinensis L.*) scientific and practical fundations of its cultivation. "Author publishing". Baku, 335p.

**Guliyev F.A., Guliyev R.F.** (2014). Tea. Baku, "Indiqo" pub. 559 p.

**Guliyev F.A., Shiraliyev M.A.** (2014). Perspective tea clones and their assessment by biological-economic indicators. Materials of the Republican scientific and Practical Conference, LSU, 38-41.

**Huseynov M.B., Suleymanova Z.C., Ojaghi J., Mammadov A.Ch.** (2020). Assessment of suitable farm for establishing tea plantations in Lankaran region and their efficient use. Scientific News of Lankaran State University, 1, 33-39.

**Kutbidze V.V., Mutovkina T. D.** (2008). Clonal selection of tea. Batum-Chakva.98 p.

**Karunarathna, K.H.T., Mewan, K.M., Weerasena, O.V.D.S.J.,Perera, S.A.C.N., Edirisinghe, E.N.U., Jayasoma, A.A.** (2018). Understanding the genetic relationships and breeding patterns of SriLanka tea cultivars with genomic and EST-SSR markers, Scientia Horticulturae, 240, 72-79.

**Mamedov M. A.** (1965). Selection and Seed breeding of tea in Azerbaijan. Journal. Subtropical Crops. 2, 24–31.

**Wambulwa, M.C., Meeghakumbura, M.K.,Kamunya, S., Muchugi, A., Möller, M., Liu, J.,Xu, J.C., Li, D.J., Gao, L.M.** (2017). Multipleorigins and anarrow genepool characterise the African tea germplasm: Concordant patterns revealed by nuclear and plastid DNA markers, Science Report,7, 4053.

# The effect of Mexidol on recovery of Liver Metabolic Disorder induced by X-RAYs

## Ismail Bagirov

*Scientific Research Center of Azerbaijan Medical University, Baku, Azerbaijan*

## Abstract

The aim of this study is to investigate the recovery of pathological changes in the liver occurred due to radiation, through pharmacological preparations. For this purpose, so called Mexidazole which is the biologically active substance, synthesized on the basis of palladium and Mexidaole was studied for its hepatoprotective properties at the Scientific Research Center. The experiments were carried out on 20 white rats of both sexes with unknown germ line. They were divided into five groups with five of rats in each. In the first group, the number of markers that characterized the normal liver metabolism were determined. In the second group the number of liver metabolic specific markers was evaluated after the X-ray exposure and in the third group the same markers were assessed 10 days after removing from the radiation area. In the fourth and fifth group the role of the biological active compound such as meksidazol on the recovery of the liver metabolic disorder induced due to the X-RAYs exposure was studied. In a way to assess the liver metabolism the concertation of the AsAT, A1AT, glutamyl transferase, KFK, LDH and alkaline phosphatase in the blood was tested.

**Key words:** Liver, enzymes, X-rays, meksidozol

## Introduction

New technologies that were integrated to the manufactory and to household along with its positive features also brought certainly new challenges to society. Nuclear power plant, hydroelectric plant, loss and waste of radioactive substances, use of imperfect technologies and other sources enrich the environment with ionizing rays (Dyuzhev 2017; Me James 2017). On the other hand, high diagnostic tools used in medical institutions (x-ray machine, magnetic resonance tomogram and also computer tomogram) and a number of household devices are able to emit radioactive radiation, even though they are in low doses (Raya-Povedano 2021; Borges de Souza 2021). Irradiation with ionizing rays affects the living organism as a whole and

disrupts the physiological functions of individual organs, leading to the development of pathological processes. It has been established that any harmful impact directed at the organism primarily affects the liver and disrupts its physiological function (Ehrhardt 2020; Roth 2017). By this time, the metabolites formed as a result of the destructive process in hepatocytes become a source of endogenous intoxication (Pavlov 2021; Djuzhev 2018). The resulting endogenous intoxication aggravates subclinical and chronic diseases in the body. All above emphasizes the importance of the synthesis of new drugs to eliminate the effects of ionizing radiation.

**Materials and methods**

The research was conducted on 25 white rats of both sexes raised in the vivarium at the Scientific Research Center of the Azerbaijan Medical University. The experimental animals were kept in the vivarium at a temperature of $20C^0$ and were fed based on the received food regimen. Depending on the task and purpose, experimental animals were divided into 5 main groups, each contains 5 rats. In the 1st group rats were examined in an intact state and the results obtained from it were considered as normal. In the 2nd group rats were irradiated with X-rays. In the 3rd group rats were examined for the duration of the pathological process 10 days after the X-ray irradiation. Rats from the 4th group were injected with the complex compound synthesized on the basis of Palladium and Mexidol (Mexidazole) into their abdominal cavity for 3 days at a dose of 0.02 mg/kg per day after irradiating them with X-rays. In the 5th group rats were treated with the complex compound synthesized on the basis of Mexidazole via injection into the abdominal cavity at a dose of 0.02 mg/kg per day for 7 days after irradiating them with X-rays.

Based on the literature review the blood parameters that reflect the liver metabolism were choosed (Ivashkin 2019; Dibirov 2017; Joshi 2018; Podoluzhnyi 2018; Garayeva 2020). Therefore, to assess the functional state of the liver, blood level of Alat aspartate transaminase (AsAT GOT Ş Ac J; Aspartate Aminotransferase UJ 2.6.1.1), Alanine Aminotransferase (AlAT GRT 1 FsJ) Alanine Aminotransferase (EJ 2.6.1.2), Glutamine transferase, Creatine phosphokinase (KFK), Lactate dehydrogenase (LDH), Alkaline phosphatase was determined. In addition, based on the literature review, markers that are associated with the liver metabolism impairment as well as the recovery of the disturbed metabolism were determined and used as diagnostic tests (Styashkina 2017). For this purpose, the concentration of creatinine, urea, total bilirubin, residual nitrogen and total protein in the blood were determined. The concentration of the specified markers in the blood was carried out in the Bio Skreen MS-2000 brand analyzer manufactured in the USA, which works in fully automatic mode using reagent kits manufactured by the Human company.

The experimental animals were subjected to X-rays using the "RUM-17" device within the following parameters.

• Voltage – 180 kv;
• Current intensity – 15 m;
• Filters – 0.5 mm Cu + 1.0 mm Al.
• Focal distance factor - 3
• Dose strength without tube - 0.86 Gr/sec

Based on the recommendation of A.U. Eminov (2014), a single dose of 4 g was used during the irradiation of experimental animals. Experimental animals were irradiated with the indicated dose for 5 days.

**Result and discussion**

In the first group the blood concentration of chosen parameters was as follows; the concentration of AST enzyme was 25-33 u/l, ALT enzyme was 30-40 u/l, glutamine transferase enzyme was between 28-58 u/l, LDH enzyme was 270-440 u/l, KFK was between 243-275 u/l, and the concentration of alkaline phosphatase enzyme varied between 150-300 u/l. In the second experimental group, the average concentration of AST enzyme in the blood was 27% (P<0.05), the ALT enzyme was 30% (P<0.05), the glutamine transaminase enzyme was 17%, the average concentration of the LDH enzyme increased by 31% (P<0.05), the KFK enzyme by 52% (P<0.001) and the alkaline phosphatase by 29% (P<0.05).

Based on the obtained results, the effect of the X-rays irradiation on the blood level of enzymes that are associated with the physiological function of the liver, was higher in compare with the normal stage. It was determined that the concentration of KFK enzyme increased due to the effect of X-rays exposure. In comparison with other parameters, the increase of concentration of γ-glutamine transferase enzyme was slightly increased.

It was observed that in the 3rd group the elevated blood concentration of liver enzymes modestly decreased (Table 1). Thus, in compare to the intact condition, the average concentration of AST enzyme increased by 22% (P=0.05),of ALT enzyme by 23%, of glutamyl transferase enzyme by 13%, the LDH enzyme by 27% (P<0.05), the KFK enzyme by 34% (P<0.05), and the alkaline phosphatase increased by 22%.

Based on the obtained results from 2nd and 3rd groups, X-rays have a serious negative effect on the enzyme synthesis and function of the liver. In addition, the function of the liver damaged by X-rays cannot be restored even after the transfer of the experimental animals from the radiation area.

The results obtained from the 4-th group showed that the injection of mexidazole at a dose of 0.02 mg/kg per day into the abdominal cavity of experimental animals irradiated with X-rays for a period of 3 days prevents abnormal liver enzyme synthesis at a certain extent.

Thus, in compare with the normal condition the average concertation of the AST enzyme increased by 14% (P=0.05), while the average concentration of ALT enzyme increased by 15% (P=0.05). In contrast to AST and ALT enzymes, the average concentration of glutamine transferase enzyme remained at the same level as in the intact state. Meanwhile, the average concentration of LDH enzyme decreased by 20% and the concentration of CFC decreased by 39.5% (P<0.01).

The average concentration of alkaline phosphatase enzyme was 16% (P=0.05) higher than that in the normal state. Thus, based on the results obtained from the 4th group, it can be concluded that as a result of injecting the mexidazole drug into the abdominal cavity for 3 days, the increased concentration of enzymes in the blood during the irradiation was significantly reduced (Table 1). Meanwhile, the results obtained from the 5th group showed that with the increase of the duration of intra-abdominal injection of mexidazole, the elevated concentration of enzymes in the blood approaches the normal level.

Thus, after the injection of mexidazole drug into the stomach of experimental animals that were exposed to X-rays for 7 days, the average concentration of AST enzyme in the blood reached the same level as it was in a normal state. The average concentration of ALT and LDH enzyme was only 6% and 10% higher respectively (P=0.05) in compare to the concentration of those in the blood of experimental animals included in the 1st group. However, the average concentration of KFK enzyme in the blood was significantly higher by 32% (P<0.01) than that in the normal stage.

Positive dynamics were observed in the concentration of alkaline phosphatase due to the effect of mexidazole in the blood. In all white rats included in the 5th group, the concentration of alkaline phosphatase enzyme in their blood was the same as the level in the intact state.

Thus, due to intra-abdominal injection of mexidazole for 7 days, the blood concentration of enzymes that are markers for the liver disorder decreased significantly.

The following results were obtained from the non-enzymatic marker of liver metabolism. The mean concentration of creatinine in the blood of white rats exposed to X-rays increased dramatically by 43.5% (P<0.05) compared to the intact

condition. The concentration of urea in the blood also increased dramatically by 72% (P<0.05) compared to the level in the intact state. The concentration of total bilirubin was 70% (P<0.05) higher than that in the intact state.

Due to the effect of X-rays, there was a significant difference (51%) in the concentration of residual nitrogen in the blood in compare with the intact state.

Unlike the mentioned markers, the total protein concentration in the blood decreased slightly by 7% in compare to the intact state.

Thus, based on the obtained results, the elevated blood concentration of creatinine, urea, total bilirubin, and residual nitrogen that were determined in the 2nd group proved that hepatitis develops in the liver of white rats under the influence of X-rays.

**Table 1. Effect of mexidazole on elevated blood enzymes cocncetration of white rats exposed to X-rays.**

| № | Groups | Statistical parameters | ASTul | ALTul | QTul | LDHul | KFKul | QFul |
|---|--------|------------------------|-------|-------|------|-------|-------|------|
| 1 | I | Min | 25 | 30 | 28 | 270 | 243 | 150 |
|   |   | Max | 33 | 40 | 58 | 440 | 275 | 300 |
|   |   | M | 29,4 | 35,2 | 43,2 | 368 | 260,4 | 23,4 |
|   |   | m | 1,50 | 1,85 | 5,43 | 28,53 | 6,00 | 27,13 |
| 2 | II | Min | 28 | 33 | 33 | 320 | 315 | 280 |
|   |   | Max | 50 | 57 | 60 | 590 | 463 | 330 |
|   |   | M | 37,4** | 45,8** | 50,6* | 482** | 394,8*** | 302** |
|   |   | m | 3,78 | 4,53 | 5,18 | 45,54 | 24.25 | 8,60 |
| 3 | III | Min | 48 | 52 | 67 | 560 | 426 | 420 |
|   |   | Max | 70 | 73 | 110 | 800 | 625 | 600 |
|   |   | M | 58,6**** | 63,8**** | 88,2*** | 724**** | 528,4**** | 530**** |
|   |   | m | 4,24 | 4,50 | 8,45 | 43,89 | 38,94 | 35,92 |
| 4 | IV | Min | 24 | 30 | 28 | 300 | 285 | 240 |
|   |   | Max | 45 | 52 | 53 | 530 | 420 | 300 |
|   |   | M | 33,6* | 40,6* | 43,4* | 422* | 363,2*** | 272* |
|   |   | m | 3,44 | 4,07 | 4,72 | 36,80 | 23,32 | 10,68 |
| 5 | V | Min | 23 | 27 | 0- | 300 | 277 | 220 |
|   |   | Max | 40 | 47 | - | 480 | 410 | 260 |
|   |   | M | 29,6* | 37,4* | - | 404* | 344,8*** | 240 |
|   |   | m | 3,04 | 3,76 | - | 33,26 | 22,59 | 7,07 |

$*$ - p = 0,05

$**$ - p < 0,05

$***$ - p < 0,05

**** - p < 0,05

In the table 2 the results obtained 10 days after stopping irradiation are shown. In compare to the normal state the blood concentration of following markers were increased: creatinine by 39% (P<0.05), urea content by 68% (P<0.05), total bilirubin content by 62.5% (P<0.05), residual nitrogen content by 46% (P<0.05). In contrast the total protein concentration decreased by 2% (P=0.05).

Thus, based on the experimental results, it can be concluded that X-rays permanently disrupt the metabolism of the liver. Since, even 10 days after of transporting the white rats from the radiation area, the average concentration of non-enzymatic markers characterizing the liver metabolism in the blood were still significantly higher than the level in the steady-state.

It was shown that administration of mercidozole at a dose of 0.02 mg/kg for 3 days to white rats exposed to X-rays led to the stabilization of the level of metabolic indicators via improving the detoxification function of the liver.

It was determined that the concentration of urea in the blood taken from the experimental animals was significantly decreased by 33.5% (P<0.05), but it was still higher (14.5% (P=0.05)) than the concentration of that in the unexposed state.

The concentration of the total bilirubin, which is one of the antitoxic indicators of the liver, decreased by 26.5% (P<0.05) and its blood concentration of most of the experimental animals was within the normal range. However, despite this positive dynamics, the average concentration of bilirubin in the blood was 25% (P=0.05) higher than that in the unexposed state.

In contrast to these indicators, the concentration of residual nitrogen in the blood has sharply decreased, but was by 2% higher than that in the unexposed state.

Positive dynamics were also observed for the total protein concentration in the blood. So, its average concentration increased by 4% (P=0.05) in compare to the 3rd group. However, it did not fall to the level of the unexposed state, and remained to be by 3% (P=0.05) higher than that.

Thus, as a result of intraperitoneal injection of 0.02 mg/kg of mexidazole for 3 days in white rats irradiated with X-rays, the elevated amount of specific indicators of liver damage was significantly reduced and approached the normal range (table 2).

In order to study the therapeutic effect of mexidazole the treatment duration was extended up to 7 days after irradiating white rats in 5th group with X-rays. Since the elevated level of other indicators in the blood was close to the normal limit, the concentration of total bilirubin and total protein in the blood in the 5th group was determined.

It was determined that as a result of injecting mexidazole into the abdominal cavity for 7 days, the increased concentration of total bilirubin in the blood due to the effect of X-rays was sharply reduced. Compared to 2nd group, the difference was by 34% ($p<0.01$), but the concentration of total bilirubin in the blood could not reach the level of the intact state, by being 12.5% higher.

Meanwhile, the average concentration of total protein decreased by 3% compared to the 2nd group and reached the normal level.

Thus, the results of our experiments have shown that liver metabolism is seriously disturbed by exposure to X-rays. According to the results obtained from the examinations of its markers in the blood, X-rays cause the development of hepatitis in the liver. Positive dynamics of metabolic indicators in the blood were recorded after administration of a newly synthesized biologically active substance so called mexidazole into the body. Based on the result it can be conclude that mexidazole has radioprotective properties.

**Table 2. Effect of mexidazole on the concentration of non-enzymatic markers of liver metabolism in the blood of white rats exposed to X-rays.**

| № | Groups | Statistical parameters | Creatinine | Urea | Total bilirubin | Residual nitrogen | Total protein |
|---|--------|------------------------|-----------|------|-----------------|-------------------|---------------|
| 1 | I | Min | 0,7 | 16 | 0,3 | 6 | 66 |
|   |   | Max | 1,2 | 45 | 1,1 | 18 | 85 |
|   |   | M | 0,92 | 33 | 0,8 | 12,2 | 75,4 |
|   |   | m | 0,09 | 5,08 | 0,14 | 2,06 | 3,47 |
| 2 | II | Min | 1 | 32 | 1,1 | 10 | 59 |
|   |   | Max | 1,7 | 74 | 1,6 | 27 | 81 |
|   |   | M | 1,32 | 56,8 | 1,36 | 18,4 | 70,2 |
|   |   | m | 0,12 | 7,60 | 0,09 | 2,80 | 4.71 |
| 3 | III | Min | 1 | 32 | 1,1 | 10 | 61 |
|   |   | Max | 1,7 | 70 | 1,5 | 25 | 81 |
|   |   | M | 1,28** | 53,6** | 1,3** | 17,8** | 71,4** |
|   |   | m | 0,12 | | 0,07 | 2,46 | 4,27 |
| 4 | IV | Min | 0,7 | 22 | 0,8 | 8 | 63 |
|   |   | Max | 1,3 | 54 | 1,2 | 20 | 82 |
|   |   | M | 0,94 | 37,8 | 1 | 12,4 | 73 |
|   |   | m | 0,10 | 5,82 | 0,07 | 2,25 | 3,86 |
| 5 | V | Min | - | - | 0,7 | - | 67 |
|   |   | Max | - | - | 1,1 | - | 83 |
|   |   | M | - | - | 0,9 | - | 75 |
|   |   | m | - | - | 0,07 | - | 3,21 |

\* - p = 0,05

\** - p < 0,05

# Reference

**Borges de Souza P, McCabe C.** (2021). Radioiodine treatment: An historical and future perspective. Endocr Relat Cancer. 28 (10):121-124.

**Dibirov M.D., Rybakov G.S., Domarev V.L., Vasilyeva M.A.** (2017). Algorithm for diagnosis and treatment of elderly and senile patients with acute cholecystitis, choledocholithiasis and obstructive jaundice, Emergency medical care.6 (2): 145–148

**Djuzhev N.A., Demin G.D., Gryazneva T.A., Kireev V.Yu., Novikov D.V.** (2018). Investigation of the Concept of a Miniature X-ray Source Based on Nanoscale Vacuum Field-emission Triode Controlled by Cut-off Grid Voltage. 1974-1978.

**Dyuzhev N.A.** (2017). Microfocus X-ray tubes with silicon field emission nanocathode as a source of X-ray radiation. Brief communications on physics FIAN. No. 12, 2017.

**Ehrhardt Jr J, Güleç S.** (2020). A Review of the History of Radioactive Iodine Theranostics: The Origin of Nuclear Ontology. Mol Imaging Radionucl Ther. 29 (3):88-97.

**Garayeva K.G.** (2020). Dynamics of liver tests in pregnant women with hepatitis of non-infectious origin when prescribed ademetionine. Kazan Medical Journal. 2: 296-303.

**Ivashkin V.T., Baranovsky A.Yu., Raikhelson K.L., Palgova L.K., Mayevskaya M.V., Kondrashina E.A., Marchenko N.V., Nekrasova T.P., Nikitin I.D.** (2019). Drug-induced liver damage (clinical recommendations for doctors). Russian Journal of Gastroenterology, Hepatology, Coloproctology. 29 (1): 101–131.

**Joshi D, Keane D, Brind E.** (2018). Visual hepatology. Moscow: GEOTAR-Media. 168 p.

**Me James A. Heslop.** (2017). Chanistic evaluation of primary human hepatocyte culture using global proteomic analysis reveals a selective dedifferentiation profile, Arch Toxicol. 91: 439-452.

**Pavlov N.A., Andreichenko A.E., Vladzimirsky A.V.** (2021). Reference medical datasets (MosMedData) for independent external evaluation of algorithms based on artificial intelligence in diagnostics, Digital Diagnostics. 2 (1): 49–66.

**Podoluzhnyi V.I.** (2018). Obstructive jaundice: current principles of diagnosis and treatment. Fundamental and Clinical Medicine. 3 (2): 82-92.

**Raya-Povedano J.L. et al.** (2021). AI-based Strategies to Reduce Workload in Breast Cancer Screening with Mammography and Tomosynthesis: A Retrospective Evaluation, Radiology. 300 (1), 57–65.

**Roth, A.** (2017). Idiosyncratic Drug-Induced Liver Injury (IDILI): Potential Mechanisms and Predictive Assays / Alexander D. Roth, Moo-Yeal Lee. BioMed Research International. 1-23.

**Styashkina S.N., Gadelshchina A.A., Voronchikhina E.M.** (2017). Mechanical jaundice-basic complication of the hepatopacreatobilar system. Bulletin of science and education. 1 (5): 103-105

# Sanfilippo A Syndrome Genetic Studies in the Patient from Azerbaijan Republic

## Sevda Alizada[1], Elkhan Rasulov[2]

[1]*Azerbaijan Medical University, Baku, Azerbaijan*
[2]*Clinical laboratory Genome, Baku, Azerbaijan*
\**Corresponding author:* *alizadasevda@yahoo.com*

**Abstract**

First time in the patient from Azerbaijan Republic, genetics of Mucopolysaccharidosis Type III - Sanfilippo A syndrome was identified and studied. In order to study Sanfilippo A genetics, authors used complex of modern molecular-genetic methods and techniques. During patient's medical-genetic consultation with doctor pediatrician and doctor geneticist in the Central Hospital of Gyanja City, a patient, originated from Lachin region of the Republic, was identified as an affected one relied on the clinical manifestations. Parents had a consanguineous marriage first cousins. Clinical studies showed cognitive changes, speech disorder, aggressiveness, hyperactivity, autistic signs, troubles in motions, hepatomegaly, failure in gaining weight, and physical development lag. For diagnostics capillary and venous blood samples were used. Blood from the patient was sampled into 2 ml-tubes with anticoagulant and absorbed to DBS (Dry Blood Spot) cards. Urine analysis was carried out with thin-layer chromatography. Enzyme activity was valued with mass spectrometry technique, and the DNA level analysis for SGSH gene was conducted with NGS technique. Urine analysis results allowed us to diagnose provisionally Sanfilippo syndrome MPS III based on increased values of heparan sulfate and keratan sulfate. Specification of Sanfilippo syndrome type (A, B, C or D) was conducted with activity evaluation of all four lysosomal enzymes: N-sulfoglucosamine sulfohydrolase (for TypeA), alpha-N-acetyl-D-glucoseaminidase (for Type B), heparan acetyl-CoA-glucoseaminide-N-acetyltransferase (for Type C), N-acetylglucoseamine-6-sulfatase (for Type D). We have got N-sulfoglucosamine sulfohydrolase 0 activity specific for Sanfilippo A syndrome. Molecular analysis identified mutation c.7_16del, p.Cys3ProfsTer8 of SGSH gene: (NM_000199.5) in homozygous state. Taking into account reproductive age of parents, fetus prenatal diagnostics is being planned for the next pregnancies.

**Key words:** Sanfilippo A syndrome, Mucopolysaccharidosis Type III, N-sulfoglucosamine sulfohydrolase, enzyme, SGSH gene, NGS technique, sequencing

**Introduction**

Sanfilippo syndrome (Mucopolysaccharidosis Type III) is named after Doctor Sylvester Sanfilippo who first described this disorder in 1963. Sanfilippo syndrome is a hereditary lysosomal storage disorder, genetically heterogeneous, conditioned with heparin sulfate (HS) storage and specified with progressing mental retardation, and moderate skeletal alterations (Aronovich et.al., 2000; Cleary et.al., 1993; Cross et.al., 2014; Esposito et.al., 2000).

Four subtypes of Sanfilippo Syndrome were identified, each of them arise with enzyme deficiencies: N-sulfoglucoseamine sulfohydrolase (Sanfilippo A), Alpha-N-acetyl-D-glucoseaminidase (Sanfilippo B), Heparan acetyl-CoA-glucoseaminide-N-acetyltransferase (Sanfilippo C), N-acetylglucoseamine-6-sulfatase (Sanfilippo D). Those enzymes' genes are located on 8, 12 and 17 chromosomes. Each enzyme deficiency leads to heparan sulfate (HS) (Esposito et.al., 2000). Every type of this disease is inherited as autosome-recessive, and parents of the index patient are heterozygotes on pathologic gene (Aronovich et.al., 2000; Bhattacharyya et.al., 2001; Valstar et.al., 2010; Xiong et.al., 2015).

Sanfilippo A type causing N-sulfoglucoseamine sulfohydrolase gene (SGSH: 605270) is located on the long shoulder of chromosome 17 (17q25) and modifies synthesis of the same named enzyme N-sulfoglucoseamine sulfohydrolase (Esposito et.al., 2000).

Sanfilippo syndrome takes the third place according to frequency among all nowadays known mucopolysaccharidoses (Khan et.al., 2017; Valstar et.al. 2008).

In British Columbia province, Canada only four out of 325617 examined newborns had got Sanfilippo syndrome (0.0012%). N-sulfoglucoseamine sulfohydrolase (Lowry et.al., 1990). In West Australia five newborns out of 58000 manifested and identified Sanfilippo A type syndrome, where frequency was counted as 0.0086% (Nelson et.al., 2003). In Netherlands frequency of the disease was 0.88-1.15:100000 among alive newborns (Poorthuis et.al., 1999).

It should be noticed that the problem in diagnostics and treatment of lysosomal storage diseases exists, and particularly of mucopolysaccharidoses. In consequence, goal of our studies is to study molecular basics of Sanfilippo syndrome using modern molecular-genetic methods and techniques of diagnostics, taking into account unexplored the disease genetics for the Azerbaijan Republic population.

**Materials and methods**

Index patient is a 4-year-old girl examined by doctor pediatrician and doctor geneticist in Central Hospital in Gyanja city in 2021. As to clinical manifestations the disease was provisionally diagnosed as lysosomal disease Mucopolysaccharidosis and specifically Sanfilippo syndrome. For this diagnostics urine, and 2 ml capillary and venous blood samples were collected on DBS (Dry Blood Spot) cards and tubes with anticoagulant. Urine analysis was carried out with thin-layer chromatography technique.

To identify disease type the following enzymes were used: N-sulfoglucoseamine sulfohydrolase (Sanfilippo A), Alpha-N-acetyl-D-glucoseaminidase (Sanfilippo B), Heparan acetyl-CoA-glucoseaminide-N-acetyltransferase (Sanfilippo C) and N-acetylglucoseamine-6-sulfatase (Sanfilippo D). Enzymes activity evaluation was conducted with mass-spectrometry technique.

DNA obtained from patient's peripheral blood sample was studied with NGS (New Generation Sequencing) technique. «A custom double stranded DNA capture bait pool was used to selectively enrich the coding regions, 10 bp of flanking intronic sequences, and known relevant variants beyond the coding regions, based on HGMD® and CentoMD® for the 166 panel genes. Libraries are generated with Illumina compatible adaptors, and sequenced on an Illumina platform to obtain ≥ 50x coverage depth for >99.5% of the targeted bases. Mean depth of reading consists of 1559 indications. All potential disease-causing variants, including the ones reported in HGMD®, in ClinVar and in CentoMD® are considered. The investigation for relevant variants is focused on coding exons and flanking +/-10 intronic bases. All potential modes of inheritance patterns are considered. Centogene® has established stringent quality criteria and validation processes for variants detected by NGS. Pathogeny classification of the obtained results was considered according to «Guidelines of ACMG*». At the same time sequencing of SGSH gene was carried out.

**Results and discussions**

During genetic consultation, doctor pediatrician and doctor geneticist examined genetically burdened patients in Central Hospital of Gyanja city, and identified a four-year-old patient with clinical manifestations of lysosomal storage disease which is Mucopolysaccharidosis Type III (MPS III).

When examining clinically, doctors observed cognitive change, cognitive changes, speech disorder, aggressiveness, hyperactivity, autistic signs, troubles in motions, hepatomegaly, failure in gaining weight, and physical development lag. Patient's photo is presented in **Figure 1**.



**Figure 1.** Patient's photo suspicious with MPS III (Sanfilippo syndrome)

Patient was born from the consanguineous marriage (parent's mothers are sisters). Parents were originated from Lachin region of the Republic.

First of all urine analysis was carried out for lysosomal storage disease - Mucopolysaccharodosis, and that was conducted with thin-layer chromatography technique. Increase of glucoseaminoglycans (GAG) - 52.12 mg/µmol when norm must be 7.60-14.40 mg/µmol because of heparan sulfate (HS) increase and keratan sulphate (KS) for Sanfilippo syndrome (MPS III).

MPS III is heterogeneous and has four subtypes. Consequently, for diagnostics and identification of Sanfilippo syndrome, the following enzymes activity evaluation was used: N-sulfoglucoseamine sulfohydrolase (Sanfilippo A), Alpha-N-acetyl-D-glucoseaminidase (Sanfilippo B), Heparan acetyl-CoA-glucoseaminide-N-acetyltransferase (Sanfilippo C) and N-acetylglucoseamine-6-sulfatase (Sanfilippo D). Enzyme analysis was conducted in dried blood samples from DBS (Dry Blood Spot) cards.

Enzyme analysis results showed 0-activity only for one enzyme - N-sulfoglucoseamine sulfohydrolase - that corresponds with Sanfilippo A syndrome. The patient was suspicious of Sanfilippo A syndrome, and her family members' enzyme analyses results are presented in Table 1.

**Table 1. Enzyme analyses results of Sanfilippo A syndrome patient family members.**

| Patient | Result | Reference | Zygosity | Inter-pretation | Method |
|---------|--------|-----------|----------|----------------|--------|
| Index patient | 0 (LOD) µmol/L/h LOD = limit of quantification | ≥ 5,0 µmol/L/h | Homozygote | Pathologic, class 1 | mass spectrometry |
| Mother | 1,81 (LOD) µmol/L/h LOD = limit of detection | ≥ 5,0 µmol/L/h | Heterozygote | Pathologic, class 1 | mass spectrometry |
| Father | 2,0 (LOD) µmol/L/h LOD = limit of detection | ≥ 5,0 µmol/L/h | Heterozygote | Pathologic, class 1 | mass spectrometry |

As it is seen from the Table 1, patient showed 0-activity of N-sulfoglucoseamine sulfohydrolase enzyme that corresponds with homozygous state of enzyme deficit. To genetically confirm the diagnosis Sanfilippo A syndrome we carried out SGSH gene genetic analysis. This analysis was conducted with two methods: NGS technique and sequencing method. Results of SGSH gene sequencing are presented in Figure2.
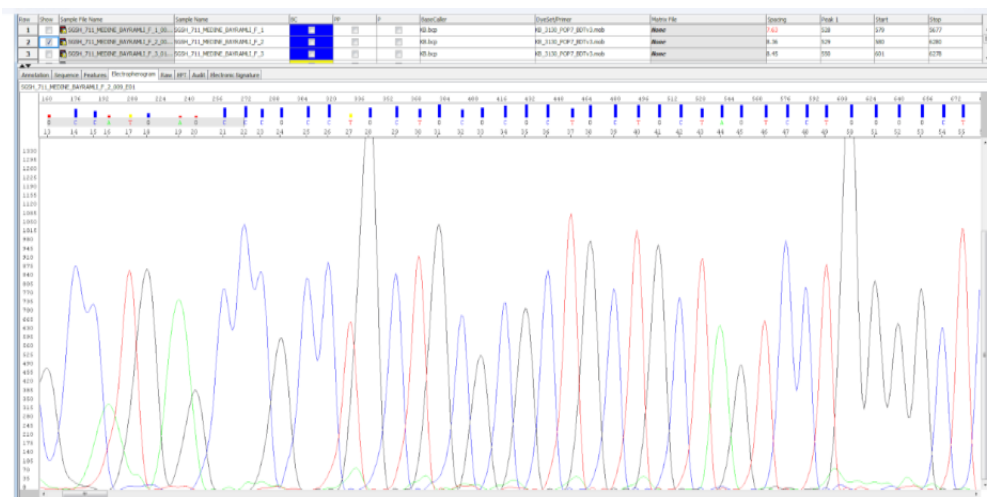


**Figure 2.** SGSH gene sequencing results

We coped to identify SGSH gene mutation c.7_16del гена SGSH: (NM_000199.5) for patient with 0-activity of N-sulfoglucoseamine sulfohydrolase enzyme. Here

deletion of 10 bp from 7 to 16 nucleotides is observed. As a result a substitution of amino acid Cysteine with amino acid Proline in codon 3 exists on the level of protein (enzyme). Mutation leads to formation terminating codon 8. The said mutation is pathogenic class 1 (see Table 2).

**Table 2. SGSH and HGSNA genes genetic analyses results**

| MPS III | Gene | Gene mutation | Protein |
|---|---|---|---|
| Sanfilippo A syndrome | SGSH: NM_000199.5 | c.7_16del | p.Cys3ProfsTer8 |

Patient manifests homozygous state of the mutation. Both parents had heterozygous carriage of this mutation.

Sanfilippo A syndrome is the mostly spread subtype. Course of the disease in this form is the severest with early onset and speediest progressing symptoms and short life expectancy (Bhattacharyya et.al., 2001).

Frequency for MPS in Japan valued 1.43 for 100000 among live newborns. Sanfilippo syndrome comprised only 16% out of all MPS types. In Switzerland MPS counted 1.56 for 100000 newborns. And MPS III considered 24% for all MPS types, Average frequency of Sanfilippo A syndrome here comprised 60% among all MPS disease types. Epidemiologic studies in British Columbia province of Canada identified 4 cases of Sanfilippo A syndrome between years 1952 and 1986, and that was counted as 1: 325,617 living newborns. (Esposito et.al., 2000; Khan et.al., 2017; Lowry et.al., 1990; Nelson et.al., 2003).

Thus, in patient suspicious with lysosomal disease Mucopolysaccharidosis Type III - Sanfilippo syndrome - genetics of the disease is studied at the level of glycosaminoglycan in urine and the level of enzyme and SGSH gene. SGSH gene mutation was identified: c.7_16del (NM_000199.5) in homozygous state. Taking into account parents' reproductive age, fetus prenatal diagnostics is recommended during the course of next pregnancies.

**Conclusion**

During genetic consultation, doctor pediatrician and doctor geneticist examined and identified patient with clinical manifestations of mucopolysaccharidosis - lysosomal storage disease.

2. On the basis of results of thin-layer chromatography urine analysis that showed increased values of heparan sulfate and keratan sulfate we were able to identify provisional diagnosis as Sanfilippo syndrome (MPS III).

3. Patient's blood sample was analyzed with all four enzymes for identification certain type of Sanfilippo syndrome (MPS III). As a result we got 0-activity for N-sulfoglucosamine sulfohydrolase enzyme that confirms Sanfilippo A syndrome in the patient.

4. Molecular analysis identified SGSH gene mutation c.7_16del, p.Cys3ProfsTer8: (NM_000199.5) in homozygous state.

5. Taking into account reproductive age of parents, fetus prenatal diagnostics is being planned for the next pregnancies.

## References

**Aronovich E.L., Carmichael K.P., Morizono H., Koutlas I.G., Deanching M., Hoganson G., Fischer A., Whitley C.B.** (2000) Canine heparan sulfate sulfamidase and the molecular pathology underlying Sanfilippo syndrome type A in Dachshunds. Genomics Aug 15;68(1):80-84

**Bhattacharyya R., Gliddon B., Beccari T., Hopwood J.J., Stanley P.** (2001) A novel missense mutation in lysosomal sulfamidase is the basis of MPS III A in a spontaneous mouse mutant. Glycobiology. Jan;11(1):99-103

**Cleary M.A., Wraith J.E. Management of mucopolysaccharidosis type III.** (1993) Arch Dis Child. Sep; 69(3):403-406

**Cross E.M., Grant S., Jones S., Bigger B.W., Wraith J.E., Mahon L.V., Lomax M., Hare D.J.** (2014) An investigation of the middle and late behavioural phenotypes of Mucopolysaccharidosis Type-III. J Neurodev Disord. 6(1):46

**Esposito S., Balzano N., Daniele A., Villani G.R., Perkins K., Weber B., Hopwood J.J., Di Natale P.** (2000) Heparan N-sulfatase gene: two novel mutations and transient expression of 15 defects. Biochim. Biophys. Acta. Apr 15;1501(1):1-11

**Haron B., Mikaeloff Y., Froissart R., Caridade G., Maire I., Caillaud C., Levade T., Chabrol B., Feillet F., Ogier H., Valayannopoulos V., Michelakakis H., Zafeiriou D., Lavery L., Wraith E., Danos O., Heard JM., Tardieu M.** (2011) Incidence and natural history of mucopolysaccharidosis type III in France and comparison with United Kingdom and Greece. Am J Med Genet A. Jan;155A(1):58-68

**Khan S.A., Peracha H., Ballhausen D., Wiesbauer A., Rohrbach M., Gautschi M., Mason R.W., Giugliani R., Suzuki Y., Orii K.E., Orii T., Tomatsu S. (**2017) Epidemiology of mucopolysaccharidoses. Molec. Genet. Metab. Jul;121(3):227-240

**Lowry R.B., Applegarth D.A., Toone J.R., MacDonald E., Thunem N.Y.** (1990) An update on the frequency of mucopolysaccharide syndromes in British Columbia. Hum. Genet. Aug;85(3):389-390

**Nelson J., Crowhurst J., Carey B., Greed L.** (2003) Incidence of the mucopolysac-charidoses in Western Australia. Am. J. Med. Genet. A. Dec 15;123A:(3):310-313

**Poorthuis B.J.H.M., Wevers R.A., Kleijer W.J., Groener J.E.M., De Jong J., Van Weely S., Niezen-Koning K., Van Diggelen O.P.** (1999) The frequency of lysosomal storage diseases in The Netherlands. August. Hum. Genet. 105(1-2):151-156

**Valstar M.J., Marchal J.P., Grootenhuis M., Colland V., Wijburg F.A.** (2011) Cognitive development in patients with Mucopolysaccharidosis type III (Sanfilippo syndrome). Orphanet Journal of Rare Diseases, Jun 20;6:43

**Valstar M.J., Ruijter G.J., Van Diggelen O.P., Poorthuis B.J., Wijburg F.A.** (2008) Sanfilippo syndrome: a mini-review. J Inherit Metab Dis. Apr;31(2):240-252

**Valstar M.J., Neijs S., Bruggenwirth H.T., Olmer R., Ruijter G.J., Wevers R.A., Van Diggelen O.P., Poorthuis B.J., Halley D.J., Wijburg F.A.** (2010) Mucopolysaccharidosis type IIIA: clinical spectrum and genotype-phenotype correlations. Ann. Neurol. Dec;68(6):876-887

**Xiong H.Y.et al.,** (2015) RNA splicing/The human splicing code reveals new insights into the genetic determinants of disease. Science Jan 9;347(6218):1254806

# Phages and Immunity

**Jamila Talibova[1], Matanat Novruzova[2], Safada Taghiyeva[2], Sara Gurbanova[2], Fakhraddin Shikhaliyev[2]**

*[1]Children's Rehabilitation Center of the Scientific Research Pediatric Institute named after K.Y. Farajova, Baku, Azerbaijan*
*[2]Department of Medical Microbiology and Immunology, Azerbaijan Medical University, Baku, Azerbaijan*
*Corresponding author: Safada.tagiyeva@yahoo.com*

**Abstract**

In recent years, the microbiome and its role in the pathophysiology of diseases and the development of other human pathophysiological conditions have attracted great interest. Only recently has the presence of bacteriophages been identified in the microbiome and their potential role in maintaining normal immunity. The progress of our knowledge in this area opens up completely new perspectives for understanding the normal physiology of the human body, the treatment of diseases, including the most difficult ones for modern medicine. Of particular interest are studies of the interaction of the microbiome with the immune system.

**Keywords:** phages; immunity; pathophysiology; microbiome; lymphocytes.

## Introduction

According to the current situation of COVID-19 pandemia in over the world detailed and deep investigation of the human immun system, formulation and adaptation of its components to the environment factors such us different microbial and non-microbial agression to the organism is very important. The topic have great actuality not only for medicals, but for all biology specialists.

## Localisation and occurance of the phages to the intestine

The increased interest to the microbiome and the application of advanced sequencing technologies have provided possibility to assess the impact of the microbiome in the pathophysiology of the disease and its potential modulation for therapeutic purposes (Hargreaves et al., 2014). Interactions between the intestinal immune system, the

epithelial barrier, and bacteria residing on it are fundamental to maintaining healthy intestine homeostasis (Erez et al., 2017; Jain et al., 2017). The microbiota plays an important role in the formation of the human immune system. For example, inter-individual differences in responses to vaccines, chemotherapy, and immunomodulatory agents depend on differences in the gut microbiota. From the discovery of phages 100 years ago until the end of the 20th century, the vast majority of research focused on the well-known antibacterial effect of phages. Although phages have been used for immunization and to assess humoral immunity in animals and patients with immunodeficiency syndromes, there are no data on the interaction of phages with the immune system and the potential consequences of such events for the formation of the immune system (Burcelin, 2016; Sausset et al., 2020). Temperate phages modify the biochemical pathways between host bacteria and affect communication between infected and uninfected cells. Engineering of the bacterial host genome by prophages has beneficial effects on bacterial cellular processes. Prophages influence the metabolism of host bacteria because they modify the resistance of bacteria to other bacteriophages, the development of bacterial cells, or the production of virulence factors. Once released, these bacteriophages are able to lyse competing strains, genetically and physiologically alter the association between bacteria. In addition, phage-mediated release of intracellular substances such as nutrients to surrounding cells has been described (Barr et al., 2013). Undoubtedly, phages can cause lysis of other bacteria, being harmless to cells lysogenic for the same phage species (Żaczek et al., 2016). Finally, temperate bacteriophages also play an important role in protecting their host from various phage infections (Alcami et al., 2002). It has long been known that the microorganisms that naturally inhabit the digestive system are extremely important for maintaining proper homeostasis and therefore for the normal functioning of the immune system. The diversity of the human microbiota can be controlled by the phages present in the intestinal tract. Based on current viral genome sequencing techniques, it is argued that there is great virion variability among humans, and only a small proportion of intestinal phages is common. Reyes et al. (2010) suggested that temperate bacteriophages make up the majority of enteric viruses (Burcelin, 2016; Park et al., 2014]. However, other results have shown that the concentration of phages may be higher, about 10 10 -10 12 bacteriophage particles per gram of stool. There is evidence that about 82% of adult intestinal bacteria are lysogens, which contain the genetic material of prophages in their genomes (Fortier, 2017). It is also possible to induce prophages from intestinal bacteria under the influence of widely used drugs (Jancheva and Böttcher, 2021). Bifidobacteria bacteriophages influence the diversity and composition of intestinal strains. Maternal bifidophages are able to be transmitted to infants and regulate the composition of the intestinal microbiota of infants (Abeles and Pride, 2014; Lugli et al., 2016). It was found also  that the

adhesion of pathogenic bacterial strains to human HT29 cells was reduced after administration of the probiotic lysogenic strains S. thermophilus J34. This suggests that probiotic strains with prophages may have a beneficial effect on the human gastrointestinal tract (Brodin and Davis, 2017; Górski et al., 2006). It is estimated that more than 3% of the bifidobacteria genome consists of bifidoprophages [Górski et al., 2016; Jończyk-Matysiak et al., 2015; Mazaheri Nezhad et al., 2011). This can be beneficial for bacterial strains, but, on the other hand, it can also cause host cell lysis (Górski et al., 2006; Górski et al., 2012). Immediately after birth, the diversity of infant phages remains at a high level, and a week after birth, this correlation tends to decrease (Abeles and Pride, 2014; Pabary et al., 2015). It has been suggested that transmission of maternal bacteriophages occurs through the activation of microbial prophages in milk, vagina, or placental tissue (Jamet et al., 2017; Łobocka et al., 2014; Miernikiewicz et al., 2016). Microscopic analysis of feces and caecum samples showed that in the intestine of an adult, most of the detected phages were derivatives of activated prophages of the families Podoviridae, Siphoviridae, and Myoviridae (Brussow and Hendrix, 2002). Phages can change the microbiological composition in the intestines by reducing the dominant bacteria and allow other strains to develop, creating diverse microbial communities. Thus, phages play an important role in the evolution, diversity, and composition of the human gut microbiota (Thammavongsa et al., 2015). Intestinal phages may have a protective potential, contributing not only to the elimination of bacteria, but also to the regulation of local immune and inflammatory reactions, thereby contributing to the maintenance of immune homeostasis (Alcami et al., 2002; Górski et al., 2015; Relman, 2015). In addition, the phenomenon of translocation may allow phages to migrate to distant tissues and interact with local and distant cells of the immune system. Some phages (for example, T4) can interact with cells of the immune system using the Lys-Gly-Asp sequence present in the gp24 capsid protein and the corresponding β-3 cell receptor integrin, also used by some pathogenic viruses (Abeles and Pride, 2014). Interestingly, this sequence is also present in the CD40 ligand, which is known to activate the endothelium and platelets, promote inflammation, and is critical for T- and B-lymphocyte activation, as interruption of CD40-CD40L interactions has strong immunosuppressive properties. Barr et al., described a symbiotic relationship between a phage and a multicellular host providing antimicrobial protection actively protecting intestinal mucosal surfaces from bacterial invasion (Jończyk-Matysiak et al., 2015). Many authors have observed an increased ratio of phages to bacteria on all studied mucosal surfaces. This enrichment occurs through binding interactions between mucin glycoproteins and the domains of immunoglobulin-like proteins exposed on phage capsids and confer mucosal immunity (Górski and Weber-Dąbrowska, 2005; Górski et al., 2017).

**Stimulation and inhibition of phagocytosis**

Phagocytosis, one of the types of endocytosis, is an extremely important mechanism of innate immunity that helps Figureht against various pathogens. The whole arsenal of cytostatics directed against bacteria (including both oxygen-dependent and independent mechanisms), after their absorption by phagocytes, causes a number of effects leading to its elimination (Górski et al., 2015). Some drug molecules can be taken in by cells by phagocytosis and can also inhibit this process (Howard-Varona et al., 2017). Therefore, it is important to understand the influence of various factors on endocytic processes. Due to the fact that many bacteria have integrated prophages in their genomes that can detect their presence only under certain conditions, at some point attention began to be paid to the possible effect of these temperate phages on phagocytes and the process of intracellular killing. It has been found that prophages can modulate the human immune response to bacterial infection (Borysowski et al., 2010). Scientists Młynarczyk et al. (1989) described the process of lysogenic conversion, which may affect the susceptibility of a Staphylococcus aureus strain to phagocytosis (Castro-Mejia et al., 2015). The authors investigated the intracellular destruction of non-lysogenic S. aureus strain 8325-4 and its eight lysogenic variants by granulocytes isolated from human blood. After one hour of incubation, the level of intracellular killing was assessed. For lysogenic strains, the level of intracellular killing after an hour ranged from 29–38%, while for a non-lysogenic strain it was 63%. These observations confirmed that the lysogenic staphylococcal strain 8325-4 was less susceptible to intracellular killing by granulocytes compared to the strain without the prophage. It is likely that the observed phenomenon is associated with prophage genes, which may affect the synthesis of antiphagocytic surface receptors or may be the result of the presence of R-plasmids in cells. The authors also investigated the effect of the presence of a prophage in S. aureus.8325-4 on the intensity of leukocyte stimulation using a bioluminescent test. The results showed that the bioluminescence of leukocytes after stimulation with lysogenic strains was lower than that of non-lysogenic strains (Pabary et al., 2015; Ravin, 2015). In addition, other studies have examined the effect of group F prophages on bacterial stimulation of human leukocytes (Bondy-Denomy and Davidson, 2014; Eriksson, 2009; Łusiak-Szelachowska et al., 2017). Leukocyte chemiluminescence for lysogenic S. aureus 8325-4 was at the level of 15.4–37.2% compared to the control strain without prophage (100% bioluminescence). Intracellular leasing of the non-lysogenic strain after 30 and 60 minutes was at the level of 19 and 63%, respectively. For two strains with prophages, after 30 min of incubation with human leukocytes, the level of intracellular killing was very low, and 32–38% of bacteria died after 60 minutes. The decrease in leukocyte stimulation by lysogenic strains may be associated with an increase in the pathogenicity of bacteria that have prophage genes integrated into the genome, compared with strains without prophage. Interestingly,

the Pf prophage genes are very widespread in the genome of Pseudomonas biofilm-forming strains. In addition, the growth of the P. aeruginosa biofilm promotes the production of the Pf phage (Majewska et al., 2015). As shown in a mouse model of pneumonia, P. aeruginosa biofilm formation and production of the Pf prophage inhibit the spread of bacteria from the lungs to other tissues. In addition, these phages contributed to the inhibition of P. aeruginosa during the invasion of airway epithelial cells. This suggests that Pf phage particles can interact with the host bacterium in the lungs. In vivo studies have shown that Pf phages inhibit neutrophil recruitment, reduce cytokine levels, and protect the lungs from damage caused by infection. In addition, the production of Pf phages by bacteria leads to less efficient phagocytosis by macrophages in vivo compared to non-lysogenic strains.

Decreased phagocytosis at the presence of the temperate bacteriophage Pf has been known for a long time and has been described in detail. Pf phages internalized into the endosomes of phagocytic cells activate TLR3 receptors, which leads to stimulation of extracellular secretion of interferons, which in turn inhibit TNF-α secretion. Switching off pro - inflammatory mediators weakens the phagocytosis of pathogenic bacteria.


**Role of prophages in biofilm formation.**

Biofilm formation has a great impact on the physiology and survival of bacteria, allowing cells to withstand various harmful environmental factors. The biofilm is of great importance in the pathogenicity of many bacteria, including P. aeruginosa, making it extremely difficult to control these bacteria. The role of bacterial biofilm is especially noticeable in the development of diseases such as periodontitis and caries, pneumonia or urinary tract infections. Surprisingly, prophages have been found to play an important role in the production of biofilms by various bacterial species. Bacillus anthraces are unable to form a biofilm when deprived of prophages. The Wip4 prophage encodes the sigma factor of RNA polymerase, which is responsible for activating the expression of genes whose products are necessary for biofilm formation. It was found that the P. aeruginosa cells included in the biofilm most efficiently express the genes present in the genome of the Pf4 prophage.

Extracellular DNA is an essential element of the regular biofilm produced by various bacteria. It has been shown that such DNA appears in a biofilm formed by Streptococcus pneumoniae due to spontaneous induction of the SV1 prophage and lysis of a small proportion of cells initially included in the structure of an immature biofilm. This can be seen as another example of "bacterial altruism" where a small fraction of bacterial cells are sacrificed to make it easier for the rest of the population

to survive. Toll-like receptors (TLRs) are the most studied class of pattern recognition receptors that recognize conserved microbial components called pathogen-associated molecular patterns. Recognition of pathogen-associated molecular patterns by pattern recognition receptors, including TLRs, is essential for the induction of innate immune responses to pathogenic viruses (Górski et al., 2006; Górski et al., 2016). However, while knowledge about the interaction between pathogenic viruses and TLRs is very extensive, data on the effect of phages on TLRs are extremely scarce. There are only two studies that suggest that phage virions can stimulate TLR (Żaczek et al., 2016). In the first study, mice deficient in MyD88, a protein essential for signaling through all TLRs (except TLR3), did not respond to immunization with M13 phage, unlike wild-type mice. However, it must be emphasized that so far no studies have been conducted to evaluate direct interactions between phage particles and individual TLRs. Studies have shown that neither purified T4 phage nor E. coli phage lysate significantly affects the expression of TLR2 and TLR4 on human monocytes (Burke et al., 2001).

## Influence of phages to the tumor growth

Over the past two decades, evidence has accumulated to suggest that phages can effectively inhibit tumor growth and metastasis formation. This confirms observations made as early as 1940 indicating that phages have antitumor activity in mice and rabbits. Interestingly, molecular mechanisms similar to those described above may be at least partially responsible for the antimetastatic effects of T4 phage and its HAP1 substrain against melanoma cells in mouse experimental cancer models. In addition, using various mouse models, it was noted that oral administration of phage was more effective than intraperitoneal administration of phage: 3% inhibition of metastases was noted with intraperitoneal administration of purified T-phage compared to 29% inhibition with oral administration; these values were 19 and 80%, respectively, for the purified HAP1 phage. Another anticancer effect of phages may depend on their ability to enhance the antitumor response initiated by vaccines based on dendritic cells (Łobocka et al., 2014; Soto, 2014).

## Influence of the phages to the virulence factors.

Van Wamel et al. (2006) used 5 classical laboratory and 85 clinical strains of S. aureus to study the distribution of temperate βC-ϕs phages (Bae et al., 2006). Their results showed that βC-ϕs were present in 88.9% of the staphylococcal strains analyzed. The presence of various virulence factors encoded by them is also

described. SAK (staphylokinase), CHIPS (chemotaxis inhibiting protein) and two superantigens SEA and SEP were found in 76.6, 56.6, 27.8 and 7.8% of the strains, respectively. The aforementioned modulators of the human innate immune system can be easily and efficiently transferred by β-hemolysin (βC-ϕs) converting phages between staphylococcal strains (Jamet et al., 2017). CHİPS (encoded by the chp gene) is a protein that has a stronger inhibition of calcium mobilization induced by complement protein C5a. Consequently, the activation of phages in response to formylated peptides and C5a, as well as the chemotaxis of human neutrophils, is inhibited. CHIPS as a virulence factor of S. aureus strains protects bacteria from the innate immune system (Soto, 2014; Thammavongsa et al., 2015). SAK (staphylococcal antigen) affects the innate immune system in various ways, for example by inhibiting opsonization (Żaczek et al., 2016). Staphylococcal superantigens have the ability to directly bind to MHC class II molecules, which can lead to the activation of monocytes and, consequently, their stimulation to increase the secretion of chemokines and other pro-inflammatory cytokines (Żaczek et al., 2016).

Panton-Valentine leukocidin is a factor that significantly increases the pathogenicity of MRSA strains. Depending on the concentration, PVL causes necrosis or apoptosis of human cells in vitro due to the formation of pores in cells or their organelles, such as mitochondria. About 30% of the isolated strains are PVL-positive, which is associated with the presence of prophage genes in their genome. Interestingly, it was shown that the distribution of individual phages carrying the PVL toxin gene depended on the geographic location from which the bacterial strain was obtained. PVL induces an anti-inflammatory response by binding to monocytes and macrophages, resulting in the release of caspase-1 dependent cytokines (IL-18 and IL-1β). The cytotoxic effect on neutrophils also causes the release of PAMP (pathogen-associated molecular patterns) and DAMP (damage-associated molecular patterns) particles from them and, consequently, an increase in the level of pro-IL-1β in monocytes and macrophages. However, there are also conflicting data on that PVL at the appropriate concentration may have a protective effect and increase the ability of the immune system to Figureht against staph infections. As can be seen, the genes carried by prophages significantly modulate the immune response.

**Conclusion**

• Phages are present in high concentrations in the intestinal tract, where they can interact not only with bacteria, but also with intestinal lymphoid tissue cells.

• Phages can interact with cells of the immune system through their proteins and cell receptors. Some of these receptors belong to the β-integrin family.

• Phage interactions with immune cells appear to have an immunomodulatory effect, suppressing elevated responses both in vitro and in vivo without causing immune deficiency.

## References

**Abeles SR, Pride DT. (2014).** Molecular bases and role of viruses in the human microbiome. J. Mol. Biol. 426 (23), 3892–3906. An article presenting what is currently known about the presence of viruses in the human microbiome.

**Alcami A, Ghazal P, Yewdell JW. (2002).** Viruses in control of the immune system. Workshop on molecular mechanisms of immune modulation: lessons from viruses. EMBO Rep. 3(10), 927–932.

**Bae T., Baba T., Hiramatsu K., Schneewind O. (2006).** Prophages of Staphylococcus aureus Newman and their contribution to virulence. Mol. Microbiol. 62:1035–1047.

**Barr JJ, Auro R, Furlan M. (2013).** Bacteriophage adhering to mucus provide a non-host-derived immunity. Proc. Natl Acad. Sci. USA, 110 (26): 10771–10776.

**Bloch H. (1940).** Experimental studies on the relationship between bacteriophages and malignant tumors. Archive for all virus research. 1(4): 481-496. Bondy-Denomy J., Davidson A.R. (2014). When a virus is not a parasite: The beneficial effects of prophages on bacterial fitness. J. Microbiol. 52:235–242.

**Borysowski J, Wierzbicki P, Kłosowska D, Korczak-Kowalska G, Weber-Dąbrowska B, Górski A. (2010).** The effects of T4 and A3/R phage preparations on whole-blood monocyte and neutrophil respiratory burst. Viral Immunol. 23(5): 541–544.

**Brodin P, Davis MM. (2017).** Human immune system variation. Nat. Rev. Immunol. 17(1), 21–29. Summary of current knowledge on how the bacterial microbiota affects the immune system.

**Brussow H., Hendrix R.W. (2002).** Phage genomics: Small is beautiful. Cell. 108:13–16.

Bruttin A, Brüssow H. (2005). Human volunteers receiving Escherichia coli phage T4 orally: a safety test of phage therapy. Antimicrob. Agents Chemother. 49(7): 2874–2878.

**Burcelin R. (2016).** Gut microbiota and immune crosstalk in metabolic disease. Mol. Metab. 5(9): 771–781.

**Burke J., Schneider D., Westpheling J. (2001).** Generalized transduction in Streptomyces coelicolor. Proc. Natl. Acad. Sci. USA. 98:6289–6294.

**Castro-Mejia J.L., Muhammed M.K., Kot W., Neve H., Franz C.M., Hansen L.H., Vogensen F.K., Nielsen D.S. (2015).** Optimizing protocols for extraction of bacteriophages prior to metagenomic analyses of phage communities in the human gut. Microbiome. 3:64.

**Dąbrowska K, Miernikiewicz P, Piotrowicz A et al. (2014).** Immunogenicity studies of proteins forming the T4 phage head surface. J. Virol. 88 (21): 12551–12557.

**Dąbrowska K, Opolski A, Wietrzyk J et al.** Activity of bacteriophages in murine tumor models depends on the route of phage administration. Oncol. Res. 15(4): 183–187.

Erez Z., Steinberger-Levy I., Shamir M., Doron S., Stokar-Avihail A., Peleg Y., Melamed S., Leavitt A., Savidor A., Albeck S., et al. (2017). Communication between viruses guides lysis-lysogeny decisions. Nature. 541:488–493.

Eriksson F, Tsagozis P, Lundberg K et al. (2009). Tumor-specific bacteriophages induce tumor destruction through activation of tumor-associated macrophages. J. Immunol. 182(5): 3105–3111.

Fortier L.C. (2017). The Contribution of Bacteriophages to the Biology and Virulence of Pathogenic Clostridia. Adv. Appl. Microbiol. 101:169–200.

Garrett WS. (2017). Gut microbiota in 2016: a banner year for gut microbiota research. Nat. Rev. Gastroenterol. Hepatol. 14(2): 78–80.

Górski A, Dąbrowska K, Hodyra-Stefaniak K, Borysowski J, Międzybrodzki R, Weber-Dąbrowska B. (2015). Phages targeting infected tissues: novel approach to phage therapy. Future Microbiol. 10(2): 199–204.

Górski A, Kniotek M, Perkowska-Ptasińska A et al. (2006). Bacteriophages and transplantation tolerance. Transplant. Proc. 38(1): 331–333.

Górski A, Międzybrodzki R, Borysowski J et al. (2012). Phage as a modulator of immune responses: practical implications for phage therapy. Adv. Virus Res. 83: 41–71.

Górski A, Międzybrodzki R, Weber-Dąbrowska B. (2016). Phage therapy: combating infections with potential for evolving from merely a treatment for complications to targeting diseases. Front. Microbiol. 7: 1515

Górski A, Ważna E, Weber-Dąbrowska B, Dąbrowska K, Świtała-Jeleń K, Międzybrodzki R. (2006). Bacteriophage translocation. FEMS Immunol. Med. Microbiol. 46(3): 313–319.

Górski A, Weber-Dąbrowska B. (2005). The potential role of endogenous bacteriophages in controlling invading pathogens. Cell. Mol. Life Sci. 62(5): 511–519.

Górski A., Dąbrowska K., Międzybrodzki R., Weber-Dąbrowska B., Łusiak-Szelachowska M., Jończyk-Matysiak E., Borysowski J. (2017). Phages and immunomodulation. Future Microbiol. 12: 905–914.

Howard-Varona C., Hargreaves K.R., Abedon S.T., Sullivan M.B. (2017). Lysogeny in nature: Mechanisms, impact and ecology of temperate phages. ISME J. 11:1511–1520.

Hargreaves K.R., Kropinski A.M., Clokie M.R. (2014). Bacteriophage behavioral ecology: How phages alter their bacterial host's habits. Bacteriophage. 4:e29866.

Jamet A., Touchon M., Ribeiro-Goncalves B., Carrico J.A., Charbit A., Nassif X., Ramirez M., Rocha E.P.C. (2017). A widespread family of polymorphic toxins encoded by temperate phages. BMC Biol. 15:75.

Jancheva M., Böttcher T. (2021). A Metabolite of Pseudomonas Triggers Prophage-Selective Lysogenic to Lytic Conversion in Staphylococcus aureus. J. Am. Chem. Soc.

Jain L, Rawat M, Ramakrishnan S, Kumar B. (2017). Active immunization with Brucella abortus S19 phage lysate elicits serum IgG that protects guinea pigs against virulent B. abortus and protects mice by passive immunization. Biologicals 45: 27–32.

**Jończyk-Matysiak E. (2015).** Ph.D. Thesis. Ludwik Hirszfeld Institute of Immunology and Experimental Therapy Polish Academy of Sciences; Wrocław, Poland: The Effect of Bacteriophage Preparations on Intracellular Killing of Bacteria by Phagocytes.

**Jończyk-Matysiak E., Łusiak-Szelachowska M., Kłak M., Bubak B., Międzybrodzki R., Weber-Dąbrowska B., Żaczek M., Fortuna W., Rogóż P., Letkiewicz S., et al. (2015).** The Effect of Bacteriophage Preparations on Intracellular Killing of Bacteria by Phagocytes. J. Immunol. Res. 2015:482863.

**Kazmi S.U., Kansal R., Aziz R.K., Hooshdaran M., Norrby-Teglund A., Low D.E., Halim A.-B., Kotb M. (2001**). Reciprocal, temporal expression of SpeA and SpeB by invasive M1T1 group a streptococcal isolates in vivo. Infect. Immun. 69:4988–4995.

**Kim KP, Cha JD, Jang EH et al. (2008).** PEGylation of bacteriophages increases blood circulation time and reduces T-helper type 1 immune response. Microb. Biotechnol. 1(3), 247–257.

**Lasserre J.F., Brecx M.C., Toma S. (2018).** Oral Microbes, Biofilms and Their Role in Periodontal and Peri-Implant Diseases. Materials. 11:1802.

**Łobocka M., Hejnowicz M.S., Gągała U., Weber-Dąbrowska B., Węgrzyn G., Dadlez M. (2014).** The first step to bacteriophage therapy—How to choose the correct phage. In: Borysowski J., Międzybrodzki R., Górski A., editors. Phage Therapy: Current Research and Applications. Caister Academic Press; Norfolk, UK: 23–69.

**Lugli G.A., Milani C., Turroni F., Tremblay D., Ferrario C., Mancabelli L., Duranti S., Ward D.V., Ossiprandi M.C., Moineau S., et al. (2016).** Prophages of the genus Bifidobacterium as modulating agents of the infant gut microbiota. Environ. Microbiol. 18:2196–2213.

**Łusiak-Szelachowska M, Żaczek M, Weber-Dąbrowska B et al. (2017).** Antiphage activity of sera during phage therapy in relations to its outcome. Future Microbiol. 12(2): 109–117.

**Mai-Prochnow A., Hui J.G., Kjelleberg S., Rakonjac J., McDougald D., Rice S.A. (2015).** Big things in small packages: The genetics of filamentous phage and effects on fitness of their host. FEMS Microbiol. Rev. 39:465–487.

**Majewska J, Beta W, Lecion D et al. (2015).** Oral application of T4 phage induces weak antibody production in the gut and in the blood. Viruses 7(8), 4783–4799.

**Mazaheri Nezhad Fard R., Barton M.D., Heuzenroeder M.W. (2011).** Bacteriophage-mediated transduction of antibiotic resistance in enterococci. Lett. Appl. Microbiol. 52:559–564.

**Miernikiewicz P, Kłopot A, Soluch R et al. (2016).** T4 phage tail adhesin gp12 counteracts LPS-induced inflammation in vivo. Front. Microbiol. 7, 1112.

**Pabary R, Singh C, Morales S et al. (2015).** Antipseudomonal bacteriophage reduces infective burden and inflammatory response in murine lung. Antimicrob. Agents Chemother. 60(2), 744–751.

**Park K, Cha KE, Myung H. (2014).** Observation of inflammatory responses in mice orally fed with bacteriophage T7. J. Appl. Microbiol. 117(3), 627–633.

**Ravin N.V. (2015).** Replication and Maintenance of Linear Phage-Plasmid N15. Microbiol. Spectr. 2:3:PLAS-0032.

**Relman D. (2015).** The human microbiome and the future practice of medicine. JAMA 314(11), 1127–1128.

**Sausset R., Petit M.A., Gaboriau-Routhiau V., De Paepe M. (2020).** New insights into intestinal phages. Mucosal. Immunol. 13:205–215.

**Soto S.M. (2014).** Importance of Biofilms in Urinary Tract Infections: New Therapeutic Approaches. Adv. Biol. 543974:13.

**Thammavongsa V, Kim HK, Missiakas D, Schneewind O. (2015).** Staphylococcal manipulation of host immune responses. Nat. Rev. Microbiol. 13(9), 529–543.

**Żaczek M, Łusiak-Szelachowska M, Jończyk-Matysiak E et al. (2016).** Antibody production in response to staphylococcal MS-1 phage cocktail in patients undergoing phage therapy. Front. Microbiol. 7, 1681.

# Prevalence of Rotavirus and Coronavirus Origin Diseases by Age Groups Among Calves in the North-West Region of Azerbaijan

## Vusal Abbasov

*Veterinary Scientific Research Institute, Baku, Azerbaijan*

**Abstract**

The purpose of the study was to identify the prevalence of diarrhea caused by rotavirus and coronavirus in newborn calves located in the North-West region of the republic using rapid testing. The study was conducted among 45 heads of calves of local races and crosses in 20 farms of the Ismailli, Gabala, and Zagatala districts. In 14 heads of calves out of 45 calves (35.5%), pathogens were not identified, and in 31 heads of calves pathogens were identified in single or mixed cases. The identified pathogens among them were distributed as follows: rotavirus in 22 calves (48.9%), coronavirus in 3 calves (6.7%), in 8 calves - (cryptosporodium parvum) 17.8%), in 5 calves calves - Giardia (11.1%) and another 5 calves had E. coli K99 (11.1%). The results of the study show that the causes of diarrhea in calves in the North-West region of the republic, among other pathogens, include rotavirus and coronavirus infections, and it is important that this be taken into account when carrying out treatment and preventive measures.

**Key words:** coronavirus, rotavirus, prevalence, express, diarrhea.

**Introduction**

Field and laboratory studies indicate that most cases of diarrhea in calves are caused by several factors, both infectious and non-infectious. Neonatal diarrhea occurs predominantly in the first 2-3 weeks after birth and is most common in calves 2-10 days of age (Bourhy, et al., 1999; Radostits, et al., 2006). Among viral diarrhea of calves, rotaviruses and coronaviruses are the most common (Hall et al., 1992). Field studies have confirmed that the most common causes of diarrhea are E. coli, rotavirus, coronavirus, cryptosporium and giardia (Svensson et al., 2003). The

incidence and location of each varies depending on the season and year, and in many cases rotaviruses and coronaviruses occur either separately or as part of mixed infections. The purpose of this study was to study the prevalence (the degree of incidence) of rotaviruses and coronaviruses in single or mixed form in the Ismailli-Zagatala-Gabala region using the rapid testing method.

**Methodology**

During the study, 1-2 samples of feces from calves with clinically observed signs of diarrhea were used, collected from calves located in the following farms - 5 farms in the village of Talistan, Ismayilli region, 5 farms in the villages of Nohur-Kishlyk and Vandan, Gabala region, 10 farms in the villages of Yeni Suvagil, Kurdamir, Aliabad and Mukha, Zagatala region. The experiment was carried out on 45 calves in 20 farms during the period July-October 2023. Of the 45 calves, 28 heads of calves are local breed calves, 11 heads of calves are a cross between Simmental and local breed calves, 3 heads of calves are a cross between Angus and local breed calves, 3 heads of calves are a cross between Swiss and local breed calves. Farms were selected on the basis of having 10-50 dairy cows. For clinical signs, factors such as animal manure moisture, its color, frequency of excretion and organoleptic characteristics of the animal manure contents were taken into account.



**Figure. 1.** Farms located in Talistan village, Ismayilli district

**Figure 2.** Zagatala region: location of farms in the villages of Yeni Suvagil, Kurdamir, Aliabad, Mukhakh.



**Figure 3.** Farms located in Gabala district, Nohur Kishlaq and Vandam villages.

To identify the pathogenic factor, the BoviD-5 Ag Test Kit (Bionote, Inc. Korea) was used - diagnostics were carried out for the presence of cryptosporosis, rotavirus, coronavirus, E. coli, and lamblia (Chen, et al., 2010; Altuğ**,** et al., 2013; Çabalar, et al., 1998). During inspections, sterile gloves, 70% alcohol, disposable uniforms and masks were used, farm owners were interviewed, and diarrhea incidence was discussed.

**Results**

As can be seen from Table 1, out of 45 calves examined using the express method, the pathogen was not detected in 14 calves (35.5%), and in single and mixed cases the pathogen was detected in 31 calves. Of these, 22 calves were diagnosed with rotavirus (48.9%), 3 calves had coronavirus (6.7%), 8 calves had (cryptosporodium parvum) 17.8%), 5 calves had lamblia (11. 1%) and 5 calves had E. coli K99 (11.1%). According to the results given in Table 2, the following forms of rotovirus were identified: 15 heads of calves had a single one, 1 head of calf had E. coli + rotovirus, 1 head of calf had rotovirus + coronavirus, 1 head of calf had rotovirus cryptosporosis, 2 heads of calves had - rotovirus + Giardia, 1 head of calf - rotovirus + cryptosporosis + coronavirus, 1 head of calf - cryptosporosis + rotovirus + Giardia. Coronaviruses were identified as follows: in 1 head of calf - coronavirus + E. coli, in 1 head of calf - rotovirus + coronavirus, in 1 head of calf - cryptosporosis + rotovirus + coronavirus. Rotoviruses were observed in 4 calves aged 3-10 days, in 12 calves aged 11-20 days and in 7 calves aged 21-28 days. There were 0 cases of coronavirus in calves 3-10 days of age, coronavirus was detected in 3 calves 11-20 days of age and 0 cases of coronavirus were observed in calves 21-28 days of age.

**Table 1. Detection rates of pathogens in animal manure samples and their percentage expression**

|   | Pathogen | Number of samples | Percentage expression % |
|---|----------|-------------------|--------------------------|
| 1 |          | 45                |                          |
| 2 | Unidentified | 14 | 31.1 |
| 3 | Identified single and mixed | 31 | 68.9 |
| 4 | Including |  |  |
| 5 | Rotavirus | 22 | 48.9 |
| 6 | Coronavirus | 3 | 6.7 |
| 7 | Cryptosporiasis | 8 | 17.8 |
| 8 | Giardia | 5 | 11.1 |
| 9 | Escherichia coli | 5 | 11.1 |

**Figure 4.** Schematic representation of diarrhea caused by various types of identified pathogens and unidentified or non-pathogenic factors.
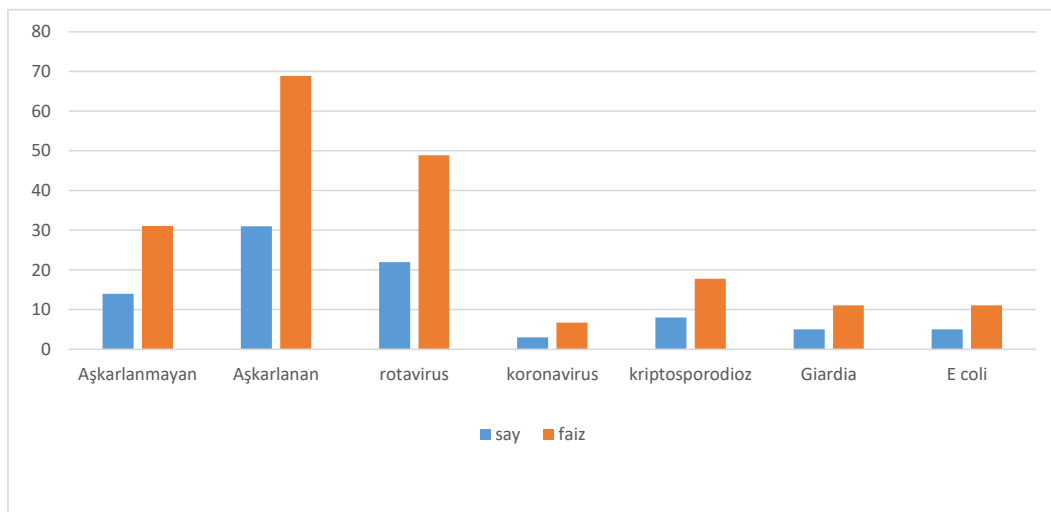


Diagram 1 shows that in 68.9% of cases of diarrhea, the main factors play the role of any identified pathogen, of which 48.9% are rotaviruses, and 6.7% are coronaviruses. 31.1% of diarrhea cases are considered either non-pathogenic or caused by pathogens not included in the rapid test.

**Table 2. Coefficients of mixed or single detection of pathogens and distribution by age groups**

| Pathogen | Quantity 45 | % | Calves aged 3-10 days | Calves aged 11-20 days | Calves aged 21-28 days |
|---|---|---|---|---|---|
| Negative | 14 | 31.11 | 5 | 6 | 3 |
| Positive | 31 | 68.9 | 6 | 15 | 10 |
| Rotavirus | 15 | 33.3 | 4 | 6 | 5 |
| Escherichia coli | 2 | 4.4 | 2 | | |
| Escherichia coli + Rotavirus | 1 | 2.2 | - | 1 | - |
| Escherichia coli Coronavirus | 1 | 2.2 | - | 1 | - |
| Cryptosporiasis | 4 | 8.9 | - | 2 | 2 |
| Giardia | 1 | 2.2 | - | - | 1 |
| Rotavirus + Coronavirus | 1 | 2.2 | - | 1 | - |
| Rotavirus + Cryptosporiasis | 1 | 2.2 | - | 1 | - |

| | | | | | |
|---|---|---|---|---|---|
| Rotavirus + Giardia | 2 | 4.4 | - | 1 | 1 |
| Cryptosporiasis Rotavirus+ Coronavirus | 1 | 2.2 | - | 1 | - |
| Cryptosporiasis, Rotavirus, Giardia | 1 | 2.2 | - | - | 1 |
| Cryptosporiasis, Escherichia coli + Giardia | 1 | 2.2 | - | 1 | - |

**Discussion**

Rotoviruses are among the most common viruses that cause acute diarrhea in calves less than one month of age, as well as in humans, indicating a high potential for zoonotic and economic impact (Al, et al., 2006; Alfieri, et al., 2012; Barrington., et al., 2002). Viral RNA viruses belong to the reoviridae family and have 7 serogroups. Group A is thought to cause disease in calves. Research shows that rotaviruses are the most common enteropathogens, accounting for 20-60% of diarrheal diseases in different countries (the prevalence of rotavirus in India ranges from 11.8% to 26.8%. Rotaviruses have been studied extensively in European countries and it has become clear that the prevalence was 24–47% in Switzerland in 1993–2006, 42% in the UK and 37–47.4% in France. Among Asian countries, the rate ranges from 0–7% in Bangladesh to 16.7% in Ethiopia (Conrad, et.al., 2011; Saif, 2007). Studies conducted among calves with diarrhea in Turkey indicate that the prevalence of rotavirus infection ranges from 0-53%, and the prevalence of coronavirus infection ranges from 13-18% (Cook, et.al., 2002; Malik, et al., 2006; De Verd, 1986; Bendali , 1999; Alkan, 1998; Abraham, 1992) .

Calf coronavirus is one of the main viruses causing enteritis in calves and wild animals (Clark, 1993; Burgu, et al., 1995). An RNA virus, it belongs to the Orthocoronavirinae subfamily of the Coronaviridae family and causes diarrhea and pneumonia in calves and winter dysentery in older cows (Saif, et al., 1990; Sezgin, 2012; Reynolds, et al., 1986). The frequency and timing of coronaviruses vary by country as follows. Until 2000, BC (bovine coronavirus) was reported as an intestinal symptom in the Americas, Europe and Asia. North and South America, Canada, the USA and Argentina have a high incidence rate, ranging from 2.41 to 84%. In the UK, Europe and Belgium, 14% and 8% were recorded in 1986 and 1999 respectively. From 2000 to 2009, incidence rates in Asia, namely Turkey and Korea, were 10.8–28.1% and 5.6–58.2% (Pesavento and Billingsley, 2003).

## Conclusion

The results of the study show that rotaviruses and coronaviruses among calves are among the main factors of calf diarrhea in the North-West region of the republic (Ismailly, Gabala, Zagatala), and both diseases can cause economic losses and losses to farmers, occurring in the form of a single or mixed infection. Timely diagnosis of the disease by checking animal manure samples taken from calves using express test kits allows for further treatment and preventive measures, which not only has a positive effect on the development of calves on farms, but also prevents the death of calves and increases the economic profitability of farmers (Çabalar, et al., 2001; Keha, et al., 2019). During the study, the prevalence of rotaviruses in the northwestern region of our republic is 48.9% (0-53%), and the prevalence of coronaviruses is 6.7% (13-18% in Turkey). Infectious diseases that occur together with rotaviruses and cause further exacerbation of the disease and deeper losses of calves should be studied separately and be the focus of attention.

## References

**Abraham G., Roeder P. L., Zewdu R.** (1992)."Agents associated with neonatal diarrhoea in Ethiopian dairy calves," Tropical Animal Health and Production. 24 (2): 74–80.

**Alam M. M., Huque A., Nigar S.** (1994). "Rotavirus infection in children and calves in association with acute gastroenteritis." Bangladesh Veterinary Journal. 28: 35–40.

**Alfieri A. A., Parazzi M.E.E.** (2006). "Frequency of group a rotavirus in diarrhoeic calves in Brazilian cattle herds, 1998–2002," Tropical Animal Health and Production. 38: 521, 2006.

**Alkan F.** (1998). Buzağı ishallerinde rotavirus ve coronavirusların rolü. Ankara Üniversitesi Veteriner Fakültesi Dergisi. 45, 29-37

**Al M. and Balıkçı E**. (2012). Neonatal İshalli Buzağılarda Rotavirus, Coronavirus, E. Coli K99 ve Cryptosporidium parvum'un Hızlı Test Kitleri ile Teşhisi ve Enteropatojen ile Maternal İmmünite İlişkisi. F.Ü. Sağ. Bil. Vet. Derg. 26 (2): 73-78.

**Altuğ N.** (2013). Neonatal Buzağı İshallerinin İmmunokromatografik Test Kitleri İle Hızlı Etiyolojik Teşhisi. YYÜ Veteriner Fakültesi Dergisi, 24 (3): 123-128.

**Arserim, N.B., Işık N., Özkan C., Kaya A.** (2013) Prevalence of Four Enteropathogens with mmunochromatographic Rapid Test in the Feces of Diarrheic Calves in East and Southeast of Turkey. Pak Vet J, 33(4): 496-499.

**Barrington G. M., Gay J. M., Evermann J. F.** (2002). "Biosecurity for neonatal gastrointestinal diseases," Veterinary Clinics of North America: Food Animal Practice 18 (1): 7–34.

**Bendali F., Bichet H., Schelcher F., Sanaa M.** (1999). Pattern of diarrhoea in newborn beef calves in South-West France," Veterinary Research. 30: 61–74.

**Bourhy H.**. (1999). Ecology and evolution of rabies virus in Europe. Journal of General Virology, 80: 2545–2557.

**Burgu I., Akça Y., Alkan F., Özkul A., Karaoğlu T.,** (1995). Yeni doğan ishalli buzağılarda rotavirusların elektron mikroskopi (EM), enzyme linked immunosorbent assay (ELISA) ve polyacrylamide gelelectrophoresis (PAGE) teknikleri ile çabuk teşhisi ve antijenik karakterizasyonu. Ankara Üniversitesi Veteriner Fakültesi Dergisi. 42. 491-498

**Clark M.A.** (1993). Bovine coronavirus / Br Vet J. 1993; 149: 51–70.

**Conrad M., Freuling, M., Beer F.** (2011). Novel Lyssavirus in Natterer's Bat, Germany, Emerging Infectious Diseases, 17(8):1519-22.

**Cook N.** (2002). Zoonotic potential of rotavirus / Journal of Infection. 48 (4): 289–302.

**Chen Q., Li J.** (2010). Comprehensive detection and identification of seven animal coronaviruses and human respiratory coronavirus 229E with a microarray hybridization assay/ Inter. Virology. 53, 95–104

**Çabalar M., Boynukara B., Gülhan T.** (2001). Prevalence of Rotavirus, Escherichia coli K99 and O157:H7 in healthy dairy cattle herds in Van, Turkey. Turkish Journal of Veterinary and Animal Science. 25: 191-196.

**Çabalar M., Voyvoda H., Sekin S.** (1998). İshalli buzağılarda rotavirusların latex aglutination (LA) ve polyacrylamide gel electrophoresis (PAGE) teknikleri ile tanısı, III. Ulusal Veteriner Mikrobiyoloji Kongresi, Bursa.

**De Verd Er.K.** (1986). Infektionspanoramat vid diarr´eer hos svenska kalvar/Vet. 58 (29).

**Hall G.A., Jones P.W., Morgan J.H.** (1992). Calf diarhoea, chapter 12. In Andrews AH, Blowey RW, Boyd H, Eddy RG (Ed): Bovine Medicine Diseases and Husbandry of Cattle, 1st ed. Blackwell Science Ltd. Oxford.

**Keha A., Xue L.** (2019). Prevalence of a novel bovine coronavirus strain with a recombinant hemagglutinin/esterase gene in dairy calves in China/Transbound Emerg. Dis., p.1971–1981

**Malik Y. S., Kumar N., Sharma K.** (2006). Epidemiology and genetic diversity of rotavirus strains associated with acute gastroenteritis in bovine, porcine, poultry and human population of Madhya Pradesh, Central India, 2004–2008/ Virus. p. 20139

**Radostits O.M**. (2006). Veterinary Medicine: A Textbook of the diseases of cattle, sheep, goats, pigs and horses. 10thed. Saunders Co, London.

**Reynolds D., Morgan J., Chanter N. et al.** (1986). Microbiology of calf diarrhoea in Southern Britain," Veterinary Record. 119 (2):, 34–39.

**Saif L.J.** (2007). Coronoviruses of domestic livestock and poultry: interspecies transmission, pathogenesis and immunity. In: Perlman S., Gallagher T., Snijder E., editors. vol. 18. ASM; Washington, DC. pp. 279–298.

**Saif L.J., Heckert R.A.** (1990). Enteric coronaviruses. In: Saif L.J., Theil K.W., editors. Viral diarrheas of man and animals. CRC Press; Boca Raton (FL):p. 185–252.

**Sezgin Ş.** (2012). Uludağ University, Faculty of Veterinary Medicine, Department of Internal Medicine. Internal Diseases of the Calves.

**Svensson C., Christensson B., Verdier K. D.** (2003). Cryptosporidium parvum and Giardia intestinalis in calf diarrhoea in Sweden/ Acta Veterinaria Scandinavica. 44 (3):145.

**Pesavento J. B., Billingsley A. M.** (2003). Structures of rotavirus reassortants demonstrate correlation of altered conformation of the VP4 spike and expression of unexpected VP4-associated phenotypes. Journal of Virology. 77 (5):3291–3296.

# The Spreadıng of Pyroplasmosıs in Pigs

## Mahir Nasibov

*Veterinary Scientific Research Institute, Department of Parasitology, Baku, Azerbaijan*
*mahirnasibov.64@gmail.com*

**Abstract**

The article concerns determining the dynamics of infection with pyroplasmosis of animals kept in pig-breeding farms located in the Khachmaz district. As a result of the conducted surveys, the epizootological situation was studied based on positive results obtained during surveys to detect the spreading of parasitic blood diseases in the territory of the Khachmaz district. In the course of the conducted studies, the causative agent of piroplasmosis *P.trautmani* was studied for their pear-shaped, amoeboid, round, oval shape. Thus, the sizes of pear - shaped parasites are 2.4-2.9x1.3-1.7 microns in peripheral blood and 0.9-1.6x0.8-1.2 microns in internal organs; amoeboid parasites were not found in peripheral blood, and 1.3-1.7x1.1-1.3 microns in internal organs; the sizes of parasites round shape in peripheral blood 0.8-1.2x2.3-2.7 microns, in internal organs - 0.6-0.7x1.7-1.9 microns; as a result of microscopy, it was found that the sizes of oval-shaped parasites range from 1.1-2.8x0.6-1.9 microns in peripheral blood and 0.8-2.3x1.0-1.3 microns in internal organs. In the internal organs of animals infected with piroplasmosis, the parasites were oval, round, single pear-shaped and amoeboid. Reproduction of pyroplasmas occurs in the internal organs of pigs (liver, lungs, heart).

**Key words:** pig, causative agent of piroplasmosis, blood smear, peripheral blood, internal organs

**Introduction**

Almost all pig-breeding farms operating in Azerbaijan are individual farms. Pork is used in the production of meat products, and a small part of it is consumed by the population as meat.

Pigs also develop blood parasitic diseases, including pyroplasmosis. In pigs, pyroplasmas first multiply in the internal organs, and then affect red blood cells in

the peripheral blood. They multiply by simple division in red blood cells. Also, the reproduction of pyroplasmas occurs in the body of ticks. Transmission of pyroplasmas by ticks occurs transovarially. The source of invasion is sick animals and carriers of pyroplasm, as well as ixod mites. The vector of the parasite is the tick *Rhipicephalus turanicus.* Pathogens are transmitted from a sick animal to a healthy one through ixodic (pasture) ticks. Pathogens of pyroplasmosis, localized in the internal organs of a sick animal, destroy, or demolish the tissues of these organs (Yengashev et al., 2022; Karimov and Timofeyev, 1986; Mamukayev, 2012).

Scientists of Azerbaijan and foreign countries have conducted several studies on the spreading of pyroplasmosis among farm animals, including pigs, on the study of ticks carrying them, on the treatment of hematopoietic parasitic diseases, etc. (Mehraliyeva, 2016; Seyidov, 2017; Abdulmagomedov et al., 2022; Belimenko, 2018; Safiullin et al., 2015; Sidorkin, 2002; Shevkoplyas and Lopatin, 2008).

Pig pyroplasmosis has also been registered in Azerbaijan. The causative agent of the disease is *P. trautmanni.* In the treatment of piroplasmosis, with flavacridine and piroplasmin give a positive result. As a preventive measure, it is necessary to bathe animals with solutions of acaricides (Mehraliyeva, 2019; Mirzabekov, 1977; Mirzabekov et al., 1949). In this research the main goal was set to study the spreading of pyroplasmosis in pigs in Azerbaijan.

**Materials and methods**

The research work was carried out in 2023 on the basis of pathological material collected from the pig-breeding farm of the Khachmaz district in the Guba-Khachmaz economic district. Conducting clinical studies among animals (pigs), smears were prepared from peripheral blood drops taken from sick animals, as well as from animals with suspicion for disease. In order to make smears, the animal's auricle was first cleaned of wool, then the ear drops were pierced with a razor and the first drop of blood was applied to the slide with a thin layer using a polishing glass. After drying, the smears were fixed in methyl alcohol under laboratory conditions and stained by the Romanovsky-Gimza method (3 drops of Romanovsky-Gimza dye were added to 1 ml of distilled water) (15). *The types of pathogens detected by smear microscopy were determined by the method of Kapustin (1949).*

Thus, in order to study the dynamics of infection with pyroplasmosis, blood smears of pigs of various ages kept in pig-breeding farms were prepared and examined in the laboratory of the Department of Parasitology of the Veterinary Scientific Research Institute.

 The study of the dynamics of infection with pyroplasmosis of the internal organs of an animal (pig) (liver, lungs, heart) was carried out by the following methods:

Smears were prepared from the internal organs of deceased or forcibly slaughtered pigs. Fixation and staining of smears from internal organs by pressing takes longer than blood smears, since the smears made by this method are thick. The smears were fixed with methyl alcohol for 10 minutes, with a mixture of ethyl ether for 15 minutes, staining took 10-15 minutes longer than a peripheral blood smear. It was painted by the Romanovsky-Gimza method for 60-70 minutes (*Yakubovsky, 2001*).

In order to determine the size and photograph blood parasites during examinations a BEL Solaris microscope, an HD- CAM camera and ImageScope software were used.

**Results and discussions**

Microscopy of blood smears obtained from pig-breeding farms located in the Khachmaz district was carried out in the Guba-Khachmaz economic district, and the dynamics of infection of animals with pyroplasmosis was determined.

As a result of the conducted surveys, the epizootological situation was studied based on positive results obtained during surveys to detect the spreading of parasitic blood diseases in the territory of the Khachmaz district. For this purpose, microscopic examination of blood smears taken from sick and clinically healthy animals was carried out, epizootological features of pyroplasmosis in Khachmaz district were studied.
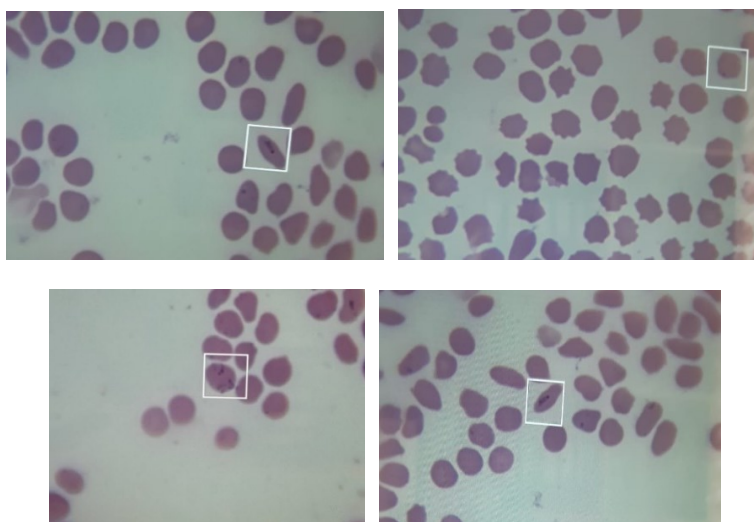
**Figure 1.** Pyroplasmas in the peripheral blood of pigs

The number of parasites in the peripheral blood of animals was 15-25 spc. (in 100 fields of the microscope). And, the number of pyroplasmas in erythrocytes was 1-2 specimens. It has been observed that parasites are mostly 1-nuclear, and in some cases 2-nuclear. The nuclei were clearly visible during microscopy, where they were localized mainly on the blunt side of the parasite edge (Figure 1).

Reproduction of pyroplasmas occurs in the internal organs of pigs (liver, lungs, heart) (Figure 2).
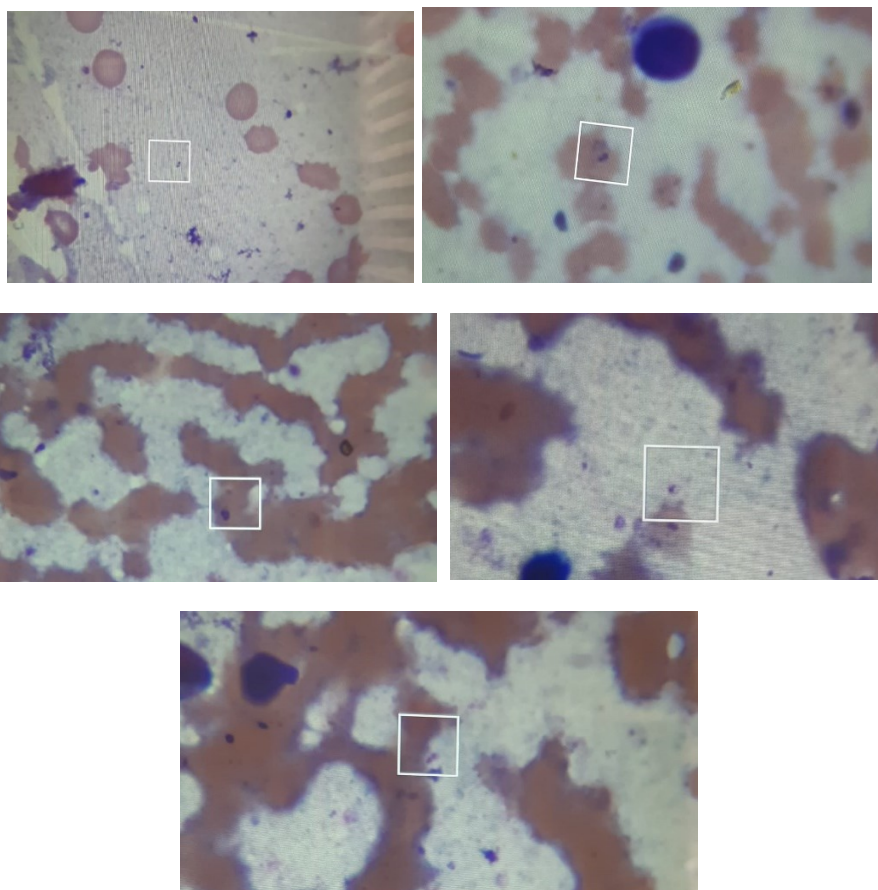


**Figure 2.** Pyroplasmas in the internal organs of pigs

Morphological differences of parasites (their shapes, sizes) both in the blood and in the internal organs of the studied animals were detected using a microscope. Parasites of pear-shaped, amoeboid, round, oval shape have been studied. The size

of parasites in the peripheral blood of pigs is larger than the size of parasites in their internal organs. Thus, the sizes of pear - shaped parasites are 2.4-2.9x1.3-1.7 microns in peripheral blood and 0.9-1.6x0.8-1.2 microns in internal organs; amoeboid parasites were not found in peripheral blood, and 1.3-1.7x1.1-1.3 microns in internal organs; the sizes of parasites round shape in peripheral blood 0.8-1.2x2.3-2.7 microns, in internal organs 0.6-0.7x1.7-1.9 microns; as a result of microscopy, it was found that the sizes of oval-shaped parasites range from 1.1-2.8x0.6-1.9 microns in peripheral blood and 0.8-2.3x1.0-1.3 microns in internal organs (Table 1).

**Table 1. Morphological differences of *P.trautmanni* in peripheral blood and internal organs of pigs**

| Forms of development of causative agent | The size of parasites in the peripheral blood of pigs (microns) | The size of the parasite (microns) in the internal organs of pigs |
|---|---|---|
| Pear-shaped | 2.4-2.9x1.3-1.7 | 0.9-1.6x0.8-1.2 |
| Amoeboid | -------- | 1.3-1.7x1.1-1.3 |
| Round shape | 0.8-1.2x2.3-2.7 | 0.6-0.7x1.7-1.9 |
| Oval-shaped | 1.1-2.8x0.6-1.9 | 0.8-2.3x1.0-1.3 |

It should be noted that in blood smears it was found that the nuclei of pyroplasmas are small and cover the volume of parasites with protoplasm. And in the internal organs, the presence of large-sized pyroplasm nuclei has been studied. Thus, in pyroplasmas, the nucleus is the main volume of the parasite, and the protoplasm is the smaller part.

In the internal organs of animals infected with piroplasmosis, the parasites were oval, round, single pear-shaped and amoeboid.

During studies conducted by our and foreign researchers on pig-breeding farms, it became clear that among pigs, as in other animals, parasitic blood diseases occur. When pigs are infected in pig-breeding farms, the productivity and quality of meat in animals decreases. From this point of view, the unhealthy state of the pig-breeding farm due to blood parasitic (pyroplasmosis) diseases leads to a decrease in meat production, which negatively affects the profitability of the farm.

In pigs, one of the important conditions is also a preventive method of combating pyroplasmosis - breaking the biological "chain" (tick-carrier, a parasitic animal, an animal susceptible to diseases). Without one of these factors, the likelihood of the

disease is also unlikely. The Figureht against ticks should be carried out with acaricidal drugs so that parasitic blood diseases do not occur.

## Conclusion

In the course of the conducted research, *P.trautmanni* was studied for its pear-shaped, amoeboid, round shape, oval-shaped forms. Thus, the sizes of pear-shaped parasites are 2.4-2.9x1.3-1.7 microns in peripheral blood and 0.9-1.6x0.8-1.2 microns in internal organs; amoeboid parasites were not found in peripheral blood, and 1,3-1.7x1.1-1,3 microns in internal organs; the sizes of parasites round shape in peripheral blood 0.8-1.2x2.3-2.7 microns, in internal organs-0.6-0.7x1.7-1.9 microns; it was found that the sizes of oval-shaped parasites range from 1.1-2.8x0.6-1.9 microns in peripheral blood and 0.8-2.3x1.0-1.3 microns in internal organs.

## References

**Abdulmagomedov, S.Sh., Bariyeva, R.M., Aliyev, A.Y., Kozikov, I.N.** (2022). Preventive efficacy of forticarb in case of pyroplasmidosis of cattle. Agrarian Science. 3: 14-16.

**Belimenko, V.V.** (2018). Animal and human diseases transmitted by ixodic ticks in the Russian Federation and the Figureht against them in modern conditions. Belimenko, V.V., Samoylovskaya N.A., Isayev Y.G. Proceedings of the All-Russian Research Institute of Experimental Veterinary named after Y.R. Kovalenko. Moscow, 1 (80): 79-87.

**Mamukayev, M.N.** (2012). Dynamics of ixodification and their role in the ecological and epizootic situation in the Sothern Regions of Russia. M.N. Mamukayev, V.K. Lolayev, D.V. Dzagoyeva, N.D. Jabiyeva. News of the Gorsky State Agrarian University. 49 (3): 191-204.

**Mirzabekov, K.D.** (1977). Invasiveness and forms of development of three species of babesia and piroplasmida in eggs of ixodic mites. Journal of "Parasitology", Leningrad. 7: 230-234.

**Mehraliyeva, U.M.** (2016). Interpretation of Pyroplasma bigeminum and Francaiella colchica in internal organs after the death of cattle. Journal of Agrarian Science. 107 – 109.

**Mirzabekov D.A., Kurchatov V.M., Abusalimov N.S., Muraki A.T.** (1949). Some data on the bioecology of ticks in the Republic of Azerbaijan. Proceedings of the Azerbaijan Scientific Research Experimental Station. Baku, 3:123-132.

**Mehraliyeva, U.M.** (2019). Blood parasitic diseases of cattle in the subtropical zone of the Republic and the spreading of ticks carrying them. Application of innovations in the direction of development of veterinary science. Materials of the International Scientific and Practical Conference. Baku:"Teacher". 244-248.

**Kapustin V.F.** (1949). Atlas of blood parasites of farm animals. Moscow, 1949.

**Karimov, B.A., Timofeyev V.A.** (1986). Efficacy of azidine and diminazine with

polyglucine in pyroplasmidosis. Veterinary Medicine. 9: 46-47.

**Safiullin, R.T., Semenychev A.V., Sarsadskikh A.A., Aliyev M.A. (2015).** Diprocarb – a reliable means of combating animal blood parasites. Journal of Veterinary. 4: 35-38.

**Seyidov, M.A.** (2017). The distribution of Ixodidae ticks across geographical zones in the Nakhchivan Autonomous Republic and the seasonal dependence of the duration of their parasitization. News of the Nakhchivan branch of ANAS. Series of Natural and Technical Sciences. 13 (2): 233- 237.

**Shevkoplyas V.N., Lopatin V.G.** (2008). Monitoring studies of ixodic ticks in the Krasnodar Territory. Journal of Veterinary Medicine. 1: 27.

**Sidorkin, V.A.** (2002). Treatment of pyroplasmidoses with diminazine+phenazone of cattle with neosidine. Veterinary Medicine. 2: 21-23.

**Yengashev, S.V., Yengasheva E.S., Kolesnikov V.I., Koshkina N.A., Filimonov D.N. (2022)**. Efficacy of the Delcid 7.5 drug against ixodic mites and diptera insects. Journal of Veterinary. 4: 41-45.

**Yakubovsky, M.V. (2001).** Diagnostics, therapy and prevention of parasitic diseases of animals, M.V. Yakubovsky, N.F.Karasev, Minsk: Khata. 375 p.

# Initial Dynamics of Carbohydrate Components in the Blood During Intensive Physical Loads

## Naila Bayramova

*Baku State University, Baku, Azerbaijan*
*naile.allahverdiyeva16@gmail.com*

**Abstract**

Blood glucose and lactic acid (lactate) levels were determined in 3-month-old rabbits at the intervals during the day after 1 hour of immobilization and 10 minutes of forced running on the treadmill. The research showed that blood glucose in intact rabbits fluctuates in the norm with a weak rhythm throughout the day. Immobilization has little effect on this dynamics, while running load leads to a significant decrease in the amount of blood glucose in the first hours, during which the amount of lactate in the blood increases significantly. These indicators quickly normalize such dynamics of important carbohydrate components of the blood are of adaptive importance for the immature animal body.

**Key words:** immobilization, forced running, blood, glucose, lactate, daily dynamics

**Introduction**

Blood as a multicomponent and multifunctional internal environmental fluid, plays an exceptional role in the human and animal organism, actively participates in a number of its adaptive reactions (Alimov, 2016, Morman, 2000). Among the multifunctional chemical components of blood, one of the substances of special physiological importance is considered to be glucose (sugar) of carbohydrate origin. In stressful situations, during the effects of physical loads and other extreme factors (lack of exogenous $O_2$, low temperature, etc.), blood glucose is an extremely important energy substrate for tissues, especially the brain, heart, and working skeletal muscles, as an "emergency fuel" (Aghayeva, 2015; Aliyev, 2017; Drozdov, 2015; Lehninger, 1985; Powers and Vaskson 2008).

The lactic acid (lactate), one of the many metabolites accumulated in the blood, is of particular interest in biochemical, physiological and clinical terms due to a number of properties. This metabolite is one of the end products of semi-disintegration reactions (glycolysis) of glucose in tissues, it is highly formed in the brain, muscle,

has a toxic effect, enters the blood from cells through a special mechanism, causes fatigue in the body, is partially metabolized in the liver, can be reabsorbed by tissues as a residual energetic material (Avital, 2008).

For experimental physiology, labour and sports physiology, medical physiology, the question of the effect of physical loads on the blood system, the amount of glucose and lactate, which are its main indicators, remains relevant. The purpose of our research is to study the initial changes in the side homeostatic levels of those substances in immature experimental animals subjected to vigorous physical exertion. There is very little experimental evidence in the literature on this issue. In our previous research, some experimental facts on this issue have been presented (Bayramova, 2022; Hajiyev and Bayramova, 2021).

**Material and methods**

The objects of the research are 3-month-old Chinchilla breed rabbits. They were fed in vivarium conditions with standard feed rations, divided into control and experimental groups. In one experiment, the animals in the group were held for 1 hour in a tightly closed position, one by one lying on their backs on a specially prepared plastic board. This was a physical load of a rigid immobilization nature applied to the animal. Another experiment involved the group placing animals one by one on the treadmill. The animal was made to run hard from its place by rotating it for 10 minutes at a speed of 40-45 revolution/minute. This was a physical load of forced running applied to the animal.

From every 3–month-old rabbit subjected to control and physical load, 0.5 to 1.0 ml of blood was taken for analysis. The blood was drawn off the ear vein of the animal. This is the method that causes the most minimal injury to the animal, complies with bioethical requirements.

In control animals, blood sampling was performed during the day in the morning, afternoon, and evening, in experimental animals 1, 3 and 6 hours after physical load.

Glucose (sugar) and lactic acid (lactate) were prescribed as carbohydrate components in the blood. The amount of glucose in the blood was studied on a portable glucometer (FIA Biomed Blood Glucose Meter, Germany), the amount of lactate in the blood was studied by colorimetric method (Filippov, 1984).

The numerical materials of the research were statistically processed (Lakin, 1980). The reliability of the results of the experiments according to the control indicators was determined according to the Student's t-tests, expressed at $p < 0.05$ and $p < 0.01$ levels.

**Results and discussion**

Table 1 shows the dynamics of blood glucose during the day in intact 3-month-old rabbits. It is clear from these materials that blood sugar homeostasis is a highly variable physiological parameter.

**Table 1. Daily dynamics of blood glucose in normal intact 3-month-old rabbits (M±m, n=5, glucose in mg/dL)**

| Objects of research | Glucose determination periods (hours) | | |
|---|---|---|---|
| | 10-11 | 13-14 | 16-17 |
| 3-month-old rabbits ( control) | $84,0 \pm 2,3$ | $91,6 \pm 3,3$ | $82,4 \pm 2,4$ |
| Average value 86,0±2,6 | | | |

As can be seen from the table, blood glucose in normal immature rabbits has a somewhat rhythmic dynamics, its maximum is observed at noon.

As an experimental method and physical load, immobilization has long been used in experimental physiology. It should also be noted that for some laboratory animals, it is not physiologically appropriate to stay tied on the back for a long time, it is accompanied by a considerable amount of nerve and muscle tension in the body, the urgent secretion of some hormonal agents, a number of metabolic changes, may play as stressor and emotiongenic factors (Elisa et al., 2008). Our experiment shows that this physical load also affects the level of glucose in the blood (Table 2). However, it was found that this effect is weak, noticeable in the first hour after immobilization.

**Table 2. Changes in blood glucose homeostasis in 3-month-old rabbits after immobilization and forced running loads (M± m, glucose, mg/dL)**

| Types of physical loads | Glucose determination periods (hours) | | |
|---|---|---|---|
| | The 1st hour | The 3rd hour | The 6th hour |
| Immobilization, number of animals, n= 5 | $79,2 \pm 2,3$ | $82,4 \pm 2,0$ | $80,3 \pm 1,8$ |
| Forced running, number of animals, n= 5 | $73,5 \pm 3,7*$ | $77,8 \pm 3,4*$ | $81,6 \pm 3,2*$ |

Note: * - Compared with the average control indicator (Table 1), the statistical reliability of the experimental indicator is $p<0,05$.

Intensive 10-minute running load on treadmill leads to a faster decrease in blood glucose in 3-months-rabbits at in the first time (in the 1st and 3rd hours). When we pay attention to the Figures of this experiment in Table 2 and compare them with the indicators we received in intact animals (Table 1), the rhythm underlying the daytime dynamics of blood glucose in normal 3-month-old rabbits weakens under the influence of intense physical load. It can be assumed that this effect may be due to the large expenditure of energy, dermal glucose, spent on muscle activity in young animals during forced jogging in treadmill.

Figure 1 shows the initial dynamics of lactate in the blood of 3-month-old rabbits that performed fast running movements on a treadmill.

The results of the research showed that after short-term intensive running on a treadmill, indoors and in a narrow area, the level of lactate in the blood increases in a statistically reliable manner compared to the control indicator, and only after a long period of time, it decreases to the normal level. This can be clearly seen from the results we obtained. In intact 3-month-old rabbits, the amount of lactate in the blood is $4.6 \pm 0.48$ mg%. It was $6.9 \pm 0.43$ mg % in the first hour after the experiment, and $4.4 \pm 0.30$ mg% in the 6th hour.
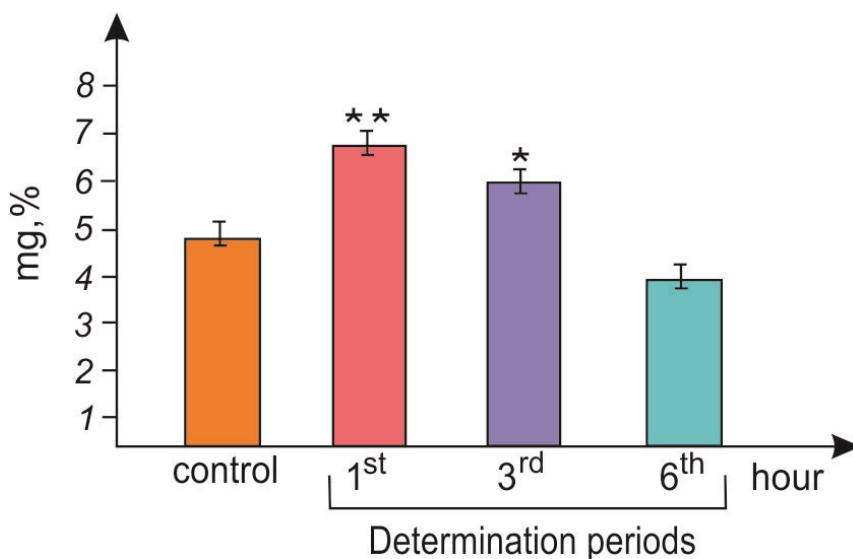


**Figure.1.** Early dynamics of lactate in the blood of 3-month-old rabbits that performed 10 minutes of forced runnimg on a treadmill. ** - $p<0.01$, * - $p<0.05$

We will see a correlative relationship if we compare the dynamics of glucose and the dynamics of lactate in the blood of 3-month-old rabbits during a forced jogging in treadbahn. Therefore, if in the first case blood glucose decreases significantly in the first period, then in the second, on the contrary, it increases. The fact is that the muscles of the skull, which work intensively during running, spend a lot of glucose, at which time glycolysis in the muscles intensifies, as a result, the amount of lactate that passes into the blood increases. In this case, adaptation in the dynamics of lactate is associated with its decrease to the norm (Shakhnova, 2000).

## Conclusion

This complex experimental study allows us to come to the following conclusions:

1. One-hour immobilization load has little effect on glucose homeostasis in the blood in 3-month-old rabbits in the first period;

2. Ten minutes of intensive running leads to an initially sharp decrease in blood glucose, an increase in lactate. There is a reverse correlation between these two dynamics.

## References

**Aghayeva S.E., Aliyev S. A. Alibayova S.S.** (2015). Biochemical indicators of blood are the criterion of adaptive processes of the athlete's body. Compendium of scientific works of the Institute of Physiology named after A.I.Garayev of ANAS. 33: 23-28

**Aliyev S.A.** (2017). Cross effects of students' adaptation to physical loads. Compendium of scientific works of the Institute of Physiology named after A.I. Garayev of ANAS. 35: 32-34.

**Alimov N.K..** (2016). Fundamentals of Medical Physiology, I., "Practice", 2016, 496.

**Avital S. Lactate.** (2008). A major and critical player in normal function of both muscle and brain. The journal of Physiology. 586 (11): 2665-2667.

**Bayramova H.U.** (2022). Primary quantitative changes in blood haemoglobin during hypoxia and physical activity in early postnatal optogenesis. Scientific and practical journal. Publication of the National Academy of Sciences of Azerbaijan. 8 (1): 40-45.

**Drozdov D.N., Kravtsov A.V.** (2015). The effect of physical activity on human blood counts. Bulletin of the Mozir State Pedagogical University I.P. Shamyakin. 4: 23-25.

**Elisa I.C., Stuart M.P, Bryan R.O. et. al.** (2008). Immobilization induces anabolic resistance in myofibrillar protein synthesis with low and high amino aced infusion. The journal of Physiology. 586 (24): 6049-6063.

**Filippov A.S. et al.** (1984). Practicum on biochemistry M., Education. 350.

**Hajiyev A.M., Bayramova B.I.** (2021). Early shifts in blood homeostasis in immature rabbits under hypoxic and physical stress. International Journal of Applied and Basic Research. NRC "Academy of Natural Sciences", Saratov. 5: 5-8.

**Lakin Q.F.** (1980). Biometrium. M., edition., "High School". 352.

**Lehninger A.** (1985). Fundamentals of biochemistry, M., "World". 2: 392.

**Morman D. Kheller L.** (2000). Physiology of the cardiovascular system. SPb , Peter. 230.

**Powers S.K., Vaskson M.I.** (2008). Exercise-induced oxidative stress. Cellular mechanisms and impart muscle force production. Physiology Rev.88: 1243-1250.

**Shakhnova A.V.** (2000). Influence of differentiated motor modes on ontogenetic development and mechanisms of adaptation. Materials intl. Conf. "Physical culture and sports at the turn of the 3rd millennium" St. Petersburg. 113-116.

# Face Recognition in Smart Cameras by Yolo8

## Farid Pashayev, Leyla Babayeva, Zuleykha Isgandarova, BehnamKiani Kalejahi

*Department of Computer Science, School of Science and Engineering, Khazar University, Baku, Azerbaijan*

## Abstract

Smart AI Cameras have become a vital tool for enhancing security in several industries, such as industrial, transportation, and retail. This study investigates the methods that might be used to recognize moving objects in both daytime and nighttime settings. In this paper, convolutional neural networks, and recurrent neural networks—two deep learning techniques for object recognition—are investigated. We look at datasets containing a range of objects, lighting conFigureurations, and camera angles to determine how well these algorithms perform. In our research, we compared results from two separate datasets using YOLOv8. After all, we compared our methods and results with other scientists' research. We discussed the importance of camera placement, lighting issues, and algorithm choice for effective object detection. We evaluate the cameras' ability to recognize and follow moving things, as well as how well they can communicate with other security systems like alarms and access control. Our research demonstrates that smart AI cameras may significantly improve security in a variety of situations and that choosing the right algorithm and placing the camera is crucial for maximizing their effectiveness. For enterprises considering the usage of smart AI cameras for security, our research offers helpful information.

*Keywords:* *Smart cameras, YOLO, YOLOv8, object recognition, person recognition,* AI, IoT

## Introduction

The explosion of artificial intelligence (AI) has had an impact on every part of community life, and deep learning (DL) and AI have made significant strides. Artificial intelligence (AI) encompasses a wide range of disciplines, including speech recognition, object identification, general algorithms, and brain modeling. As the need for safety and security has increased, more research has been done on intelligent surveillance. Intelligent surveillance can be used for a variety of purposes,

including moving object recognition, object tracking, motion segmentation, object classification and identification, event detection, and behavior interpretation and description. Current study focuses on the processing and interpretation of camera-captured video sequences. Any moving items in a scene must first be detected by several apps in this field. To find out what is happening around monitored items, for instance, video event detection must first identify and track the tracked objects. In order to implement intelligent surveillance, monitoring and object detection are crucial components. Video object segmentation, which separates the moving element from each frame of a video clip, can be used to identify moving things. For segmenting video objects, a variety of techniques have been suggested. The two subcategories of these methods are foreground extraction-based and background construction-based video object segmentation. In background construction-based video object segmentation, the background information is first obtained, and then a video object is created by deleting the backdrop from the current frame in following frames. Foreground extraction-based video object segmentation first obtains an initial video object using temporal, spatial, or temporal-spatial information. The subsequent frames' motion, change, or other feature information is used to pinpoint the video object. Fast-moving objects can be tracked using background construction-based video object segmentation. It also costs little to implement and has simple computing requirements. For background construction-based video object segmentation, background modeling is required. In many applications (like video surveillance), it is primarily utilized in background subtraction foreground identification to model the background and identify the moving objects in an image. To show a background, the simplest method is to get a still photograph with no moving parts. The camera must be fixed, the illumination must be steady, and the background must not move in order to achieve decent results while utilizing background subtraction. The background can alter in specific circumstances, such as when the lighting changes. As a result, the backdrop representation model needs to be reliable and flexible. Background modeling has been used to detect moving objects in difficult circumstances.

Techniques for steadily updating models in the presence of dynamic backgrounds and variable lighting. Background subtraction approaches, both traditional and contemporary, have been studied. Our project intends to build a device that can recognize people in a picture or video. To address this issue, we went with the YOLOv8 approach.

 Segmentation, object detection, and image categorization are among the applications for the newest and most complex YOLO model, YOLOv8. YOLOv8 was introduced by Ultralytics, the company that also created the well-known YOLOv5 concept. YOLOv8 offers a number of architectural changes and

improvements over YOLOv5. In computer vision, the YOLO (You Only Look Once) model set has gained popularity. YOLO has grown highly popular due to its high level of realism and compact model size. A wide spectrum of developers can use YOLO models because they can be trained on a single GPU. On edge hardware or in the cloud, machine learning professionals can deploy it affordably. The YOLO concept has received significant backing from the computer vision community ever since Joseph Redmond initially proposed it in 2015. Versions 1-4 of YOLO were first kept up to date in C code inside of Redmond's own Darknet deep learning platform (Kiani et al., 2022). YOLOv8 is mostly used for the following reasons:

- The results of the Roboflow 100 and COCO tests indicate that YOLOv8 has a respectable accuracy rate.

 - YOLOv8 comes with a variety of features that are beneficial to developers, including an approachable CLI and a well-thought-out Python package.

 - Because there is a sizable community surrounding YOLO and one that is growing around the YOLOv8 model, you can get help from numerous computer vision experts when you need it.

YOLOv8 obtains great accuracy on COCO. For instance, the medium YOLOv8m model yields a 50.2% mAP when assessed on COCO. Additionally, YOLOv8 outperformed YOLOv5 much better than Roboflow 100, a dataset that accurately measures model performance across a variety of task-specific domains.

 YOLOv8's developer-friendly features are also crucial. For instance, YOLOv8 offers a CLI that simplifies model training compared to other models that require many executable Python files. Additionally, compared to earlier models, developing with a Python package is more comfortable. Two datasets were employed, one of which includes 13660 photos of people and another has 11324 pictures of both humans and other things (Yazdi & Bouwmans, 2018). However, both of these datasets were trained on photos of people. We obtained 75% accuracy after training the first dataset and 96% accuracy after training the second dataset. We will look at the issue at hand as well as the solutions put forth by both us and other researchers that have looked into this issue.


1.      Related Works

An earlier article by Mehran et al. (2022) presents a summary of the most recent methods for moving object recognition in video sequences. The authors divide these methods into three groups: modeling-based background subtraction, low-rank and

sparse matrix decomposition, and object tracking. In addition to performance measurements and multiple benchmark datasets available to evaluate the performance of different moving object identification systems, they look at difficulties and important concerns in this sector (Riechmann, et al., 2022). Additionally, we cited a work by Sivachandiran et al. (2021), who developed a novel DL-driven automated person detection and tracking (DLD-APDT) model for surveillance videos to identify and track persons in the movies. Their model's input video is initially turned into a collection of frames using a frame conversion technique. Furthermore, they employ EfficientDet, a model for object detection based on BiFPN. Again, their training is based on the PascalVOC and PenFudan datasets. Finally, to choose the hyperparameters as accurately as feasible, they employ the RMSProp optimizer (Imerit.net. 2021). In their study, three cutting-edge OD systems-YOLOv3 (SPP), YOLOv4 and PANet (SPP), and CSPResNeXt50— were examined, used, and assessed., Lukas Malburg et al. (2021) propose a general framework for multi-modal monitoring of industrial processes as a first step toward video-based monitoring and tracking. Their experimental assessment shows that, in an industrial research scenario, detection accuracies for customized objects and failure locations of these objects may be increased to beyond 90%. The authors intend to use the Internet of Things to deploy OD systems along with other sensors to track the production process (Malburg et al., 2021) Wu-Chih Hu et al. (2023) show yet another practical technique for recognizing and tracking several moving objects in a video sequence captured by a moving camera without the use of additional sensors. Their method is incredibly effective; it can be applied in real-time applications, for monitoring overlapped objects and objects with different scales, as well as for identifying objects that are moving swiftly or that are being filmed by a camera that is moving quickly (Wu-Chih Hu et al. 2023) Amin Al-Habaibeh et al. (2023) consider the use of low and high-resolution infrared sensors as a component of the Internet of Things (loT) to estimate crowds in cities in order to improve and maximize the efficacy of the transportation system and other public services for low-density situations. Various image processing methods are used to compare the findings of an experiment after numerous subject counts are photographed. According to the findings, both approaches can be used to assess crowd density. A high-resolution camera is more expensive and precise to place in infrastructures, as has been made public. This comparison uses the FLIR E25, a high-resolution alternative, and the IRI 1002, a reasonably priced infrared camera with 16x16 pixels. Radiation from a healthy body temperature is infrared. The average body temperature is influenced by a variety of things, including the type of food consumed, the clothing worn, the amount of physical activity, sleeping habits, and the time of day. Between the wavelengths of 7.5 and 13, infrared energy is detectable by infrared cameras (Al-Habaibeh, et al., 2023). To prevent camera trap systems

from taking pictures of nothing, the authors of the article "Motion vectors and deep neural networks for video camera traps" by Miklas Riechmann et al. (2022) provide a solution. Utilizing less disk storage space, less bandwidth, and less time for examination later in the research process are all benefits of this method. Additionally, their approach includes a pipeline for video frame filtering based on images and motion. The use of machine learning (ML) on a live video feed powered by an RPi is suggested in light of the information above (Riechmann, et al., 2022). Several different objects in TIR pictures and videos were successfully recognized by the YOLO model-based UAV object recognition framework created for this study. The YOLO models (YOLOv3, YOLOv4, and YOLOv5) with 15 different architectures based on pre-trained checkpoints using multi-situation ground TIR video frames were used in this study to explore the vehicle and human multi-object recognition. The assignment with the highest overall mAP had a 14 MB validating job model, whereas the assignment with the highest total mAP had an 88.69%. The quickest detecting speed was 50 FPS. They used the YOLO models produced using the ground TIR dataset in the UAV object-based detection system they suggested. They also talked about using the right evaluation techniques to obtain appropriate detection results. It is predicted that the identification results and cross-application demonstrated in this work will be useful for item detection in diverse TIR datasets (DAVIDNYARKO123, 2023) The remaining comparisons can be seen here: Table1.

## 2.    Data

We used two datasets in our code. The first was downloaded from the internet, and the second one was created using various datasets. Using YOLOv8n.pt, these two datasets were trained. The first dataset (human dataset, n.d.) has 13660 images at a resolution of $416 \times 416$ pixels. The only images in this dataset are private ones. People are labeled in YOLOv8 format as pedestrians. When we run it, the accuracy is 75%. We created a second dataset using various images we acquired from the internet. Then, we used robot flow to classify them into groups. To create the group, 11324 photos were employed. The collection contains 80 classifications in addition to personal photos. It has undergone multiple training with a batch size of 16 and an epoch of 30. Although this dataset can detect a large number of objects, our accuracy with simply human image training is 96%.

## 3.    Experiments

Each image underwent the pre-processing steps of auto-alignment of pixel data using EXIF orientation stripping and scaling to $416 \times 416$ (Stretch). We have chosen a batch size of 16 and a training epoch of 30 for these datasets. These datasets were

trained over the course of about 30 hours.

On a special dataset, a YOLOv8 model is trained using the training mode. In this mode, the model is trained using a set of hyperparameters and a few carefully chosen datasets. The model's training parameters are adjusted in order for it to correctly identify the classes and locations of objects in an image.
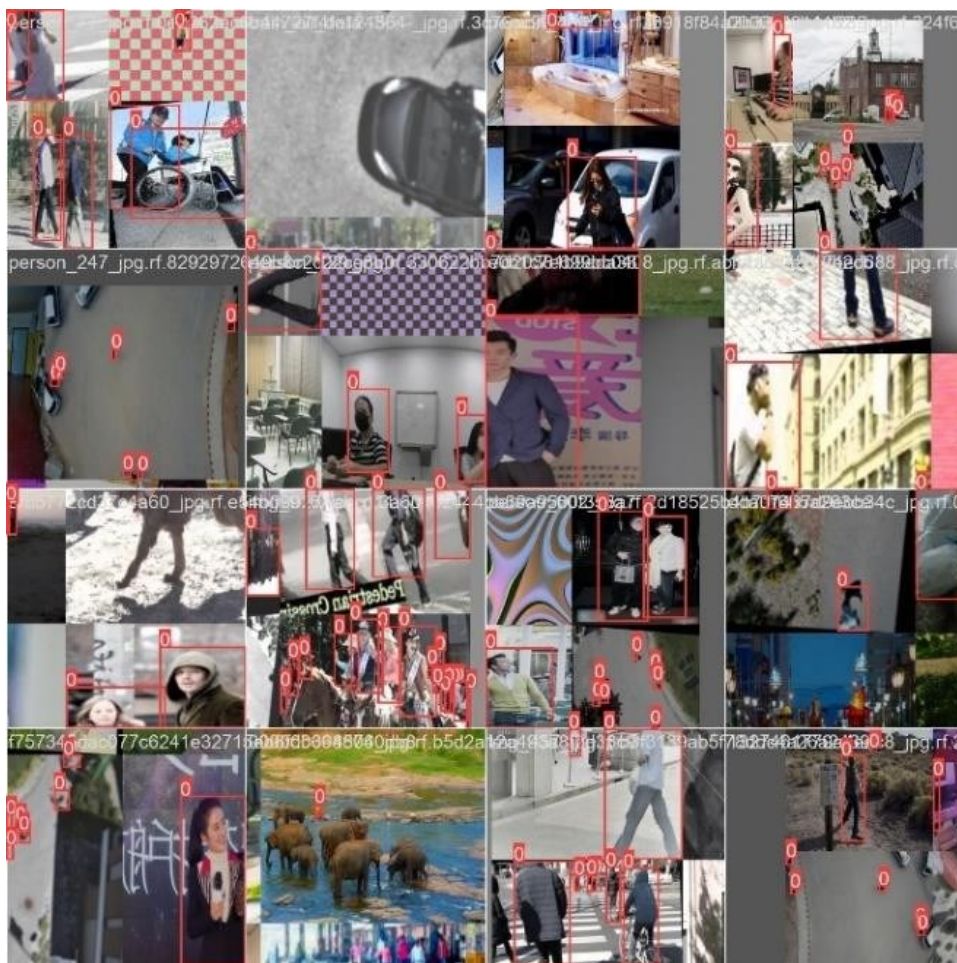


**Figure 1**. Train batch of first dataset

For YOLO models, the various conFigureurations and hyperparameters required to train the model on a dataset are referred to as "training settings". The performance, speed, and accuracy of the model can be affected by any of these options. The standard YOLO training parameters include the learning rate, momentum, weight decay, and batch size. Other factors that could affect the training procedure include

the choice of an optimizer, a loss function, and the quantity and make-up of the training dataset. For optimum performance for a certain application, these parameters need to be carefully adjusted and experimented with. A way to determine how effectively your algorithm models your dataset is by using the loss function. It is a mathematical function of the machine learning algorithm's parameters. The loss is zero if the model's forecast is accurate; otherwise, the loss is higher. b0x_loss is a loss that evaluates how "tight" the projected bounding boxes are to the item in the real world. cls_loss is a loss that measures how accurately each predicted bounding box was classified; each box may contain either an object class or "background." Cross entropy loss is the common name for this loss. Summarized data and results of each dataset used can be seen in the following Table2:

Table2. Comparison table of two used datasets

| Datasets | Number of data | Training model | Accuracy | box_loss | cls_loss |
|----------|----------------|----------------|----------|----------|----------|
| Dataset 1 | 13660 | YOLOv8 | 75% | 1,57 | 1,28 |
| Dataset 2 | 11324 | YOLOv8 | 96% | 1,17 | 1,18 |

Data labeling in machine learning is the classification of unlabeled data (such as pictures, text files, videos, etc.) and the addition of one or more educational labels to give the data context in order to learn from it using a machine learning model. For instance, labels might say if a picture shows a bird or an automobile, whether someone spoke in an audio recording, or whether a tumor is visible on an X-ray. The use cases of speech recognition, computer vision, and natural language processing all call for the labeling of data.
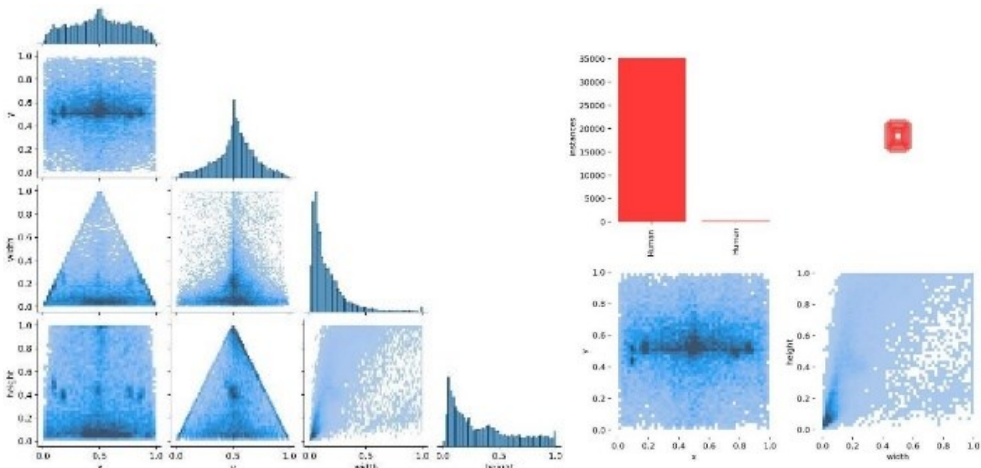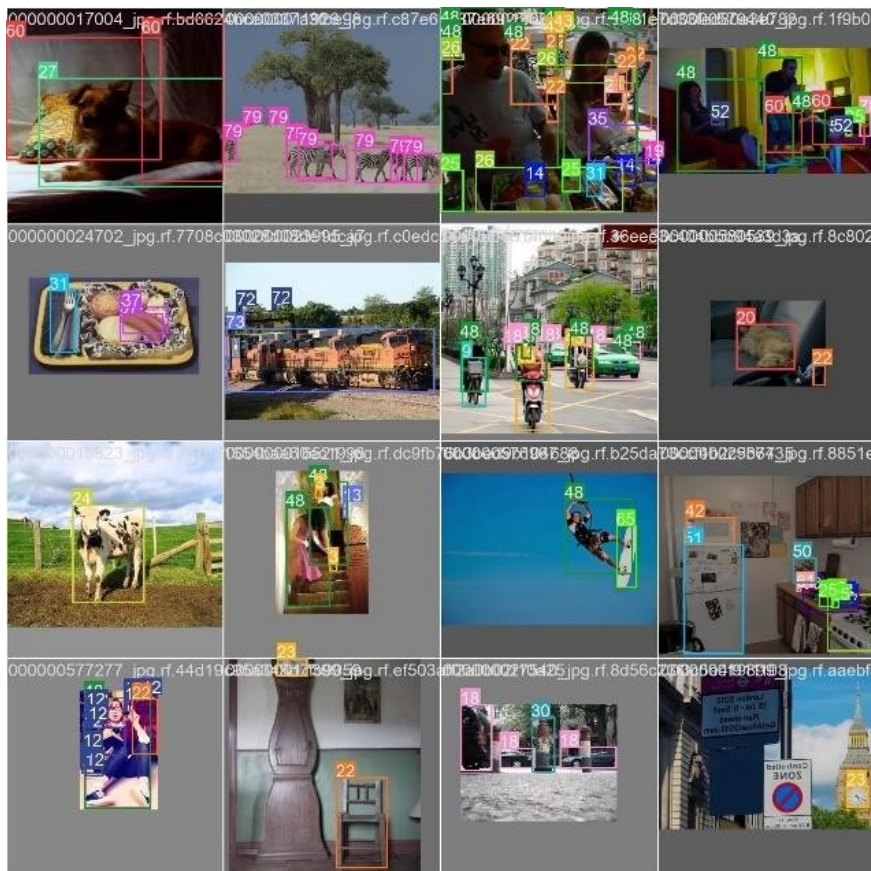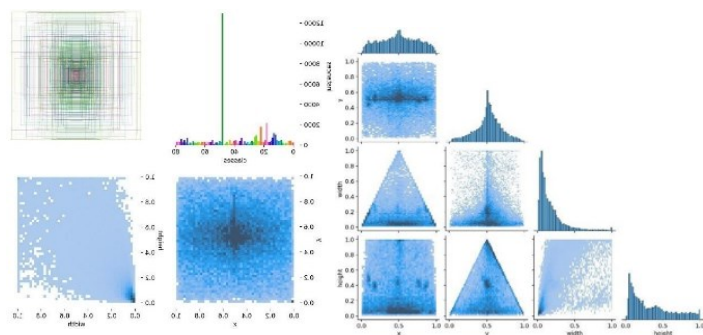


**Figure 2.** Labels and Label's Correlogram for first dataset

A set of two-dimensional histograms called a correlogram is used to compare each axis of our data to every other axis. You can view labels and labels correlograms for both datasets in Figure2 and Figure4. Train batch for second dataset:



**Figure 3.** Train batch of second dataset



**Figure 4.** Label's Correlogram for second dataset
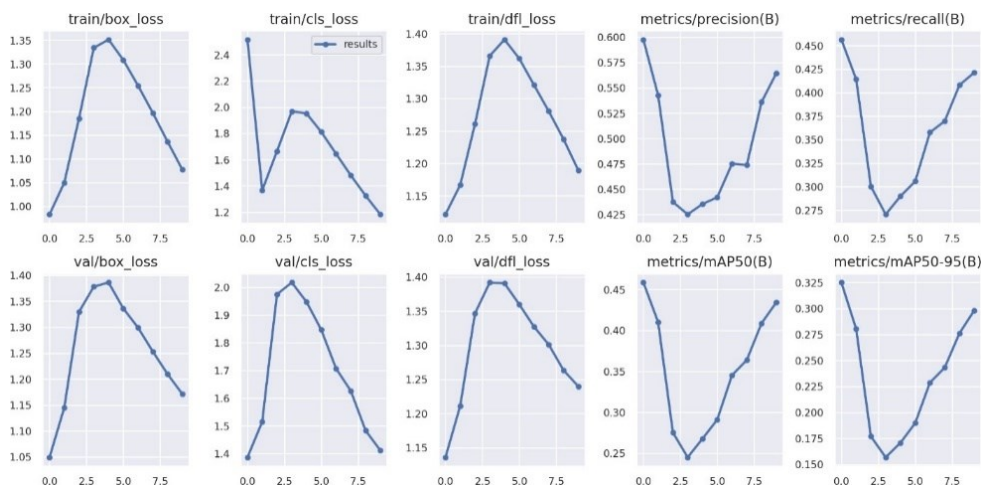
**Figure 5.** Metrics and results of second dataset

## Conclusion

In our research, we offered a method for surveillance systems' image and video cameras to use when looking for humans. The YOLOv8 method was used to train two datasets. The batch size and epoch for training the first dataset were 16 and 30, respectively. After 30 hours of training, we were 75 percent accurate. The second data set had a batch size of 16 and an epoch of 30. Using solely training images of individuals, this dataset has a 96% accuracy rate for detecting a variety of objects. Despite significant progress, there are still many problems that need to be tackled. It might be challenging to get the greatest performance due of things like occlusion, various lighting conditions, and privacy concerns. Future research should focus on developing advanced methods and algorithms to handle these problems and improve the general reliability and accuracy of human recognition systems. Furthermore, it is crucial to consider how morally questionable person recognition technology might be. The potential for abuse and privacy concerns needs to be carefully taken into account. Researchers and practitioners should aim to create transparent frameworks that prioritize privacy protection and guarantee the proper usage of smart camera systems. Person identification for smart cameras is becoming a reality as a potent technology with numerous applications in security, surveillance, and human-computer interaction. Future study in this area can be built upon the accomplishments discussed in this publication. With further effort on refining algorithms, resolving problems, and adding ethical considerations, person identification technology will progress and become widely used, ultimately making our societies safer and more efficient. In the future, we intend to go into more detail

about this and recommend it to malls for use in identifying persons and tracking, as well as in observing people's entrances and exits for increased security.

## References

**Al-Habaibeh, A., Yaseen, S., & Nweke, B.** (2023). A comparative study of low- and high-resolution infrared cameras for IoT smart city applications. Ain Shams Engineering Journal. 14(6): 102108.

**Data labeling: why it is important to manage it efficiently.** (2022). Labellerr. https://www.labellerr.com/blog/data-labeling-why-it-is-important-to-manage-it-efficiently/

**Davidnyarko123.** (2023). GitHub-DAVIDNYARKO123/yolov8-silva. GitHub. https://github.com/DAVIDNYARKO123/yolov8-silva

**Imerit.net.** (2021). This Is How You Know It's Time to Bring in Professional Data Labelers. iMerit. https://imerit.net/blog/when-to-outsource-your-data-labeling-all-sol/

**Hu, W. C., Chen, C. H., Chen, T. Y., Huang, D. Y., & Wu, Z. C.** (2015). Moving object detection and tracking from video captured by moving camera. Journal of Visual Communication and Image Representation. 30: 164–180.

**Jiang, C., Ren, H., Ye, X., Zhu, J., Zeng, H., Nan, Y., Sun, M., Ren, X., & Huo, H.** (2022). Object detection from UAV thermal infrared images and videos using YOLO models. International Journal of Applied Earth Observation and Geoinformation. 112: 102912.

**Kiani, Kalejahi, Behnam et al.** (2022). 'Diagnosis of Liver Disease by Computer- Assisted Imaging Techniques: A Literature Review'. 1 Jan: 1097 – 1114.

**Kiani Kalejahi, B., Meshgini, S. & Danishvar, S.** (2023). Brain tumor segmentation by auxiliary classifier generative adversarial network. SIViP 17, 3339–3345. https://doi.org/10.1007/s11760-023-02555-6.

**Malburg, L., Rieder, M. P., Seiger, R., Klein, P., & Bergmann, R.** (2021). Object Detection for Smart Factory Processes by Machine Learning. Procedia Computer Science. 184: 581–588.

**Mutepfe F, Kalejahi BK, Meshgini S, Danishvar S.** (2021). Generative Adversarial Network Image Synthesis Method for Skin Lesion Generation and Classification. J Med Signals Sens. 11(4):237-252.

**Paul, R., & Mukhopadhyay, S.** (2015). Foreground Object Extraction Based on Independent Component Analysis. Advances in Vision Computing: An International Journal. 2(4): 1–11.

**Riechmann, M., Gardiner, R., Waddington, K., Rueger, R., Leymarie, F. F., & Rueger, S.** (2022). Motion vectors and deep neural networks for video camera traps. Ecological Informatics. 69: 101657.

**Sivachandiran, S., Jagan Mohan, K., & Mohammed Nazer, G.** (2022). Deep Learning driven automated person detection and tracking model on surveillance videos. Measurement: Sensors. 24: 100422.

**Yazdi, M., & Bouwmans, T.** (2018). New trends on moving object detection in video images captured by a moving camera: A survey. Computer Science Review 2018; 28: 157–177.

**Table1. Comparison table of related works**

| | Models | Datasets | Experiments | Results |
|---|---|---|---|---|
| Our work | YOLOv8 | Human dataset and image dataset | We trained our model, and then tested it on our datasets. It first resizes photos, removes background, detects all objects on them and then detects which object is person | 75% and 96% |
| Mehran Yazdi et al. | They summarized different techniques in their work | Benchmark datasets | They divided multiple techniques into object tracking, low-rank and spare matrix decomposition, and modeling-based background subtraction | Summarized and compared multiple methods |
| S. Sivachandiran et al. | Used DLD-APDT | Surveillance videos | Their model first carries out a frame conversion operation, turning the input video into a collection of frames. Additionally, they use the BiFPN-based EfficientDet model as an object detector. Again, PascalVOC and PenFudan datasets are being used in their training. Finally, they use the RMSProp optimizer to select the hyperparameters as best as possible | Person detection using DL-driven automated person detection and tracking model |
| Lukas Malburg et al. | Used YOLOv3, YOLOv4 and PANet | Custom dataset | As a first step towards video-based monitoring and tracking, Lukas Malburg et al. propose a generic framework for multi- | Their experimental evaluation demonstrates that detection accuracies for custom objects and |

| | | | modal monitoring of manufacturing processes in their study and deploy and assess three cutting-edge OD systems (YOLOv3 (SPP), YOLOv4 and PANet (SPP) CSPResNeXt50) | failure places of these objects can be improved to above 90% in an industrial research setting |
|---|---|---|---|---|
| Wu-Chih Hu et al. | Method for detecting and tracking moving objects without using extra sensors | Videos of moving objects taken by moving cameras | Tested their model on moving objects from a video sequence taken by a moving camera without using extra sensors | It is effective for tracking items that overlap and objects whose scale changes, as well as for detecting fast-moving objects or things under fast-moving cameras |
| Amin Al-Habaibeh et al. | Used multiple image processing techniques | FLIR E25, a high-resolution substitute, and IRI 1002, a low-cost infrared camera with 16x16 pixels, are used in this comparison | In an experiment, multiple subject counts are photographed, and the results are then compared using different image processing techniques | The results suggest that both technologies help determine crowd density |
| Miklas Riechmann et al. | YOLO model-based UAV | TIR dataset | Their method introduces an image- and movement-based video frame filtering pipeline | The identification results and cross-application shown in this work are anticipated to be helpful for item detection in various TIR datasets |

# Quantum Dots in Semiconductors for Coming Optical Applications

## Babak Emdadi

*Institute of Physics & Electronic of Khazar University, Baku, Azerbaijan*
*emdadi.babak2021@khazar.org*

**Abstract.**

Review of semiconductor quantum dots (QDs) development and research for optical applications. The QDs are tiny crystals, around 10 nm in size, made of semiconductors III-V, II-VI, IV, and IV-VI. They are divided into two categories. The self-assembled QDs, which are grown epitaxially on a semiconductor substrate, are one type. The other type is colloidal QDs, which are chemically produced in a solvent. Due to the fact that both QDs' emission wavelengths span a broad spectrum, from visible to infrared, the QDs are appealing to a variety of application domains. In the areas of replacing current devices, quantum information devices, and solar energy conversion devices, research on both epitaxial QDs and colloidal QDs has advanced. The QD devices will be crucial to the 21st century's large-capacity information-oriented civilization and the solution to the energy crisis. The three application sectors, namely the replacement of current products, quantum information devices, and solar cells, are the main topics of this article.

**Keywords:** quantum dot, nano crystal, semiconductor laser, quantum information, solar cell

## Introduction

The quantum dots (QDs), which have an average size of around 10 nm, are tiny crystals made of semiconductors III-V, II-VI, IV, and IV-VI. QDs are divided into two groups. One type is epitaxial QDs, which self-assemble on single-crystal semiconductor substrates by using well-known epitaxial growth techniques including metalorganic vapor phase deposition (MOCVD) and molecular beam epitaxy (MBE). The other is colloidal QDs, which are created using a chemical process in a flask and a solvent. The most interesting finding is that both QDs emit light with a broad spectrum of wavelengths, ranging from visible to infrared. As a result, both are very desirable materials for use in many optical device applications.

Since epitaxial QDs are manufactured using the same equipment as semiconductor devices today, they can be simply incorporated into semiconductor device fabrication procedures. Actually, the active layer of semiconductor laser diodes for the optical communication system already uses QDs. Because of the crystal strain energy caused by the substrate's lattice mismatch, the epitaxial QDs self-assemble. Hence the self-assembled QDs' form cannot completely shield them from the effects of substrate orientation. This has advantages for managing QD location and disadvantages for producing isotropically shaped QDs, as will be discussed later.

The cost of producing colloidal QDs is exceptionally low since they may be produced in large quantities without the use of expensive equipment. Since they are not attached to a substrate, QDs are often symmetrical. The utilization of biomarkers is attracted by their excellent chemical stability. Colloidal QDs are assembled into solid devices using a polymer matrix that maintains QD functionality. In the area of optical quantum information technology, for instance quantum processing and communication, both types of QDs have advanced. The two QDs have already achieved the single photon emission. In order to achieve optical quantum repetition and optical quantum operation, the creation of the quantum-entangled photon pair is still a research goal. A significant problem for the generation is the symmetry of the QD structure. In order to construct the QD circuit for the quantum operation, it is also necessary to regulate the size, position, and connectivity of QDs.

Recent years have seen a keen demand for innovations in green nanotechnology. It has been demonstrated that the QD solar cell offers a significant solution. The intermediate energy band will be created if QDs can be stacked thickly in three dimensions, much like an artificial crystal. With the QDs' intermediate band, it is expected that the photoelectric conversion efficiency will be greater than 70%, which is significantly higher than the efficiency of the existing silicon-based solar cell. A current crucial topic is how to realize the intermediate band. This study examines semiconductor QD research and development, including our contributions, in the three areas of product replacement, quantum information devices, and solar cells.

**Materials and methods**

The primary application of quantum dot technology, which was the initial motivation for studying it, is still replacement of existing devices. The semiconductor laser diode is the most popular and sophisticated QD technology. Since it is sufficient to develop a QD layer as an active region in place of a quantum well (QW) layer, epitaxial QDs are simple to incorporate into the laser diode construction process. Thus, using QDs does not increase the price of manufacturing semiconductor lasers,

as was previously believed. Since in paper researchers (Arakawa et al., 1982) suggested that the performance of a QD laser would be significantly better than a QW laser, numerous researchers have worked to make the QD laser a reality (Mukai et al., 1998, Huffaker et al., 1998, Murray et al., 1999). Despite having to overcome numerous practical obstacles, QD lasers are now on the market thanks to QDLaser Inc., a spin-off business initiative of Fujitsu Lab. QD lasers have advanced significantly over the past several years. The realization of high modal gain, high speed modulation, and high temperature functioning was made possible by the high density of QD layers. Direct modulation at a speed of 25 Gbit/s is offered. Because the threshold current is steady between -10 and 85°C, it was possible to create a high-bit-rate, temperature-unrestricted communications transmitter. Even at 220 °C, the QD laser functions (Figure. 1).
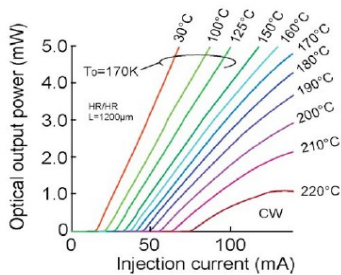


**Figure 1.** QD laser parameters of optical output power against injection current from 30 and 220°C.

Compared to epitaxial QDs, colloidal QDs have a number of advantages. Since they are cheap, the cost of QD items can be reduced. The colloidal QDs' band gap energy is depicted in Figure 2 (Rogach et al., 2007). Each bar shows the changeable energy range.
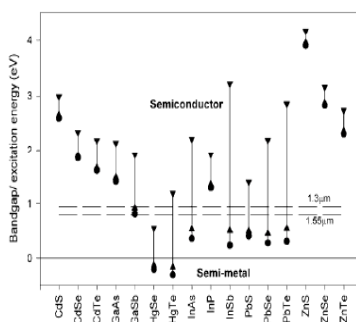


**Figure 2.** Band gap energies for bulk materials and nano crystals with diameters of 10 nm and 3 nm are displayed.

There are numerous component material options available to obtain the visible emission. The use of QDs luminescence at visible wavelengths advances the bio marker application (Michalet et al., 2005). They are suitable for use in security ink or light emitting diodes (LED) due to their chemical stability (Craig et al., 2012). Although the electronics applications are still being researched, it has been established that they function well enough for everyday use. The spectral purity of QDs permits a color gamut wider than the HDTV (High Definition Television) standard, as shown by the CIE chromaticity diagram in Figure 3. PbS, PbSe, InAs, and InSb are the materials of choice for invisible light, notably in telecommunication wavelengths.
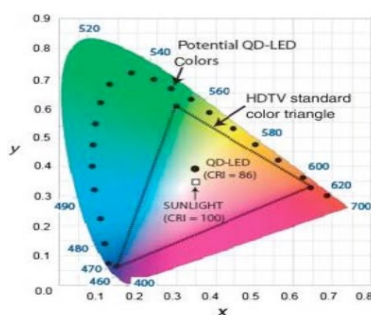


**Figure 3.** CIE chromaticity diagram displaying the QD LED's potential.

## 3. Quantum information devices

The quantum information device, which will enable entirely safe communication and incredibly rapid processing, is another significant application of QD. QDs have been researched as a source material for the single photon emitter and the entangled photon pair generator in the quantum communication technology. QDs and microcavity are integrated for the goal. QDs are employed in quantum computation as a qubit storage or a waveguide for a quantum optical circuit. In the early 2000s, epitaxial QDs produced their first single photon (Santori et al., 2002). By using HBT conFigureuration, anti-bunching of the photon count was shown as the evidence. Following that, the quantum cryptography-based communication investigations have been proven at the specific communication wavelength, as illustrated in Figure 4 (Miyazawa et al., 2005).

These emitters were created by fusing microcavity and QD. The ideal microcavity for controlling single photon properties is a three-dimensional photonic crystal (Nomura et al., 2010). Numerous researchers have attempted to combine these two ultimate artificial materials since QD can predict the single electron characteristics.

One of these final structures is depicted in Figure 5 (Tandaechanurat et al., 2009). In the manufacturing process, the stack of woodpile structures was put together on top of the active layer with the defect nanocavity sitting on top.
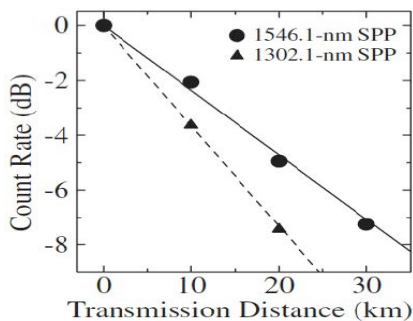


**Figure 4.** C- and O-band single photon transmission rates across the long single mode fiber.
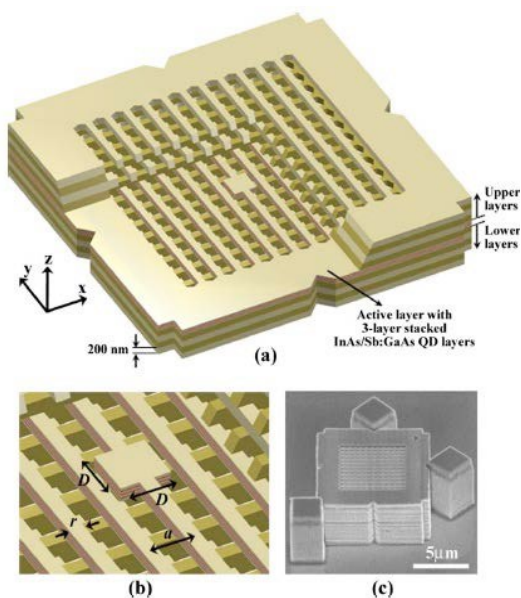


**Figure 5.** (a) Three-dimensional cavity structure schematic. (b) A cavity that has been magnified. The 25-layer woodpile structure may be seen in the (c) SEM image.

The colloidal QD has also achieved single photon emission. At visible wavelengths, the antibunching was seen (Pisanello et al., 2010). QD was placed in the straightforward cylindrical polymer microcavity for the intended use. We are also looking at the Figure 6 colloidal QD-containing simple polymer microcavity in three dimensions (Mukai et al., 2007).
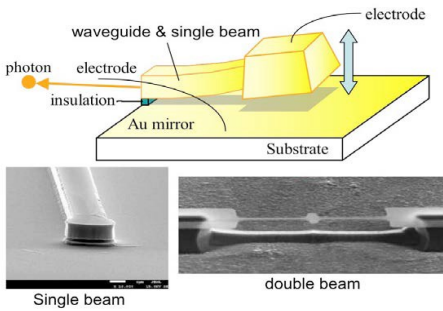
**Figure 6.** (a) Waveguide-equipped tunable photonic dot schematic. The photonic dot's head portion contains a QD. (b) A product composed of III-V compound semiconductor; (c) a product with two polymethylmethacrylate waveguides (PMMA).

QD is installed in the photonic dot portion of the microcavity head, which is supported by one or two beams. The beam serves as a waveguide guiding a photon into the planar photonic circuit, while the QD serves as a photon source. Instead of using high reflection multilayers, the upper wall, sidewalls of the head, and substrate surface are simply coated with gold. The timing of the QD's photon spontaneous emission is controlled by adjusting the distance between the head and the substrate using the micromachine approach. There have been several suggestions for employing QDs to build quantum circuits (Khan., 2006, Vartuli et al., 1994). The most fundamental concept uses QDs as the photon source, and photonic crystal waveguides are utilized to connect QDs to other optical elements like optical couplers and detectors. Another concept uses a QD waveguide to drive the quantum signal (Huang et al., 2007). The quantum circuit device cannot be created without the QD positioning technique. In this realm of study, epitaxial QD has also advanced. The groundbreaking study's two-dimensional arrangement of size-controlled QDs was depicted as qubit cells in Figure 7 (Okubo et al., 2017).
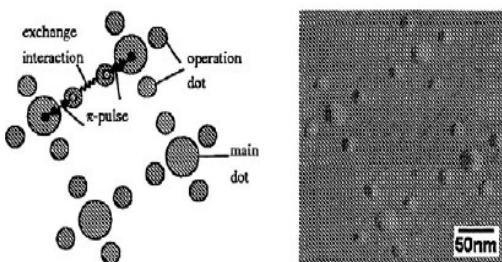


**Figure 7.** Quantum circuit arrangement in two dimensions created through SPM oxidation and subsequent epitaxial growth.

In this manufacturing, nano-sized holes on the substrate were first created by nano-spot oxidation using scanning probe microscopy (SPM), and then the oxides were selectively etched away. The preferred QD development in the holes was caused by epitaxial growth on the patterned substrate. The holes were followed by the QD position as well as the QD size. In another instance, the QD array as depicted in Figure 8 (Ohkouchi et al., 2009) was drawn using the cantilever source dropper.
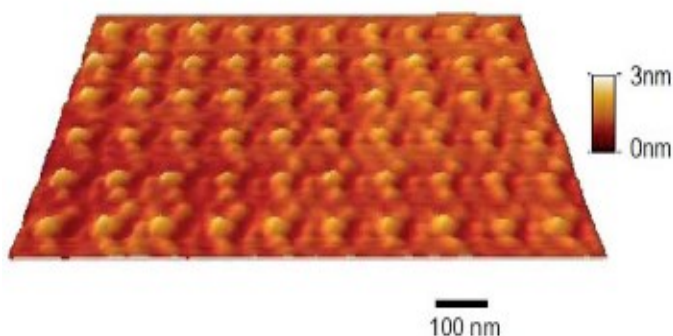


**Figure 8.** By using a nano-jet probe, a QD array was drawn.

With the help of epitaxial growth on a prepared substrate, the astounding 3D arrangement of QDs was made possible (Figure 9) (Atkinson et al., 2008). The method is based on the observation that crystal deformation causes QD nucleation to happen. It needs to be emphasized, nonetheless, that these QDs still struggle with low quantum efficiency and poor size homogeneity for use in real devices.
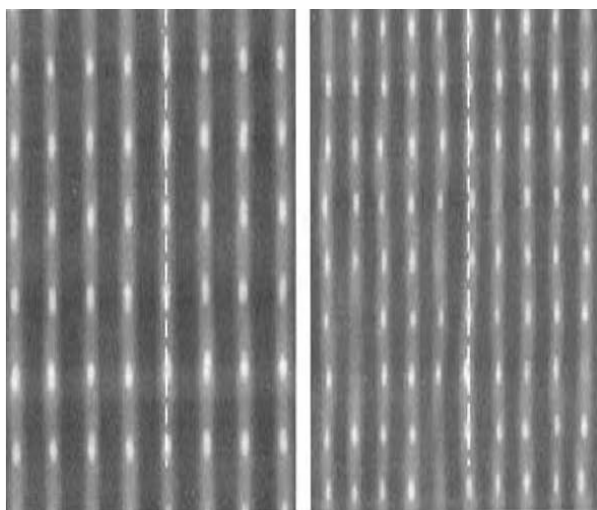


**Figure 9.** Epitaxial QDs produced in lines on a patterned substrate.

Since it is required for optical quantum repetition and optical quantum processing, the creation of the entangled photon pair is a crucial analyze topic in the field of quantum information technology. The photon pair emitted from the exciton molecules in QD has the potential to be in the polarization-entangled condition. When an exciton molecule is excited, it produces a photon that converts it into a single exciton, and the single exciton subsequently releases a second photon with a typically slightly different energy (Moreau et al., 2001). The reliability of nuclear power generation has recently been questioned, and the development of energy sources other than oil is urgently needed. The so-called "green technology" may provide several solutions, one of which is the QD solar cell. Two different forms of QD solar cells have received a lot of attention. One method includes epitaxial QDs as the compound semiconductor cell's intermediate-band photon absorber (Figure 10).
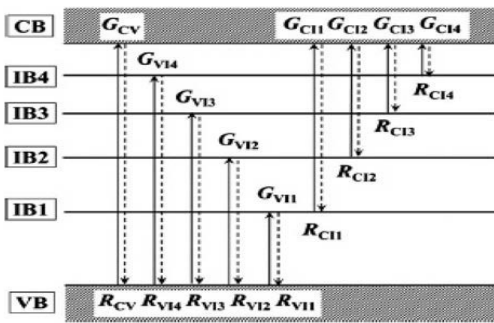


**Figure 10.** Carrier transitions and energy levels of the several QD intermediate bands are shown schematically.

The sensitizer in the organic solar cell of the other type uses colloidal QDs. The latter style of cell was anticipated to have a maximum photoelectric conversion efficiency of more than 70% (Nozawa et al., 2011). Although the latter form of cell is more readily adapted to practical use, its conversion efficiency is less than 10%. The epitaxial growth equipment has been used to study the production of the intermediate band solar cell (Ahsan et al., 2012). To create the intermediate energy band, the QDs must be packed tightly in three dimensions, but this is challenging. Existing QDs influence the development of new QDs because the crystal distortion energy serves as the basis for epitaxial QD production. As a result, it's imperative that the growth of multiplied layers be coordinated with the continual modification of the growth surface circumstances. In addition to the QD-sensitized cell, the Schottky cell or the depletion hetero junction cell has also been studied using colloidal QDs (Figure 11) (Zhou et al., 2011). In the QD layers, the QDs are accumulated at random. PbSe and CdSe QD Schottky cells still only have a 10% conversion rate. The challenges are still being solved through research and advancement. As an illustration, the ligands

around QDs serve to electrically isolate them to some extent. To increase conductivity, it has been researched how to substitute the ligands with shorter ones.
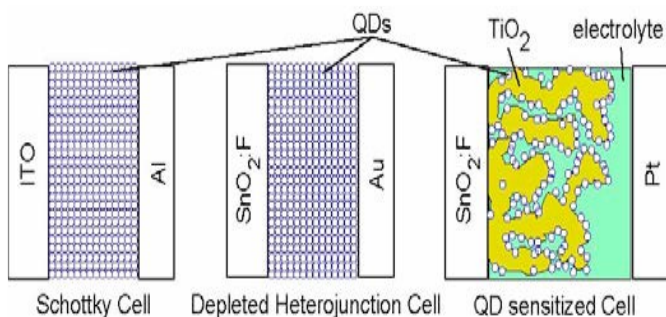


**Figure 11.** Schematic of the colloidal QD-based solar cells.

The production of a low-cost solar cell with a benefit of an intermediate band will be possible without trouble if QD superlattice is produced utilizing colloidal QDs.

## Conclusion

Overview of semiconductor QD research & innovation with an eye toward diverse applications of its optical features. Because QDs' emission wavelength spans the visual to infrared spectrum, they are appealing to a variety of application domains. In the areas of replacing current devices, quantum information devices, and solar energy conversion devices, research on both epitaxial QDs and colloidal QDs has advanced. The QD devices will be crucial to the 21st century's large-capacity information-oriented civilization and the solution to the energy crisis.

## References

Ahsan, N., Miyashita, N., Islam, M. M., Yu, K. M., Walukiewicz, W., & Okada, Y. (2012). Effect of Sb on GaNAs intermediate band solar cells. In 2012 IEEE 38th Photovoltaic Specialists Conference (PVSC) PART 2 (pp. 1-8). IEEE.

Arakawa, Y., & Sakaki, H. (1982). Multidimensional quantum well laser and temperature dependence of its threshold current. Applied physics letters, 40(11), 939-941.

Atkinson, P., Kiravittaya, S., Benyoucef, M., Rastelli, A., & Schmidt, O. G. (2008). Site-controlled growth and luminescence of InAs quantum dots using in situ Ga-assisted deoxidation of patterned substrates. Applied Physics Letters, 93(10), 101908.

Craig, D. A., Craig, R. E., & Crosby, T. K. (2012). Simuliidae (Insecta: Diptera). Fauna of New Zealand, 68.

Huang, L., Hegg, M. C., Wang, C. J., & Lin, L. Y. (2007). Fabrication of a nanophotonic quantum dot waveguide and photodetector integrated device. Micro & Nano Letters, 2(4), 103-106.

Huffaker, D. L., Park, G., Zou, Z., Shchekin, O. B., & Deppe, D. G. (1998). 1.3 μm room-temperature GaAs-based quantum-dot laser. Applied Physics Letters, 73(18), 2564-2566.

Khan, M. M. (2006). Fabrication and testing of nano-optical structures for advanced photonics and quantum information applications. Dissertation Abstracts International, 69(01).

Michalet, X., Pinaud, F. F., Bentolila, L. A., Tsay, J. M., Doose, S. J. J. L., Li, J. J., ... & Weiss, S. (2005). Quantum dots for live cells, in vivo imaging, and diagnostics. science, 307(5709), 538-544.

Miyazawa, T., Takemoto, K., Sakuma, Y., Hirose, S., Usuki, T., Yokoyama, N., ... & Arakawa, Y. (2005). Single-photon generation in the 1.55-μm optical-fiber band from an InAs/InP quantum dot. Japanese Journal of Applied Physics, 44(5L), L620.

Moreau, E., Robert, I., Manin, L., Thierry-Mieg, V., Gérard, J. M., & Abram, I. (2001). Quantum cascade of photons in semiconductor quantum dots. Physical Review Letters, 87(18), 183601.

Mukai, K., Nakata, Y., Shoji, H., Sugawara, M., Ohtsubo, K., Yokoyama, N., & Ishikawa, H. (1998). Lasing with low threshold current and high output power from columnar-shaped InAs/GaAs quantum dots. Electronics Letters, 34(16), 1588-1590.

Mukai, K., & Yamamoto, Y. (2007). Photonic dot structure which emits photons horizontally to a built-in waveguide. Journal of crystal growth, 301, 984-988.

Murray, R., Childs, D., Malik, S., Siverns, P., Roberts, C., Hartmann, J. M., & Stavrinou, P. (1999). 1.3 μm room temperature emission from inas/gaas self-assembled quantum dots. Japanese Journal of Applied Physics, 38(1S), 528.

Nomura, M., Ota, Y., Kumagai, N., Iwamoto, S., & Arakawa, Y. (2010). Zero-cell photonic crystal nanocavity laser with quantum dot gain. Applied Physics Letters, 97(19), 191108.

Nozawa, T., & Arakawa, Y. (2011). Detailed balance limit of the efficiency of multilevel intermediate band solar cells. Applied Physics Letters, 98(17), 171108.

Ohkouchi, S., Ozaki, N., Sugimoto, Y., Ishikawa, H., & Asakawa, K. (2009). Site-controlled InAs quantum dot formation grown on the templates fabricated by the Nano-Jet Probe method. Journal of crystal growth, 311(7), 1819-1821.

Okubo, S., Ohta, H., Ijima, T., Yamasaki, T., Zhang, W., Hara, S., ... & Watanabe, T. (2017). THz ESR study of Spinel Compound GeCo2O4. Zeitschrift für Physikalische Chemie, 231(4), 827-837.

Pisanello, F., Martiradonna, L., Leménager, G., Spinicelli, P., Fiore, A., Manna, L., ... & Bramati, A. (2010). Room temperature-dipolelike single photon source with a colloidal dot-in-rod. Applied Physics Letters, 96(3), 033101.

Rogach, A. L., Eychmüller, A., Hickey, S. G., & Kershaw, S. V. (2007). Infrared-emitting colloidal nanocrystals: synthesis, assembly, spectroscopy, and applications. small, 3(4), 536-557.

**Santori, C., Fattal, D., Vučković, J., Solomon, G. S., & Yamamoto, Y.** (2002). Indistinguishable photons from a single-photon device. nature, 419(6907), 594-597.

**Tandaechanurat, A., Ishida, S., Aoki, K., Guimard, D., Nomura, M., Iwamoto, S., & Arakawa, Y.** (2009). Demonstration of high-Q (> 8600) three-dimensional photonic crystal nanocavity embedding quantum dots. Applied Physics Letters, 94(17), 171115.

**Vartuli, J. C., Schmitt, K. D., Kresge, C. T., Roth, W. J., Leonowicz, M. E., McCullen, S. B., & Sheppard, E. W.** (1994). Development of a formation mechanism for M41S materials. In Studies in Surface Science and Catalysis (Vol. 84, pp. 53-60). Elsevier.

**Zhou, Y., Eck, M., Veit, C., Zimmermann, B., Rauscher, F., Niyamakom, P., ... & Krüger, M.** (2011). Efficiency enhancement for bulk-heterojunction hybrid solar cells based on acid treated CdSe quantum dots and low bandgap polymer PCPDTBT. Solar Energy Materials and Solar Cells, 95(4), 1232-1237.

# Application of Nanotechnology in Increasing Oil Recovery Coefficient of the Reservoir

## Jamal Aliyev

*SOCAR, "Oil-Gaz Scientific Research Design" İnstitute, Baku, Azerbaijan*
*camal.aliyev1965@mail.ru*

**Abstract**

When the formation is injected with a nanosystem, the demulsification process takes place in the formation water; as a result, a nanoscreen against formation water and a nano-layer between the phases are formed. In this case, the surface tension on the oil and rock surface decreases and separation of oil from the reservoir occurs. As a result of the demulsation process, the conductivity of the reservoir collectors increases, thus, the filtration of oil from the reservoir to the bottomhole accelerates. One of the most promising technologies in this area is the treatment of the bottomhole zone with specially prepared solutions - nanocompositions consisting of a complex of surfactants and nanoparticles. Nanocompositions significantly increase the compaction, lubrication and solubility properties of oil under mining conditions.

## Introduction

With the introduction of traditional methods of oil and gas fields in Azerbaijan, the latest oil ratio varies from an average of 40.3-44.2% and the bulk of the oil reserve (55.8-59.7%) remains in the subsoil, being attributed to the non-removable oil reserve.

When analyzing the positive and negative results of the methods of impacting the reservoirs being worked out for a long time, it is obvious that in most cases, obtained effects are found to be both local and short-term.

The dynamism of the water-oil-gas system is ensured by the processes arising due to the imbalance of the intralayer environment, and due to this, excess pressure is

created in the reservoir. However, at the final stage of development, this system goes from a non-equilibrium state to an equilibrium state and thus, the processes taking place in the reservoir weaken and the removal of fluid from the reservoir becomes more complicated. Therefore, it was necessary to apply a more progressive and effective new technology-nanotechnology - to improve the physicochemical properties of working solutions injected into the reservoir together with water and improve the method of water injection. The nanotechnological basis for increasing the oil yield coefficient is based on the replacement of petroleum hydrocarbons by the complex action of nanoparticles of surfactants, deemulgators, acids, alkalis and hydrocarbon-oxidizing bacterial molecules. As a result of this impact , new oil-compacting reagents such as CH4 , CO2, H2 and N2 are formed in reservoir (Shahbazov, 2019).

In addition Along with the increase in oil production by 2.0-2.5 times, it was possible to reduce energy costs due to the implementation of ” Nano oil "program in flooded and low-debit wells at SOCAR's oil and gas production facilities (Mirzajanzade, 2006].

During the transition of atoms and molecules from chaotic movement to orderly movement on the basis of ” minor impact and alarm effect ", there was an increase in oil production as a result of breakage of old communications and the formation of new ones.

As can be seen from Figure 1, electron paramagnetic resonance spectra are observed in NanoSystems. Transverse elongation of signals and volumetric expansion occurs in the system as the temperature increases. Surface tension falls down during volumetric expansion. During the studies carried out, the chemical properties and sizes of metal nanoparticles change as the temperature increases. As nanoparticles shrink in size, the temperature increases and the paramagnetic field arises. ( Aliyev, 2020) As nanoparticles shrink in size, they move along the axis from the unit atom to the mass state and a dispersed system (dipole) arises (Matiyev, 2022).

When a reservoir is impacted by a nanosystem, a thermal and electric paramagnetic field arise. At this time, the temperature increases, the volume of the formation water expands, heat and hydrogen gas produce. The addition of nanoparticles along with surfactants to the oil-bearing reservoir improves the hydrodynamic properties of the reservoir. It lowers the viscosity of the oil, reduces its specific gravity, increases permeability, expands porosity, accelerates fluidity, and a demulsification process occurs. Due to hydrophobic and hydrophilic interactions, a strong, relatively dense thin film is formed in the system at the phase separation boundary (Aliyev, 2020).
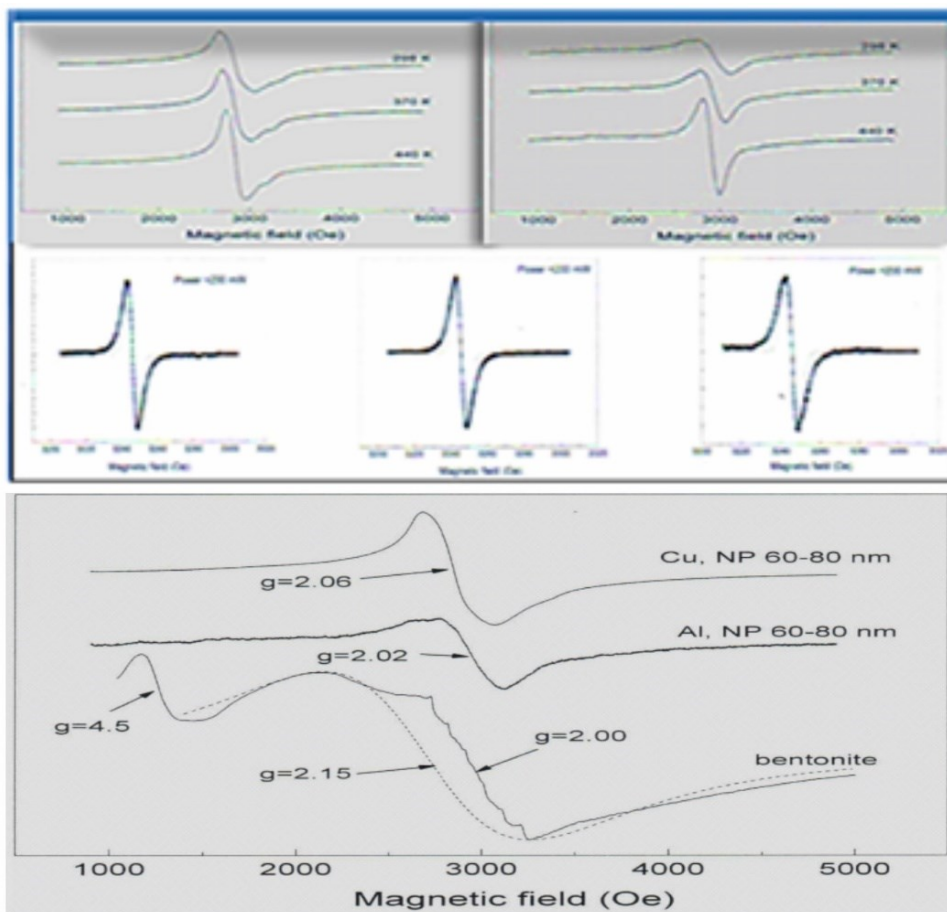
**Figure 1.** Electron paramagnetic resonance spectra in NanoSystems

Nanoparticle solutions enter the capillary pores, moving the oil and gas contained in the pores. It grinds the large gas bubbles in the pores and moves the oil there. It is unevenly distributed between phases. Metal nanoparticles guide the molecules of surfactants and accelerate their movement. Adsorption of a molecule of surfactants occurs, where, in the centers of nanoparticles there is a nanoparticle of metal, and around it are molecules of adsorbed surfactants directed with their polar side towards the metal, and with the non-polar hydrocarbon radical towards the water phase.

The molecules of surfactants are in a position perpendicular to the orientation of the nanoparticles. Due to the effect of nanoparticles, tens of thousands of molecules of surfactants are involved here.

As a result, the formation of mycelium-hedgehogs occurs. Hydrophobic mycelium-hedgehogs are unevenly distributed between the oil and water phases (Figure 2).

During movement, mycelium-hedgehogs acquire an ellipse-like shape. This shape is similar to the state that the jellyfish receives during its movement in water. Such a shape allows for rapid movement of mycels and the formation of a thin veil on the border of oil-water phases. Taking the form of jellyfish during the movement of the mycels makes it easier for the nanosystem to slide on the interphase boundary and provides easier separation of the oil-water phases. This is called the "jellyfish effect" because the shape that the mycels take during this movement resembles a jellyfish (Figure 3), (Aliyev, 2020-a).
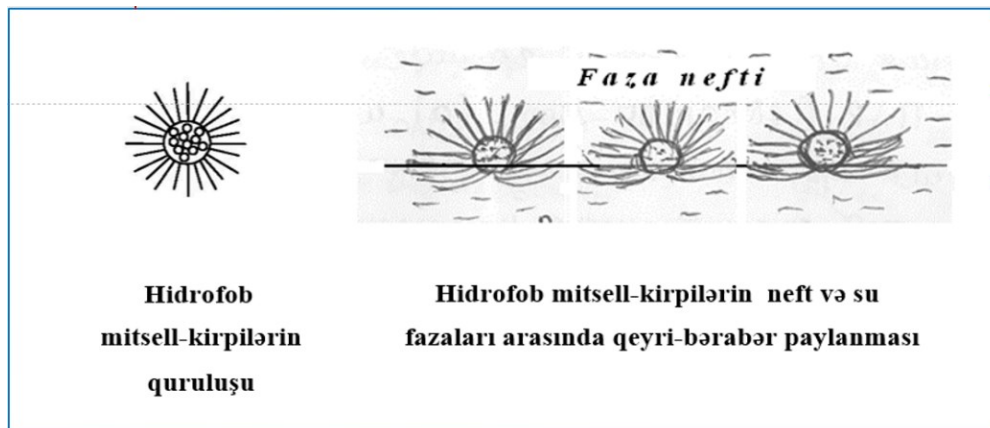


**Figure 2.** Uneven distribution of hydrophobic mycelium-hedgehogs between the oil and water phases
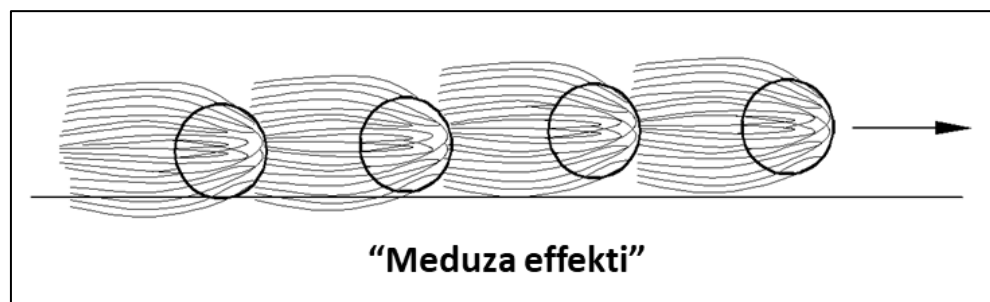


**Figure 3.** The state that the jellyfish effect takes during its movement in the water

When a nanosystem is injected into the formation, the demulsification process occurs in the formation water; as a result, a nanoscreen against formation water and a

nanolayer between the phases are formed. At this time, the surface tension on the surface of oil and rock decreases and separation of oil from formation rocks occurs. As a result of the demulsation process, the conductivity of the reservoir collectors increases, thus, the filtration of oil from the reservoir to the bottomhole accelerates (Bagirov, 1997).

One of the most promising technologies in this area is the treatment of the well zone with specially prepared solutions - nanocompositions consisting of a complex of surfactants and nanoparticles. (Figure 4).

The addition of a small amount of nanoparticles to the surfactant solution improves its oil-compacting properties, increases the hydrophobic property of the mineral matrix (pores) of the rock, thereby providing a more complete coverage (filling) of the reservoirs with the injected liquid. In this case, more effective oil compression is achieved by using multicomponent surfactants of the NANO-SAM type of various molecular compositions. (Shahbazov, 2019).
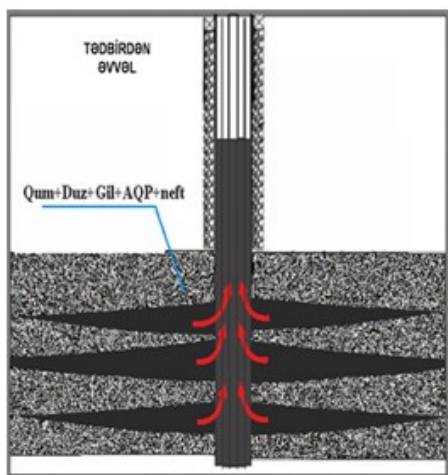


**Figure 4.** Treatment of the well bottom zone with nanosolution

According to the "minor impact and alarm effect" effect, the nanoparticles injected into the layer cause the formation of thermal effect and electromagnetic resonance at the boundary of phases. (Aliyev, 2020-c). Nanoparticles have magnetic properties that remain active up to a temperature of 1200C. By acting on mechanical mixtures (asphalt resin paraffin, salts, sands, etc.), the nanosystem passes into a new, "nano-nucleus" (nano-embryo) phase (Figure 5).

**Figure 5.** The effect of nanoparticles on the formation of thermal effect and electromagnetic resonance at the boundary of phases

It has been experimentally shown that by introducing iron (or aluminum) nanoparticles in bentonite nanocomposite and polyacrylamide into the clay-sand environment at low temperatures (33-360C), catalytic reactions occur, resulting in the separation of bubbles of carbon, hydrogen, ammonia and acetylene oxides.

Because of this, the pressure in the medium increases significantly, and it becomes easier to displace the oil from the porous medium (Abbasov and Aliyev, 2019).

The ability of surfactants to form a continuous adsorption layer on the metal surface is widely used, at the same time, the composition and structure of the adsorption layers depend on the structure of the surface being processed, the chemical properties of the reagents used and many other factors.

The addition of nano-substances to liquids leads to the appearance of unique properties in them. Specially developed nano-compositions significantly increase the oil compression, lubrication and solubility properties of working fluids used in mining conditions.

The introduction of nanotechnology is one of the promising directions for increasing the effectiveness of crude oil transportation in mining conditions. With their help, it is possible to significantly reduce consumption costs.

Nano-Systems help reduce surface tension in the liquid-metal contact area by creating a nano-coating on the inner walls of the reservoir and pipes, weaken

hydraulic resistance, and increase their transportability by creating a nano-coating on the inner walls of oil transport collectors and pipes.

Due to the anti-corrosion effect of nano-substances, there are also economic benefits, such as saving energy and extending the service life of pipes and equipment in mines. The resulting nano-coatings weaken corrosion processes, thereby increasing the service life of pipelines and oil and gas equipment.

## References

**Abbasov J.S. and Aliyev C.A.** (2019). Features of the effect of orography on the temperature change under the earth (Siyazan monocline). Azerbaijani geologist. Scientific bulletin of the society of oil geologists of Azerbaijan.19(23): 102-105.

**Aliyev J.A.** (2020-a). A nanosystem against complications in oil extraction. "Geologist of Azerbaijan" scientific bulletin of the society of oil geologists of Azerbaijan. 24: 87-90 .

**Aliyev J.A.** (2020-b). Application of nanotechnology against bed wetting. ANAS Council of Young Scientists and Specialists, "Young Researcher" scientific-practical journal. 6 (1): 73-79 .

**Aliyev J.A.** (2020-c). Increase in oil recovery of non-homogeneous layers with a new composition. Tver: Scientific and technical journal "Korotazhnik". 3:70-80.

**Bagirov B.A.** (1997). Azerbaijan's reserves are in hard-to-extract oil fields current state of development. Collection of scientific works of ADNA. 2: 3-7.

**Matiyev K.** (2022). Development of a new Flattening Inhibitor for the prevention of salt deposits. Abstracts of the Republican scientific conference "Chemistry and chemical technology".

**Mirzajanzade A.Kh.** (2006). Nanotechnology in oil and gas extraction: research, application and implications. In the report at the VII Azerbaijan International Scientific-Practical Conference.

**Shahbazov E.Q.** (2019). Application of nanotechnology in extraction and transportation of heavy oil in Bibiheybat field. News of Azerbaijan Higher Technical Schools. 21 (4): 37-4

# Building IOS App for Language Learning

## Ilaha Samadova , Leyla Muradkhanli

*Department of Computer Science, Khazar University, Baku, Azerbaijan*
*\*Corresponding author: [ilaha.samadova@khazar.org](mailto:ilaha.samadova@khazar.org)*

**Abstract**
This paper presents the development of an iOS app for language learning, aimed at enhancing user experience and engagement. The app is designed to facilitate language learning by providing definitions, vocabulary lists, and pronunciation practice in a mobile platform. The app was developed using Swift programming language and integrated with a cloud-based server to enable real-time data synchronization and user tracking. The study conducted an evaluation of the app's user experience and engagement through a usability test and user survey. Results showed that the app is effective in enhancing language learning experience and user engagement, particularly in its interactive and personalized approach. The development of the iOS app for language learning with embedded definitions was an extensive process that involved a wide range of considerations. The main objective of this project was to create an app that provides a comprehensive learning experience for English language learners. The development of this app was made possible through the use of Xcode and Swift programming language. Xcode is an integrated development environment (IDE) that allows developers to create apps for Apple devices, while Swift is a programming language developed specifically for Apple platforms. The app's design was carefully crafted to ensure that it is easy to use, engaging, and interactive. The user interface (UI) was designed to be intuitive, allowing users to navigate the app with ease. The app's color scheme and typography were chosen to be visually appealing and consistent with modern design trends. Additionally, the app's design was optimized for different screen sizes, ensuring that it looks great on all iOS devices. One of the key features of the app is its embedded definitions. This feature allows users to easily understand the meanings of new words by providing definitions within the app. This helps learners develop their vocabulary and comprehension skills in a natural way. The app also includes sample sentences to provide context for the new words and help users understand how they are used in context. The app also includes pronunciation exercises to help users improve their pronunciation skills. The app's pronunciation exercises are designed to be fun and engaging, encouraging users to practice and improve their pronunciation skills.

Overall, the development of the iOS app for English language learning with embedded definitions was a significant undertaking that involved a wide range of considerations. The app's features, design, and technological advancements were carefully crafted to provide a comprehensive learning experience for English language learners. With its embedded definitions, sample sentences, and pronunciation exercises, the app is an effective tool for improving users' vocabulary and comprehension skills.

**Keywords**: iOS, Language Learning, Swift, Xcode.

## Introduction

Language learning has become an essential skill in today's globalized world, as people become more interconnected through technology and travel. The ability to communicate in different languages is crucial for individuals to succeed in both personal and professional contexts. With the advancements in technology, mobile applications have emerged as a popular tool for language learning. Mobile language learning applications provide learners with access to language materials and practice exercises anytime and anywhere, making it easier for individuals to learn and practice a language at their convenience. The purpose of this dissertation is to develop an iOS app for language learning that enhances user experience and engagement.

Research has shown that the effectiveness of mobile applications for language learning is dependent on several factors, including the design of the app, the quality of the content, the engagement features, and the level of personalization. Furthermore, the usability of the app plays a crucial role in its effectiveness in enhancing language learning.

The purpose of this research is to develop an iOS app for language learning that enhances user experience and engagement. The study aims to evaluate the effectiveness of the app in enhancing language learning by conducting a usability test and a user survey. The findings of this study will contribute to the growing body of research on mobile applications for language learning and provide insights into the design and development of effective language learning apps.

In summary, this research aims to develop an iOS app for language learning that enhances user experience and engagement. The study will contribute to the growing body of research on mobile applications for language learning and provide insights into the design and development of effective language learning apps.

**Literature Review**

Mobile applications (apps) have become increasingly popular as a tool for language learning, offering learners access to a range of language materials and practice exercises anytime and anywhere. In recent years, several studies have investigated the effectiveness of mobile apps for language learning. This literature review will examine the findings of three studies on the use of mobile apps for language learning, focusing on the design and effectiveness of these apps.

Alharthi and Dickens (2020) conducted a review of the literature on the use of mobile apps for learning Arabic as a foreign language. The authors analyzed 18 studies and found that mobile apps can be effective in enhancing Arabic language learning, particularly in their ability to provide learners with interactive and personalized learning experiences. The authors also found that the quality of the app's content, design, and usability were crucial factors in their effectiveness (Alharthi and Dickens 2020).

Wang and Wang (2019) conducted a review of the literature on mobile learning research in English as a foreign language (EFL). The authors analyzed 45 studies and found that mobile learning can be effective in enhancing EFL learning, particularly in improving learners' vocabulary and reading comprehension. The authors also found that the use of mobile apps in language learning was associated with higher levels of engagement and motivation among learners (Wang and Wang 2019).

Kim and Jang (2021) investigated the effects of a mobile app-based vocabulary learning on EFL learners' vocabulary knowledge and attitudes. The study involved 75 Korean university students who used a mobile app to learn English vocabulary for six weeks. The results showed that the mobile app was effective in enhancing learners' vocabulary knowledge and attitudes towards vocabulary learning. The authors also found that the use of a mobile app provided learners with greater flexibility and convenience in their learning (Kim and Jang 2021).

In summary, the studies reviewed in this literature review suggest that mobile apps can be effective in enhancing language learning, particularly in their ability to provide learners with interactive and personalized learning experiences. The design, content, and usability of the app are crucial factors in its effectiveness, and the use of mobile apps is associated with higher levels of engagement and motivation among learners.

**Architecture**

Model-View-Controller (MVC) architectural pattern is used in the development of the language learning application. The model, which controls the data and business logic, the view, which shows the data to the user, and the controller, which manages user input and coordinates with the model and view, divide the app into three different parts (Table 1).

**Table 1. MVC design pattern**

| Component | Responsibilities |
|---|---|
| Model | - oversees the application's data and business logic.- Maintains user preferences, word lists, and grammatical rules in storage- Gives the controller a way to access and change the data. |
| View | - shows the user the user interface (UI) for the software.- Consists of UI components including buttons, labels, and text fields- Pays attention to user input and delivers it to the controller so it may be processed. |
| Controller | - enables communication between the model and the view and manages user input.- Analyzes user input and adjusts the model as required.- Modifies the view to match model changes. |

API is used in this app to give definitions inside language learning software. The following actions need to be taken for using API:

let key = "your_api_key_here"

let query = "lookup_here"

let url = "https://api.dictionaryapi.dev/api/v2/entries/en/ "

guard let url2 = URL(string: url) else {

  print("Invalid URL: \(url)")

  return

}

```
let result = URLSession.shared.dataTask(with: url) { data, response, error in

  guard let info = info else {

    print ("Nothing received: \(error?.localizedDescription ?? "Unknown error")")

    return

  }

  do {

    let json = try JSONSerialization.jsonObject(with: info, options: [])

    // Extract the definition(s) for the search term from the JSON object by parsing it

    // The UI of your app should display the definition(s)

  } catch {

    print("Error parsing JSON: \(error.localizedDescription)")

  }

}

result.resume()
```

## Methodology

The app was developed using Swift programming language and integrated with a cloud-based server to enable real-time data synchronization and user tracking. The app's features include interactive lessons, vocabulary lists, and conversation practice exercises. The app was evaluated using a usability test and user survey to determine its effectiveness in enhancing user experience and engagement. The usability test involved participants performing specific tasks using the app, while the user survey collected feedback on the app's usability, design, and content.

## Conclusion

The development of an iOS app for language learning is a promising approach in enhancing user experience and engagement in language learning. The app's

personalized and interactive features contribute to its effectiveness in facilitating language learning. The study's findings suggest that further development of the app, particularly in content diversity and social interaction features, can enhance user engagement and motivation. Future studies can explore the longitudinal evaluation of the app's effectiveness in language learning.

## References

**Alharthi, R., & Dickens, L.** (2020). Mobile Apps for Learning Arabic as a Foreign Language: A Review of the Literature. Language Learning & Technology, 24 (3): 118–135.

**Kim, J. H., & Jang, H. W.** (2021). The Effects of a Mobile App-Based Vocabulary Learning on EFL Learners' Vocabulary Knowledge and Attitudes. International Journal of Emerging Technologies in Learning (iJET), 16 (2): 49-62.

**Wang, M., & Wang, Y.** (2019). A review of mobile learning research in English as a foreign language. Educational Technology Research, 67(5): 1114-1148.

# Selection of Artificial Lift Method

## Khadija Gasimova

*Faculty of Graduate School of Science, Art, And Technology,*
*Khazar University, Baku, Azerbaijan*
*xadica.qasimova@khazar.org*

**Abstract**

For most of producing oil and gas wells to be profitable over the long term, the appropriate artificial lift technique must be chosen. The present research examines the key selection criteria for the eight current primary artificial lift techniques and offers useful recommendations on the performance and applicability of the techniques based on real-world and tested technology. This paper discusses plunger lift, gas lift, hydraulic jet pumping, beam pumping, progressive cavity pumping, electric submersible pumping. The main goal of this study is to choose the best method, such as natural drive and artificial lift methods for accelerating and optimizing hydrocarbon production in the ARC oil field using the PROSPER software package and fictitious well data from Well WE1. The electrical submersible pump method is the subject of the nodal analysis for both natural drive cases and artificial lift techniques on PROSPER. Natural drive, ESP have calculated oil production rates of 57.2sm3 /day, 94.4 sm3 /day respectively. According to this study, using artificial lift techniques dramatically boosts oil production.

**Keywords:** Artificial Lift techniques, Nodal Analysis, Natural Drive, Prosper.

## Introduction

Selecting the optimal lift technique correctly is frequently based on strong convictions. Operating staff unconsciously chooses the lift technique that they are most accustomed to. Equipment manufacturers or even internal experts on a certain approach frequently advise that the standards might be adjusted to meet their preferred way. Getting accurate operational cost information on the lift method over the well's life is the most challenging aspect of the analysis. If possible, data from wells that are similar should be used. The present value profit of the particular artificial-lift method can be determined using those Figures along with forecasts for salvage value, inflation, taxes, and other factors (Clegg et al., 1993). The

characteristics of reservoir fluids are distinguished using the measurement of oil reservoirs and their performance with hydrocarbon reservoirs, which is significant in numerous reservoir investigations. Using the necessary methodologies to get precise property values is therefore crucial in the various oil sectors (Abdurazzaq, 2021). The idea of production optimization became necessary when the first oil reserves began to experience serious depletion. Exploring new fields involves a lot of risk and uncertainty, thus it's critical to explore every option available in the existing reservoirs as soon as possible (Surajo, 2017).

**Petroleum Production Wells**

The parts of a naturally flowing well are the reservoir segment, wellbore, and wellhead (Figure 1). Production fluids are sent from the reservoir portion to the wellbore. The wellbore provides a pathway for the fluids to travel from the bottom hole to the surface. At the wellhead, the fluid output rate can be changed. An oil or gas reservoir is defined as a single porous and permeable subterranean rock formation that is enclosed by impermeable rock or water barriers and contains a discrete bank of fluid hydrocarbons. Based on the hydrocarbon content and initial reservoir state, engineers classify oil, gas condensate, and gas reservoirs. (Guo, 2008)
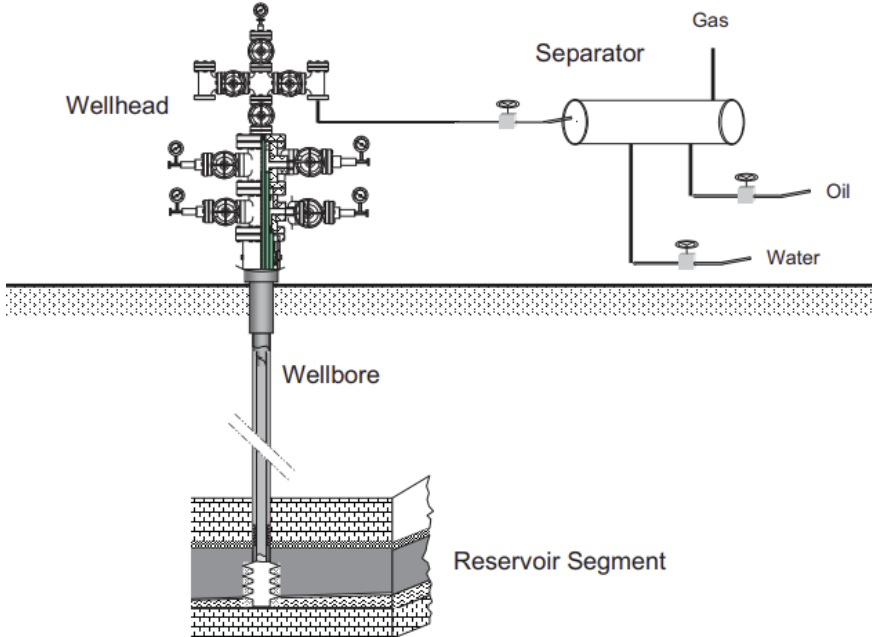


**Figure 1.** Oil and gas are produced by naturally flowing wells under their own pressure. (2008 by Gulf Publishing Company)

## Pumping

In order to raise the pressure in the well and compensate for the total flowing pressure losses, pumping is used. It can be further categorized using a variety of characteristics, such as the pump's working principle. However, the most widely used classification separates rod and rodless pumping based on how the downhole pump is operated. The surface drive mechanism and downhole pump are connected by a series of rods that, depending on the type of pump being used, either oscillate or rotate. Positive displacement pumps that needed an alternating vertical movement to work were the first types to be used in water and oil wells. A recently developed rod pumping system makes use of a progressive cavity pump, which requires rotation of the rod string to function. This pump operates on the same positive displacement concept as the plunger pumps used in other kinds of rod pumping systems, but it lacks valves. As the name indicates, rodless pumping techniques do not use a rod string to control the downhole pump from the surface. The downhole pump is therefore driven by means other than mechanical, such as electric or hydraulic. Rodless pumping can use centrifugal, positive displacement, or hydraulic pumps, among other types of pumps. A multistage centrifugal pump is powered by a submerged electrical motor in electric submersible pumping (ESP). Electricity is delivered to the motor via a cable that is run from ground level up. These machines are perfect for producing large amounts of liquid. The other rodless lifting techniques all use a high-pressure power fluid that is injected into the hole. The first technique created was hydraulic pumping, which uses downhole units with a positive displacement pump powered by a hydraulic engine. Despite being a hydraulically powered method of fluid lifting, jet pumping operates entirely differently from the rodless pumping concepts previously covered (Gabor, 2017).
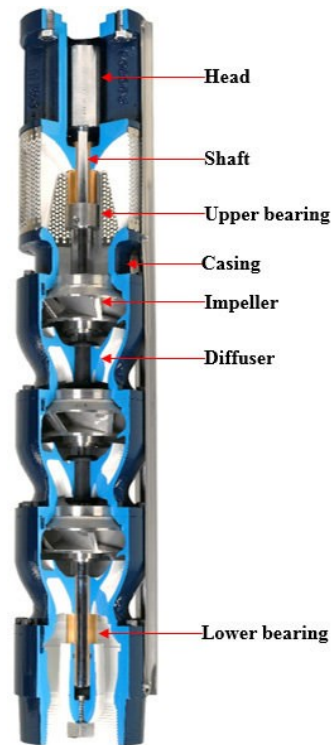


**Figure 2.** Main components of an electrical submersible pump (ESP). (Multistage assembly http://www.franklinwater.com).

## Main objective of Electrical Submersible Pumps

ESPs are frequently employed in the petroleum sector to boost the production rates of hydrocarbon fluids, particularly for offshore deep-water oil fields. The revolving

impeller and stationary diffuser are components of each stage of a multistage ESP that is typically installed in series (Figure 2). Due to the substantial depth of the reservoir, the ESP system in oil fields often consists of hundreds of stages to achieve the boosting pressure need. The impeller, which spins the blades to force fluid flow and impart kinetic energy to the fluids, is the main component of ESP. The majority of the fluid's kinetic energy is transformed to pressure potential by diffuser vanes at the impeller's exit. (Zhu and Zhang, 2018).

ESP has a higher flow rate and a greater drawdown than the majority of other artificial lift techniques. (Yudi, S., 2013). However, ESP has the following advantages and disadvantages:

 The benefits of ESPs

- ✓        Adaptable to wells with high deviations, up to 80°.
- ✓        Adjustable to needed 6'-diameter subsurface wellheads.
- ✓        Quiet, secure, and hygienic for proper operations.
- ✓        Usually regarded as a large volume pump.

ESP drawbacks as well

- ✓        Will put up with low levels of sand production.
- ✓        Expensive pulling operations to fix downhole issues
- ✓        Production decline when on a DHF
- ✓        Less than 150 B/D gross in volume does not work well.

**Gas Lift Technique**

Gas is often injected during the gas lift operation into the space between the production tube and casing. A single or more typically a number of gas lift valves then permit the gas to enter the flow stream within the production tubing at a particular depth. The fluids flowing in the tubing at that depth and throughout the tubing above the injection point have a gradual increase in the gas liquid ratio due to the injection of gas into the production tubing. (Production Technology - 1, 2015). Compressors are used to supply the gas pressure necessary for pipeline gas transportation as well as to raise oil in gas-lift activities. The two main types of compressors utilized in the production of natural gas nowadays are reciprocating and rotary compressors. In the natural gas business, reciprocating compressors are the most widely utilized equipment. Practically all pressures and volumetric capabilities are supported by their design. (Guo, 2007).

**Details of the Simulation Model's components**

After collecting all data for the reservoir simulation model related to reservoir fluid properties is taken https://www.researchgate.net/publication/355270858 with some additional parameters, and table containing the data needed for the software is created for well. The Prosper Software is used to enter the data, and the model with the lowest error rate is chosen. The program then uses the black oil model, which functions at the expense of the characteristics of the other reservoir fluids, to match the input values.

**Prosper Information**

One of the most critical aspects of well analysis is evaluating whether wells may be capable of producing at a higher rate than the existing one. PROSPER, a well modeling software, is intended to help ensure that well models are accurate and consistent. It also handles every component of well modeling, including PVT (fluid description), VLP correlations (for computing flow-line and conduit pressure loss), and IPR (reservoir inflow).

**Simulated Well Modelling.**

The ARC field produces oil and gas via WE1 wells . The long-term plan for the ARC field, optimization of oil well output in the ARC field, and the efficiency of gas production to improve oil well production are all factors driving the implementation of this research. The goal of this research is to examine oil wells in the ARC Field that have the potential to boost production through Artificial Lift.

**Methodology**

The PROSPER software package, which aims to get inflow/outflow performance curves, create IPR and VLP models, select the best artificial lift method, perform well perforation design, and so on based on the minimum required input data, is used to generate the inflow performance relationship (IPR) and vertical lift performance (VLP) curves for this study. To improve the accuracy of models created using the program, genuine manufacturing history data can also be entered. The program is a creation of Petroleum Experts Limited (PETEX), a UK-based company that produces some of the petroleum industry's most frequently utilized software (IPM PROSPER User Manual, Version 11.5, January 2010).

**Data Requirements**

✓     PVT data
✓     Reservoir Data
✓     Equipment data, including as downhole equipment, deviation surveys, geothermal gradients, and average head capacities
✓     ESP case data

**Table 1. Reservoir and fluid properties**

| Properties,Unit | Value |
|---|---|
| Reservoir pressure, atm | 89 |
| Bubble point pressure, psi | 3600 |
| Reservoir Temperature, F | 250 |
| Gas Oil Ratio, scf/stb | 800 |
| Water cut, % | 50 |
| API | 35 |
| Gas specific gravity | 0.78 |
| Water salinity, ppm | 80.000 |
| Oil FVF, bbl/stb | 1.45 |
| Oil viscosity, cp | 0.3 |
| Reservoir permeability ,md | 20 |
| Reservoir thickness ,m | 15 |
| Drainage area,$m^2$ | 820000 |
| Dietz shape factor, unitless | 23.9 |
| Skin factor, unitless | 2 |
| Wellbore radius, inches | 9 |
| TD,m | 780 |
| MD,m | 560 |

**Table 2. Input PVT Data**

| PVT properties, Unit | Value |
|---|---|
| Solution GOR, scf/STB | 800 |
| Oil gravity ,API | 35 |
| Gas gravity,sp | 0.78 |
| Water salinity,ppm | 80000 |
| Mole percent H2S, % | 0 |
| Mole percent CO2 ,% | 0 |
| Mole percent N2,% | 0 |

## The Well Model

Building a Model for Well-Performance PROSPER is used.
There are 6 areas on the PROSPER primary screen:
1.        Options Summary
2.        PVT Data
3.        IPR Data
4.        Equipment Data
5.        Analysis Summary
6.        PROSPER Version

## Model ConFigureuration for Natural Drive Case



**Figure 2.** Prosper System Summary

The software use the Vogel's model below the bubble point and the Darcy's equation above the bubble point.Vogel's method is one of the most often used techniques for creating inflow curves.The "Darcy" model is applied here. To build the IPR curve,

production rates at varied drawdown pressures are used. In order to match the PVT test data to the Black Oil correlations that are available on PROSPER, basic PVT input data from offset wells, such as GOR, API gravity, Gas gravity, Water salinity, and impurities present in reservoir fluid, are first introduced into the software. The software calculates the previously mentioned PVT properties after taking into account the entirety of the available data as well as the "Calculate" option used for building the IPR curve.
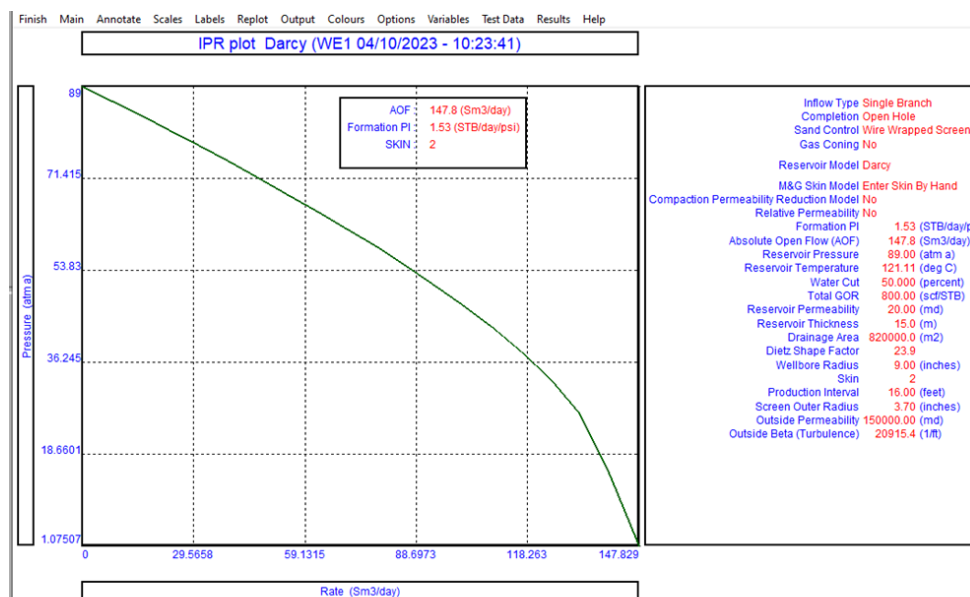


**Figure 3.** Plot of IPR according to Darcy Reservoir Mode

According to the Figure observed above, the estimated absolute open flow (AOF) 147.8 $sm^3$ /day and the formation productivity index (PI) is 1.53 STB/day/psi.

As seen in the graphic above, the oil rate and bottom hole flowing pressure (BHFP) are 57.2 $sm^3$ per day and 39.63 atm, respectively. It means that the intended well may flow naturally based on the input parameters.

**Model ConFigureuration for ESP Case**

The PROSPER model requires that the PVT data be matched with the matching parameters using the appropriate correlation. There are numerous relationships that might be relevant. In order to get the optimal correlation to represent the features of

the reservoir fluid, Prosper software will go through numerous iterations. A combination of a pump, motor, and cable is chosen from a list provided by PROSPER as the last step in the ESP design process. The Schlumberger REDA D1440 (101.6 mm OD) pump, which offers the finest performance among the pumps, is chosen to provide the most efficiency.
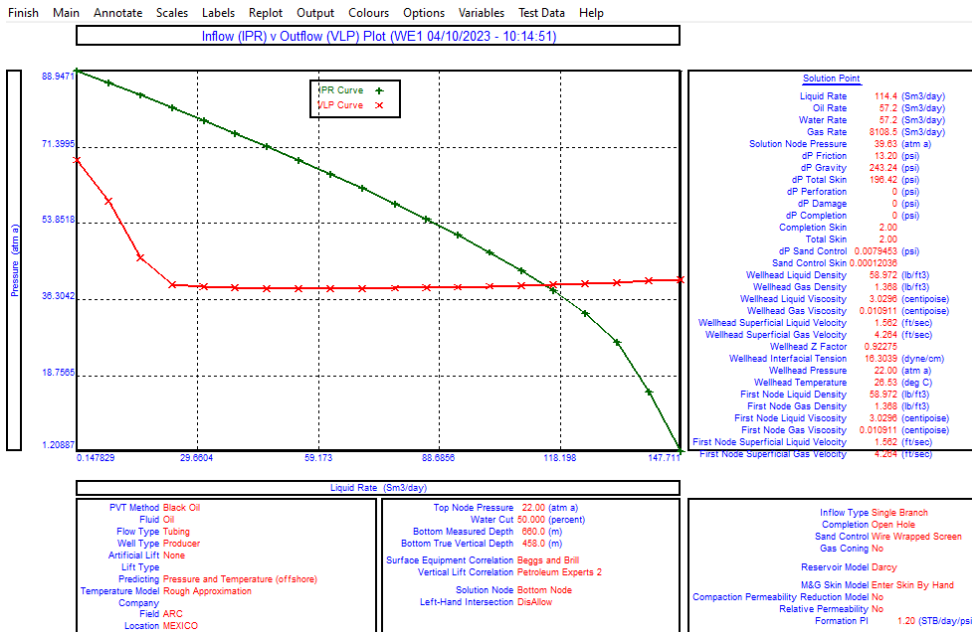


**Figure 4.** IPR and VLP curves for the natural drive situation

From the wellhead to the pump discharge, the Pump Discharge Pressure is displayed in the picture above as a blue curve, the IPR as a green curve, and the VLP as a red curve.

The liquid rate and oil rate determined by PROSPER for this scenario are clearly shown in the above Figure to be 188.9 $sm^3$ per day and 94.4 $sm^3$ per day, respectively. In order to get the best performance out of the pump, the ESP case is modelled on PROSPER.

**Discussion and Conclusions**

The software receives all necessary data from PVT, deviation survey, geothermal temperature profile, and downhole equipment, and then creates the IPR curve. Following the modeling of the natural drive case and the ESP case the operating

points at the intersection of the IPR and VLP curves are obtained for each scenario using the system calculations menu. The obtained findings demonstrate that the well modelled oil production in the natural drive case for the oil rate and bottom hole flowing pressure (BHFP) are 57.2 $sm^3$/day and 39.63 atm, respectively. However, the production rate is dramatically raised when artificial lift techniques are used. It is clear from the data that applying ESP results in increased production rates, and that this can be used to improve and optimize production. Given that ESPs have a limited existence and that it will be necessary to replace the downhole ESP lifted wells, careful planning is essential to completing this project. In order to get the best performance out of the pump, the ESP case is modelled on PROSPER. The system calculations show that the oil production rate is equal to 94.4 $sm^3$/day.
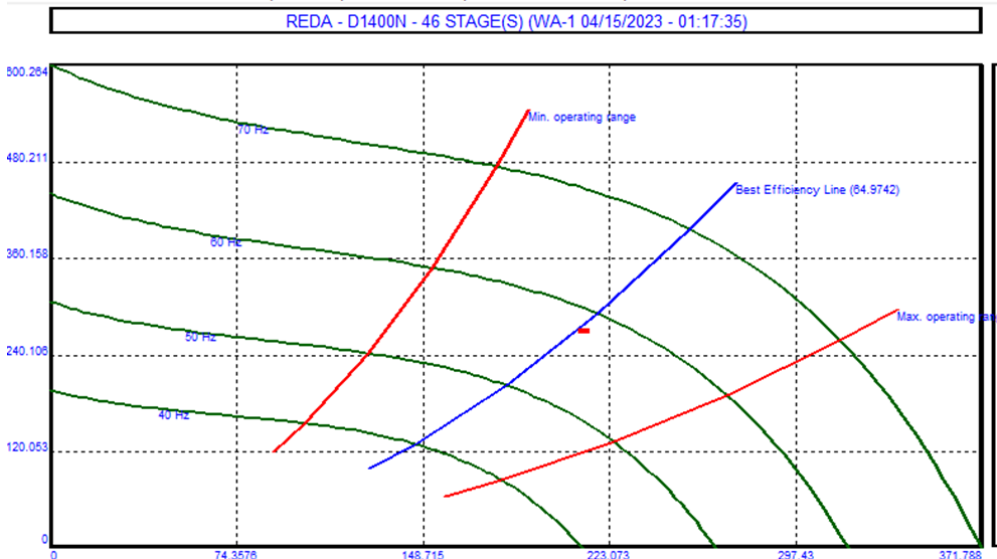


**Figure 5.** Performance Curve of REDA1440

**Recommendations**

The PROSPER modeling used for this research was effective and the best choice for maximizing and optimizing hydrocarbon output. More advanced software is needed to make an integrated approach when it comes to field production optimization and enhancement, taking into account the surface network of existing wells and available subsurface data.
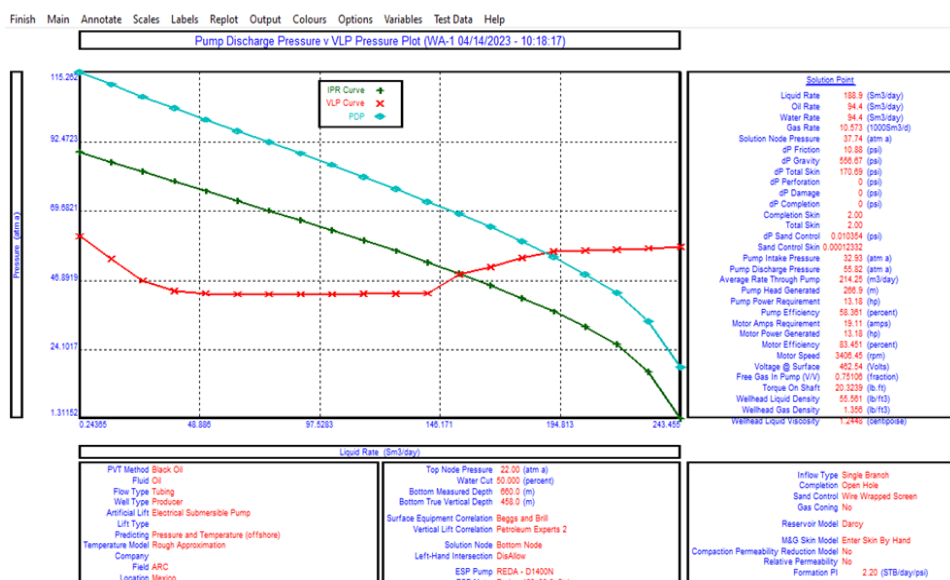
**Figure 6**. Pump Discharge Pressure vs VLP Plot for ESP-lifted well

## References

**Abdelhady, A., Gomaa, S., Ramzi, H., Hisham, H., Galal, A., Abdelfattah, A.** (2020). Electrical Submersible Pump Design in Vertical Oil Wells, Pet Petro Chem Eng J. 4(5): 000237.

**Abdurazzaq, T., Togun, H., Haider, D., Hamadi**, M.A. (2021) Determining of reservoir fluids properties using PVTP simulation software- a case study of buzurgan oilfield ,1-2

**Clegg, J.D. et al**. (1993). Recommendations and Comparisons for Selecting Artificial-Lift Methods. 6-8.

**Gabor, T.** (2017). Electrical Submersible Pumps Manual Design, Operations, and Maintenance. 43-44.

**Guo, B.** (2007). Petroleum Production Engineering, A Computer-Assisted Approach. Gulf Professional Publishing. 31-32.

**Guo, B., Sun, K., Ghalambor A.** (2008). Well productivity handbook by Gulf Publishing Company.10-11

**IPM PROSPER User Manual,Version 11.5**. (2010). United Kingdom: Petroleum Experts.58-60.

**Production Technology.** (2015). Edinburgh, United Kingdom: Heriot Watt University, Institute of Petroleum Engineering. 22-23.

**Surajo, A. I. K.** (2017). Nodal Analysis and Artificial Lift Methods. 24-25.

**Yudi, S.** (2013). Analytical Study of Oil Recovery on Gas Lift and ESP Methods. 5-6.

**Zhu, J., Zhang, Hong-Quan.** (2018). A Review of Experiments and Modeling of Gas-Liquid Flow in Electrical Submersible Pumps. 2-3.

# The Impact of Augmented Reality Application Development on University Teaching Curricula

## Mutaz Mohammed Abuhashish, Leyla Muradkhanli

*Department of Computer Science, Khazar University, Baku, Azerbaijan*
*mutaz.mohammed@khazar.org*

**Abstract**

The rapidly developing field of augmented reality (AR), which has the potential to completely transform the educational system, is called "augmented reality." AR applications may be utilized to build learning environments that are immersive and engaging, which can help students better absorb and remember the content they are being taught. In this article, we examine the research that has been conducted about the influence that AR has had on the growth of educational curricula in higher education institutions. We highlight the benefits of employing AR in education, such as higher learning outcomes, greater problem-solving abilities, and increased student engagement. We also go through some of the difficulties associated with implementing augmented reality in educational settings, such as the high cost of AR hardware and the prerequisite of specialized instruction. In conclusion, we provide some suggestions as to how universities may benefit from incorporating augmented reality into their existing instructional programs.

**Keywords:** augmented reality, educational curricula, learning, student, developing.

**Introduction**

Augmented Reality (AR) technology is growing and developing rapidly, and its potential to develop and improve teachers' experiences has received a lot of attention in recent years. Augmented reality applications have been increasingly used in various fields, including education, as they can improve student engagement and understanding of complex ideas and concepts associated with undergraduate educational curricula,(Chiang et al., 2022) augmented reality technology can change traditional classroom learning environments by providing an interactive and immersive learning experience. (Lampropoulos et al., 2022)The impact of the application of Augmented Reality in university (Manuri & Sanna, 2016) educational curricula plans is a topic of extraordinary interest and importance for teachers,

students, and researchers. This technology has been shown to improve knowledge retention and retrieval, as well as problem-solving and critical thinking skills.

However, there are some challenges to integrating AR technology into school curricula, such as the need for specialized software development skills, and access to appropriate hardware. Augmented Reality technology is becoming more accessible with the rise of smartphones and tablets equipped with AR capabilities, such as Apple's ARKit and Google's AR-Core. (Yuliono & Rintayati, 2018) This technology allows users to experience a blend of the physical and digital worlds by overlaying virtual objects onto the real world in real time.

This presents unique opportunities for educators to create immersive and engaging learning experiences that can increase student motivation and interest in the subject matter.(Chen et al., 2022) One potential application of AR in university education is in the teaching of STEM (Science, Technology, Engineering, and Mathematics) subjects. AR can be used to visualize complex concepts such as molecular structures or engineering designs, allowing students to interact with virtual objects in a way that was not possible before(Duan et al., 2022). AR can also provide opportunities for hands-on experimentation without the need for expensive equipment or facilities.

AR can also be used to enhance language learning by providing students with immersive language experiences. For example, students can use AR to practice language skills by interacting with virtual objects and characters in a simulated real-world environment. However, there are challenges associated with integrating AR technology into university curricula. One difficulty is the need for specialized software development skills, as creating augmented reality applications requires knowledge of programming languages and software development tools, which not all educators have access to.

Teachers may need to invest in equipment such as smartphones or tablets. Despite these challenges, the potential benefits of AR in education make it an area of growing interest and research. Incorporating AR technology into university curricula has the potential to improve student engagement and understanding of complex concepts, leading to better learning outcomes increased and retention of knowledge. (Arulanand et al., 2020)His paper aims to explore the potential impact of AR application development in university educational curricula. It will examine the benefits and challenges associated with the use of AR technology in education and provide examples of how AR has been successfully integrated into university courses.

The paper will also explore the skills and knowledge required to develop AR applications(Tang et al., 2020) and the role of educators in guiding students through

the development process. Ultimately, this paper will argue that the integration of AR technology in university curricula has the potential to improve student learning outcomes and enhance the overall quality of the educational experience. the research topic arises from answering the following key question: What is the Role of Augmented Reality Application Development in Teaching Undergraduate Courses?

The following are the study hypotheses: Augmented reality is quite useful in a variety of educational settings? One of the most essential educational digital applications is augmented reality. Using augmented reality applications in teaching has a major positive influence? Maintaining a widespread culture of digital education apps that use augmented reality? There have been several earlier experiences using augmented reality in teaching? Augmented reality makes a vital contribution to educational applications?

Science, engineering, and medicine are the most common AR uses for education. The usage of augmented reality (AR) is being utilized to increase student engagement, motivation, and learning results. According to these Figures, augmented reality is quickly becoming a mainstream technology in education. As AR technology advances, we should expect to see much more widespread use of AR in university education.

## Augmented Reality

Augmented Reality is a technology based on projecting virtual objects and information into the user's real environment to provide additional information or act as a guide for him, in contrast to virtual reality based on projecting real objects into a virtual environment(Arulanand et al., 2020). Aller can deal with information and virtual objects in augmented reality through several devices, whether they are portable such as a smartphone or through devices that are worn such as glasses and contact lenses.(Karagozlu, 2018) All of these devices use a tracking system that provides accurate projection, displaying information in the appropriate place such as the global positioning system (Global Positioning System), camera, and compass as inputs that are interacted with through applications.

Augmented reality is an enhanced, interactive version of a real-world environment that is achieved through digital visuals, sounds, and other sensory stimuli via holographic technology. Augmented reality includes three features: a combination of the digital and physical worlds, real-time interactions, and precise 3D identification of real and virtual objects.

Augmented reality provides a better way to design, organize, and deliver consumables by overlaying digital content in real-world work environments(Mota et

al., 2018). When a business understands augmented reality and how to use it successfully, everyone can work remotely while collaborating efficiently.

## Types of augmented reality

When deciding what kind of augmented reality technology you'll need for your business, you'll first have to decide what kind of augmented reality you want to use. There are two types of augmented reality: tag-based and taggles.(Edwards-Stewart et al., 2016) Choosing one of these types of augmented reality will determine how you will be able to view your images and information.

Tag-based AR is created using image recognition to identify objects already programmed into your AR device or app.(Peddie & Peddie, 2017) By placing objects as reference points, they can help the augmented reality device determine the camera's position and orientation. This is generally achieved by switching the camera to grayscale and detecting a tag to compare that tag with all the other tags in its databank. (Jasche et al., 2021)Once your device finds a match, it uses that data to mathematically determine the position and place the AR image in the right place.

Marker-less augmented reality is the most complex as there is no point for your device to focus on. For this reason,(Jasche et al., 2021) your device must recognize the items as they appear in the display. Using a recognition algorithm, the device will look for colors, patterns, and similar features to determine what that object is and then, using time, accelerometer, GPS, and compass information, will orient itself and use the camera to overlay an image of whatever you want in your real-world surroundings.

## The future of augmented reality in education

There is no doubt that learning through practice is more effective than different teaching methods such as reading and writing.(Özeren & Top, 2023) Thus, augmented reality can participate strongly in this field, and enter the classroom, which would be a stimulus for learning and increase concentration (Ozdemir et al., 2018). The nature of augmented reality by displaying virtual objects in the real environment for students would be beneficial in improving student performance and increasing their interaction. Moreover, it provides them with the opportunity to see, move, and interact with three-dimensional images through books designed for that.

Augmented reality contributes to much scientific research, especially those that cannot be dealt with in a traditional way, for example, to do chemical reactions for the course of chemistry; Augmented reality provides the possibility to use virtual materials, mix them and see the results in the classroom without the need for these

materials or laboratories.(Yuliono & Rintayati, 2018) Space science is one of the most important areas in which augmented reality can be applied due to the ambiguity it contains and the lack of infrastructure for monitoring from astronomical observatories, especially in the Arab world, so that augmented reality applications are used to display planets and galaxies on mobile devices such as smart phones that have (GPS) to determine the user's location (longitude and latitude) and the compass and to determine the user's direction and the accelerator to determine the height, the global system for determining time (universal time) all of these four elements work together through a series of operations and calculations to determine the destination (Shirazi & Behzadan, 2015)The user is then shown galaxies, planets...etc. Perhaps the most notable application in this field is observing the "Gazing star" sky.

The application of augmented reality in education still faces several challenges, which is that displaying educational content requires technical experts,(Kurt & Öztürk, 2021; Sari et al., 2017) and investment in this field is costly and requires advanced devices such as cameras and projectors, and experts are needed to repair any malfunctions. In addition, augmented reality is still not accurate in displaying objects in the right place and time.

**The importance of augmented reality in education**

Augmented reality holds great importance in the field of education and can have a positive impact on the learning process.(Han et al., 2022) Here are some reasons why augmented reality is important in education:

Exciting Learning Experience: Augmented Reality provides an exciting and interesting learning experience for students.(Pasaréti et al., 2011) By integrating digital elements with the real world, learning becomes an interactive and innovative experience that engages students and motivates them to explore the subjects.

Enhancing interaction and participation: Augmented reality can contribute to enhancing interaction and participation among students. (Wu et al., 2013)It gives them the opportunity to interact with and interact with digital objects in a real-world context, which promotes collaboration and engagement among students.

Provide real-world experiences: Augmented reality allows learning elements to be experienced in real-world contexts.(Elmqaddem, 2019) Students can explore educational places, objects and phenomena in a more realistic and detailed manner, which contributes to a better understanding and practical application of academic concepts.

Enhancing critical thinking: Augmented reality can contribute to enhancing students' critical thinking. When students interact with digital elements and explore concepts first-hand, critical and analytical thinking and creativity speak(P. Chen et al., 2017).

Developing practical skills: Augmented reality provides an opportunity to develop a range of practical skills in students. Students can collaborate on learning projects that use augmented technology, enhancing communication, collaboration, and problem-solving skills.

Expanding access and communication: Augmented reality can expand students' access to learning materials and resources. Students in remote or inaccessible areas can access exciting learning experiences through augmented reality technology.

Augmented reality can improve the learning experience and contribute to students' skills, interaction, and participation in the learning process. Thus, augmented reality plays an important role in developing education and improving learning outcomes.

**Augmented reality applications in education**

Augmented reality technology has multiple applications in the field of education. Here are some examples of how augmented reality can be used in education:

Enhanced Science Experiments: Augmented reality can be used to enhance science, chemistry, and physics experiments. Students can explore scientific processes first-hand and watch and interact with 3D experiments for a better understanding of scientific concepts(Tzima et al., 2019).

Virtual educational tours: Augmented reality can be used to organize virtual educational tours of museums and historical and cultural sites. Students can visit remote or hard-to-reach locations and explore them realistically and interactively (Tekedere & Göke, 2016).

Teaching foreign languages: Augmented reality can be used in learning foreign languages by creating interactive virtual environments to interact with the target language. Students can practice conversations and learn vocabulary and grammar through interactive experiences(Crandall et al., 2015).

Learn practical skills: Augmented reality can be used to develop practical skills such as engineering, design, and architecture. Students can create and interact with 3D models to develop hands-on skills and experience practical operations more realistically(Iqbal et al., 2022).

Develop stories and narratives: Augmented reality can be used to transform stories and narratives into exciting visual experiences. Students can see and interact with the characters and events in the novel in 3D, which enhances understanding and imagination of the story.

Teaching motor skills: Augmented reality can be used to teach motor skills such as dance and sports. Students can watch motion models and simulate movements to improve their technique and performance(Bacca Acosta et al., 2014).

These are some examples of how augmented reality can be used in education. Applications and uses are constantly evolving, enhancing the learning experience, and enhancing student engagement and interaction in the educational process.

**Materials and methods**

Augmented reality (AR) is a technology that superimposes a computer-generated image on a user's view of the real world, thus providing a composite view. AR has the potential to revolutionize education by creating immersive and interactive learning experiences that can help students to better understand and retain information. In this research, we follow the most important methods to answer the research hypotheses.

 **1-Development of educational applications commensurate with the requirements of modern technological technology.**

Several major elements must be considered while developing educational applications that fulfil the criteria of contemporary technological technologies. The utilization of interactive and immersive technology such as augmented reality (AR) and virtual reality (VR) is one of the most essential components. These technologies can provide a more interesting and immersive learning experience, which can allow students' attention to be captured and maintained. Another critical factor to consider is the use of personalized learning strategies that address individual student demands and learning styles. Furthermore, the development of educational applications should focus on improving students' critical thinking, problem-solving, and teamwork abilities, as they are necessary for success in the modern workforce. Finally, educational apps must be accessible and inclusive for all students, including those with disabilities or special needs, to benefit from them. Taking these elements into consideration, educational apps that are consistent with the requirements of contemporary technological technology and that may assist to improve the quality of education for all students can be produced.

## 2- The urgent need to develop modern training and education methods.

The rapid rate of technological progress, globalization, and evolving worker expectations have produced an urgent need for contemporary training and education approaches to be developed. Traditional education and training systems are no longer adequate to fulfil the demands of the modern workforce, which expects employees to be adaptive, inventive, and adept in developing technology. Furthermore, the current COVID-19 epidemic has emphasized the need for creative and adaptable training approaches that may be taught remotely or via hybrid learning models. To meet these difficulties, current training and education techniques must emphasize critical thinking, problem-solving, and teamwork abilities, as well as the incorporation of emerging technologies like augmented reality, virtual reality, and artificial intelligence. Furthermore, current training and education techniques should be accessible, adaptable, and personalized in order to suit to learners' specific requirements and learning styles. We can help to guarantee that individuals are prepared with the skills and information required to thrive in the contemporary workforce and to adapt to the continuous changes and challenges of the twenty-first century by establishing new training and education approaches.

## 3- keeping pace with the rapid developments of Augmented Reality applications in education.

Augmented Reality (AR) is a fast-expanding discipline, with new technology and applications emerging at a rapid rate. As a result, educators and educational institutions have huge difficulty in keeping up with the newest innovations in AR applications in education. However, staying current on these advances is critical to guarantee that educational programs are relevant, interesting, and successful in preparing students for the needs of the modern workforce. Furthermore, by staying up to date on the newest AR apps and tools, educators may remain ahead of the curve in terms of adopting cutting-edge technology into their teaching practices, which can help attract and retain students while also improving overall educational quality. Educators and institutions may keep up with the newest advances in AR applications in education by attending conferences, seminars, and other professional development opportunities, as well as reviewing relevant material and engaging with the AR community on a regular basis. Furthermore, it is critical to interact with industry partners and other stakeholders to ensure that the educational curriculum corresponds with the most recent workforce demands and trends.

**Results and discussions**

**Manifesting the role of augmented reality in various fields of education.**

Augmented Reality (AR) has a function in education that goes beyond the usual STEM professions. AR may be used in a variety of disciplines and fields, such as art, history, literature, and language acquisition. AR may be utilized in the realm of art to bring paintings and sculptures to life, allowing students to understand the artistic styles and techniques of many eras and artists. AR in history may give students a more immersive and interactive experience, allowing them to examine historical locations and events in a more engaging and memorable manner. AR can give a more dynamic and engaging experience for students in language learning, allowing them to practice their language abilities in a realistic and immersive setting. Furthermore, augmented reality (AR) can assist to bridge the gap between theory and practice by allowing students to apply their knowledge in real-world settings and build practical abilities that employers greatly value. As a result, the function of augmented reality in education is broad and multidimensional, having the potential to alter how students engage with instructional information across a wide range of courses and areas.

**Emphasize the importance of employing augmented reality applications as an integrated educational medium.**

In today's digital world, using Augmented Reality (AR) applications as an integrated instructional medium is critical. AR may make learning more interesting and interactive for students by allowing them to actively engage in the learning process and explore instructional information in a more immersive manner. By incorporating AR into the curriculum, educational institutions may offer a more dynamic and personalized learning experience that responds to individual learners' different requirements and preferences. Furthermore, AR may assist students bridge the gap between theory and practice by allowing them to apply their knowledge in real-world circumstances and build practical abilities that employers greatly value. Furthermore, incorporating AR can aid in the promotion of digital literacy and 21st-century skills among students, preparing them for the needs of modern jobs. As a result, the significance of using augmented reality as an integrated educational media cannot be emphasized, as it has the potential to alter the way students engage with educational information and prepare them for success in their future employment.

**Develop applications for bachelor's education using augmented reality technology.**

The development of bachelor's education applications employing augmented reality technology has the potential to improve the quality and efficacy of educational delivery. Students may experience a more immersive and engaging learning environment by incorporating AR into the curriculum, which allows them to engage with digital information in a way that closely matches real-life settings. AR, for example, may be used to imitate laboratory activities, giving students the opportunity to practice scientific ideas in a safe and controlled environment. AR may also be utilized to provide students with virtual tours of historical monuments and landmarks, letting them experience the world's cultural legacy in a more participatory and memorable way. Furthermore, because AR provides a new and interesting manner of providing instructional information, it may be utilized to improve student engagement and motivation. As a result, the creation of bachelor's education apps employing AR technology is a significant step towards fostering creative and effective teaching practices and improving the quality of education provided to students.

## Conclusion

AR is a promising technology with the potential to transform education. Educators may utilize AR to create immersive and engaging learning experiences that help students better absorb and remember material by overcoming the hurdles of adopting AR in education. There has been a surge of interest in the use of Augmented Reality (AR) technology in educational settings in recent years, with a particular emphasis on its potential to improve student engagement, motivation, and learning results. AR is a technology that superimposes digital information on top of the actual environment, allowing users to engage with digital content in a more immersive and engaging manner.

AR has the potential to alter the way students engage with educational information in higher education by providing a more dynamic and personalized learning experience. The incorporation of augmented reality apps into university courses can have a major influence on student learning results. AR technology has been proved in studies to improve student engagement and motivation by providing a new and entertaining manner of presenting instructional information. AR may bring abstract concepts to life and help students grasp difficult topics in a more realistic and concrete way by superimposing digital information over the actual environment. AR, for example, may be used to imitate scientific investigations, giving pupils the opportunity to practice scientific ideas in a safe and controlled setting. This can assist to improve student learning outcomes by making learning more interactive and interesting for pupils. AR technology can also be utilized to improve pupil

information retention. AR can assist in boosting the efficacy of educational material delivery and promote long-term retention of information by presenting students with a more dynamic and immersive learning experience.

This is especially true in higher education, where students are frequently asked to study complicated and abstract topics that can be difficult to understand without the assistance of interactive and engaging instructional tools. AR technology can assist bridge the gap between theory and practice, in addition to increasing student engagement and knowledge retention. AR can help students build practical abilities that employers appreciate by giving them access to simulated real-world events. For example, in professions like engineering, architecture, and medicine, AR may be used to recreate work-related settings, allowing students to gain practical abilities that are extremely relevant to their future employment. Despite the potential benefits of AR technology in educational contexts, several difficulties must be overcome before its full potential can be realized.

One of the most significant hurdles is the requirement for specialized technical skills and experience to build AR applications. For educational institutions that do not have access to specialized technological competence, this might be a substantial impediment. Another issue is the lack of necessary infrastructure to enable the usage of AR technology, such as high-quality hardware and software, dependable network access, and acceptable bandwidth. Finally, the incorporation of augmented reality apps into university courses has the potential to improve student engagement, motivation, and learning results. AR can assist bridge the gap between theory and practice by giving students with an innovative and dynamic learning experience, as well as build practical abilities that employers greatly value. However, to fully realize the promise of AR technology in educational settings, specialized technical skills, and expertise, as well as suitable infrastructure to enable AR technology use, are required.

## References

**Arulanand, N., Babu, A. R., & Rajesh, P. K.** (2020). Enriched learning experience using augmented reality framework in engineering education. Procedia Computer Science, 172, 937–942.

**Bacca Acosta, J. L., Baldiris Navarro, S. M., Fabregat Gesa, R., & Graf, S.** (2014). Augmented reality trends in education: a systematic review of research and applications. Journal of Educational Technology and Society, 2014, Vol. 17, Núm. 4, p. 133-149.

**Chen, C.-C., Chen, H.-R., & Wang, T.-Y.** (2022). Creative situated augmented reality learning for astronomy curricula. Educational Technology & Society, 25(2), 148–162.

**Chen, P., Liu, X., Cheng, W., & Huang, R.** (2017). A review of using Augmented Reality in Education from 2011 to 2016. Innovations in Smart Learning, 13–18.

**Chiang, F.-K., Shang, X., & Qiao, L.** (2022). Augmented reality in vocational training: A systematic review of research and applications. Computers in Human Behavior, 129, 107125.

**Crandall, P. G., Engler III, R. K., Beck, D. E., Killian, S. A., O'Bryan, C. A., Jarvis, N., & Clausen, E.** (2015). Development of an augmented reality game to teach abstract concepts in food chemistry. Journal of Food Science Education, 14(1), 18–23.

**Duan, H., Shen, W., Min, X., Tu, D., Li, J., & Zhai, G.** (2022). Saliency in augmented reality. Proceedings of the 30th ACM International Conference on Multimedia, 6549–6558.

**Edwards-Stewart, A., Hoyt, T., & Reger, G.** (2016). Classifying different types of augmented reality technology. Annual Review of CyberTherapy and Telemedicine, 14, 199–202.

**Elmqaddem, N.** (2019). Augmented reality and virtual reality in education. Myth or reality? International Journal of Emerging Technologies in Learning, 14(3).

**Han, X., Chen, Y., Feng, Q., & Luo, H.** (2022). Augmented reality in professional training: A review of the literature from 2001 to 2020. Applied Sciences, 12(3), 1024.

**Iqbal, M. Z., Mangina, E., & Campbell, A. G.** (2022). Current challenges and future research directions in augmented reality for education. Multimodal Technologies and Interaction, 6(9), 75.

**Jasche, F., Hoffmann, S., Ludwig, T., & Wulf, V.** (2021). Comparison of different types of augmented reality visualizations for instructions. Proceedings of the 2021 CHI Conference on Human Factors in Computing Systems, 1–13.

**Karagozlu, D.** (2018). Determination of the impact of augmented reality application on the success and problem-solving skills of students. Quality & Quantity, 52(5), 2393–2402.

**Kurt, Y., & Öztürk, H.** (2021). The effect of mobile augmented reality application developed for injections on the knowledge and skill levels of nursing students: An experimental controlled study. Nurse Education Today, 103, 104955.

**Lampropoulos, G., Keramopoulos, E., Diamantaras, K., & Evangelidis, G.** (2022). Augmented reality and gamification in education: A systematic literature review of research, applications, and empirical studies. Applied Sciences, 12(13), 6809.

**Manuri, F., & Sanna, A.** (2016). A survey on applications of augmented reality. ACSIJ Advances in Computer Science: An International Journal, 5(1), 18–27.

**Mota, J. M., Ruiz-Rube, I., Dodero, J. M., & Arnedillo-Sánchez, I.** (2018). Augmented reality mobile app development for all. Computers & Electrical Engineering, 65, 250–260.

**Ozdemir, M., Sahin, C., Arcagok, S., & Demir, M. K.** (2018). The effect of augmented reality applications in the learning process: A meta-analysis study. Eurasian Journal of Educational Research, 18(74), 165–186.

**Özeren, S., & Top, E.** (2023). The effects of Augmented Reality applications on the academic achievement and motivation of secondary school students. Malaysian Online Journal of Educational Technology, 11(1), 25–40.

**Pasaréti, O., Hajdin, H., Matusaka, T., Jambori, A., Molnar, I., & Tucsányi-Szabó, M.** (2011). Augmented Reality in education. INFODIDACT 2011 Informatika Szakmódszertani Konferencia.

**Peddie, J., & Peddie, J.** (2017). Types of augmented reality. Augmented Reality: Where We Will All Live, 29–46.

**Sari, A., Akkaya, M., & Abdalla, B.** (2017). Assessing e-Government systems success in Jordan (e-JC): A validation of TAM and IS Success model. International Journal of Computer Science and Information Security (IJCSIS), 15(2).

**Shirazi, A., & Behzadan, A. H.** (2015). Design and assessment of a mobile augmented reality-based information delivery tool for construction and civil engineering curriculum. Journal of Professional Issues in Engineering Education and Practice, 141(3), 4014012.

**Tang, K. S., Cheng, D. L., Mi, E., & Greenberg, P. B.** (2020). Augmented reality in medical education: a systematic review. Canadian Medical Education Journal, 11(1), e81.

**Tekedere, H., & Göke, H.** (2016). Examining the effectiveness of augmented reality applications in education: A meta-analysis. International Journal of Environmental and Science Education, 11(16), 9469–9481.

**Tzima, S., Styliaras, G., & Bassounas, A.** (2019). Augmented reality applications in education: Teachers point of view. Education Sciences, 9(2), 99.

**Wu, H.-K., Lee, S. W.-Y., Chang, H.-Y., & Liang, J.-C.** (2013). Current status, opportunities and challenges of augmented reality in education. Computers & Education, 62, 41–49.

**Yuliono, T., & Rintayati, P.** (2018). The promising roles of augmented reality in educational setting: A review of the literature. International Journal of Educational Methodology, 4(3), 125–132.

# Analyzing Credit Card Fraud Cases with Supervised Machine Learning Methods: Logistic Regression and Naive Bayes

## Naila Habibullayeva, Behnam Kiani Kalejahi

*Computer Engineering Department, Khazar University, Baku, Azerbaijan*
*＊Corresponding author: naila.habibullayeva@khazar.org*

**Abstract**

Frauds involving credit cards are simple and simple to target. With the rise of online payment credit cards have had a huge role in our daily life and economy for the past two decades and it is an important task for companies to identify fraud and non-fraud transactions. As the number of credit cards grows every day and the volume of transactions increases quickly in tandem, fraudsters who wish to exploit this market for illegitimate gains have come to light. Nowadays, it's quite simple to access anyone's credit card information, which makes it simpler for card fraudsters to do their crimes. Thanks to advances in technology, it is now possible to determine whether information gained with malicious intent has been used by looking at the costs and time involved in altering account transactions. The Credit Card Fraud analysis data set, which was obtained from the Kaggle database, was used in the modeling process together with The Logistic regression method and Naive Bayes algorithms. Using the Knime platform, we are going to apply machine learning techniques to practical data in this study. The goal of this study is to identify who performed the transaction by examining the periods when people used their credit cards. The Logistic regression approach and the Naive Bayes method both had success rates of 99.83%, which was the highest. The two methods' results are based on Cohen's kappa, accuracy, precision, recall, and other metrics. These and many more outcomes are shown in the confusion matrix.

**Keywords:** Credit card fraud, supervised Machine Learning, Logistic Regression modeling, Naive Bayes modeling, imbalanced classification

**Introduction**

Payments can be made using credit cards and POST devices used at shopping points, provided by banks to the people they serve. You can also withdraw cash from ATMs. Credit cards also make people's lives easier when it comes to paying their expenses in installments.

In this way, people reduce their monthly expenses by dividing them into a certain number of months instead of paying all at once. Thanks to its prevalence and strong infrastructure around the world, credit cards have become a payment tool that people can use easily and frequently in a very short time. In today's society, fraud on credit cards has considered a significant worry, with increased fraud in political agencies, corporate sectors, financial commerce, as well as other associations. The credit card is indeed an efficient and easy target for fraudsters since a significant volume of money may be stolen swiftly and without risk. Criminals perpetrate fraud on credit cards by stealing personal statistics including credit account values, banking information, and passwords. Fraudulent individuals attempt to constitute their malicious attack seem legal, making fraud reporting difficult. Credit card fraud has risen as a result of our society's growing reliance on the internet; yet, theft has grown not just internet but also offline. In 2022, global cybercrime expenses were $408.50 billion. To combat the problem, several corporations, such as VISA, are resorting to Machine learning solutions. Using machine learning to identify credit card fraud has several advantages, such as:

• Pattern classification
• Data processing efficiency
• Prediction accuracy

Although the use of certain data mining methods, the results in identifying credit card fraud are not particularly accurate. Only by detecting fraud with advanced algorithms, which is a promising mechanism for minimizing credit card fraud, can these expenses be reduced. As the use of the internet expands, the financial business issues credit cards.

In addition to this situation, many problems have arisen as the usage areas of credit cards have increased, and the reasons why people prefer them have increased. The most important problem that occurs when people use credit cards so much is that their information falls into the hands of other people and is misused. Credit card fraud can occur by copying an existing card exactly to a new card, or by stealing the information on the existing card from e-commerce sites and using it as the owner of the card or transferring money from it. Fraud with credit cards causes enormous

financial losses for every nation on the planet. For this reason, certain analyses are made using data obtained from credit card transactions in the study, and as a result this analysis, it is aimed to prevent credit card fraud.

## Literature Review

A plethora of traditional machine learning methods including Decision Tree, K-Nearest Neighbour (KNN), SVM, Logistic Regression, Random Forest, XGBoost, and other deep learning methods were applied to the process of the detection of credit card fraud. Including ANN and Logistic Regression, tree-based cooperative methods proved effective. From past work on this topic, I have learned that it is important to balance the data as there is a large imbalance in the data set between fraud and non-fraud transactions. In this section, a significant number of works have been presented.

Rimpal R. Popat et al. (2019) tried an interesting approach. This team uses the end clustering technique to divide the data into three different groups according to the transaction amount. They used range partitioning for it. In the next step, they used the sliding window method by aggregating transactions into groups and then extracting patterns in cardholders' behavior. Minimum, maximum, and average transaction amounts made by cardholders were calculated. And whenever there is a new transaction made the new transactions are fed to the window while the old one is removed from it

Pranjal Saxena et al. (2021) used supervised machine learning methods such as Random Forest, Stacking Classifier, and Logistic Regression and compared them with different metrics like Recall, Accuracy, Precision, etc. They eventually found out that Logistic Regression was the most accurate when it was picked as the base estimate of the r of Stacking classified followed by Random Forest and XGB classifier.

In another study, Tince Etlin Tallo et al. (2018) compared the advantages and drawbacks of fraud detection methods. For instance, they have Figured out that although the Hidden Markov Model is fast at detection, its accuracy is low, and it is not scalable for large data sets. On the other hand, Bayesian networks are good at accuracy while being expensive. Moreover, when it comes to artificial neural networks, they are portable and, effective in dealing with noisy data while being difficult to set up and having bad explanation capabilities. Another interesting point from this study was that they mentioned that there are no suitable metrics to evaluate the results of these prediction models as well as a lack of adaptive fraudulent insident of credit card detection systems.

The research on SVM, random forests, decision trees, and logistic regression by Navanushu Khare et al. (2018) was described. They experimented with a

significantly unbalanced dataset. The effectiveness criteria include specificity, accuracy, sensitivity, and precision. According to the statistics, a logistic regression model is 97.7% accurate, Decision Trees are 95.5% true the random forest method is 98.6% accurate, and the classifier using SVM is 97.5% accurate. They determined that the Random Forest method is a highly efficient and precise method for detecting fraud. They also determined that, owing to the data imbalance problem, the SVM method did not execute any better in detecting fraud with credit cards

To identify outliers, Vaishnavi Nath Dornadula et al. (2019) employed novel machine learning methods. That team used Local Outlier Factor and Isolation Forest algorithm which at the moment are considered the most popular outlier detection methods in the industry. Their accuracy was 99.6% while they had lower precision at 33%. The reason for the low precision in the data is a huge imbalance.

## Methods and Materials

The data set and methods employing to help detect fraud of credit card are explained in this section.

## The Dataset

The data collection includes a total of 2,84,807 transactions from the website (www.kaggle.com) website, of which 492 are false. The data set has to be handled since it is so severely unbalanced before a model can be built Credit card companies need to be able to spot fraud financing card transactions to stop charging customers for goods they did not purchase.

The dataset consists of September 2013 payment card operations made by users across Europe. In our data of operations that occurred throughout two days, we found 492 errors out of 284,807 operations. The sample is heavily biased with criminal activity accounting for 0.172% of all positive activities. All of the quantitative data parameters in the collection of data have completed PCA treatment. Regrettably, the disclosure of the initial characteristics and additional contextual details of the data is precluded by confidentiality concerns. The characteristics denoted as V1, V2, and so forth. The principal components derived from PCA are represented by V28, while the features 'Time' and 'Amount' remain untransformed.

| Time | V1 | V2 | V3 | V4 | V5 | V6 | V7 | V8 | V9 | V10 |
|---|---|---|---|---|---|---|---|---|---|---|
| 0 | -1.35981 | -0.07278 | 2.536347 | 1.378155 | -0.33832 | 0.462388 | 0.239599 | 0.098698 | 0.363787 | 0.090794 |
| 0 | 1.191857 | 0.266151 | 0.16648 | 0.448154 | 0.060018 | -0.08236 | -0.0788 | 0.085102 | -0.25543 | -0.16697 |
| 1 | -1.35835 | -1.34016 | 1.773209 | 0.37978 | -0.5032 | 1.800499 | 0.791461 | 0.247676 | -1.51465 | 0.207643 |
| 1 | -0.96627 | -0.18523 | 1.792993 | -0.86329 | -0.01031 | 1.247203 | 0.237609 | 0.377436 | -1.38702 | -0.05495 |
| 2 | -1.15823 | 0.877737 | 1.548718 | 0.403034 | -0.40719 | 0.095921 | 0.592941 | -0.27053 | 0.817739 | 0.753074 |
| 2 | -0.42597 | 0.960523 | 1.141109 | -0.16825 | 0.420987 | -0.02973 | 0.476201 | 0.260314 | -0.56867 | -0.37141 |
| 4 | 1.229658 | 0.141004 | 0.045371 | 1.202613 | 0.191881 | 0.272708 | -0.00516 | 0.081213 | 0.46496 | -0.09925 |
| 7 | -0.64427 | 1.417964 | 1.07438 | -0.4922 | 0.948934 | 0.428118 | 1.120631 | -3.80786 | 0.615375 | 1.249376 |
| 7 | -0.89429 | 0.286157 | -0.11319 | -0.27153 | 2.669599 | 3.721818 | 0.370145 | 0.851084 | -0.39205 | -0.41043 |
| 9 | -0.33826 | 1.119593 | 1.044367 | -0.22219 | 0.499361 | -0.24676 | 0.651583 | 0.069539 | -0.73673 | -0.36685 |
| 10 | 1.449044 | -1.17634 | 0.91386 | -1.37567 | -1.97138 | -0.62915 | -1.42324 | 0.048456 | -1.72041 | 1.626659 |
| 10 | 0.384978 | 0.616109 | -0.8743 | -0.09402 | 2.924584 | 3.317027 | 0.470455 | 0.538247 | -0.55889 | 0.309755 |
| 10 | 1.249999 | -1.22164 | 0.38393 | -1.2349 | -1.48542 | -0.75323 | -0.6894 | -0.22749 | -2.09401 | 1.323729 |
| 11 | 1.069374 | 0.287722 | 0.828613 | 2.71252 | -0.1784 | 0.337544 | -0.09672 | 0.115982 | -0.22108 | 0.46023 |
| 12 | -2.79185 | -0.32777 | 1.64175 | 1.767473 | -0.13659 | 0.807596 | -0.42291 | -1.90711 | 0.755713 | 1.151087 |
| 12 | -0.75242 | 0.345485 | 2.057323 | -1.46864 | -1.15839 | -0.07785 | -0.60858 | 0.003603 | -0.43617 | 0.747731 |
| 12 | 1.103215 | -0.0403 | 1.267332 | 1.289091 | -0.736 | 0.288069 | -0.58606 | 0.18938 | 0.782333 | -0.26798 |
| 13 | -0.43691 | 0.918966 | 0.924591 | -0.72722 | 0.915679 | -0.12787 | 0.707642 | 0.087962 | -0.66527 | -0.73798 |
| 14 | -5.40126 | -5.45015 | 1.186305 | 1.736239 | 3.049106 | -1.76341 | -1.55974 | 0.160842 | 1.23309 | 0.345173 |

**Figure 1.** A part of the Credit Card Fraud dataset

## The Performance Metrics

The *Confusion matrix* displays the node's particular output along with the amount of similarities in every single cell. Correctness facts are displayed in a separate column. The results include the average accuracy, Cohen's kappa, recall, precision, sensitivity, preciseness, the F-value, and the following: true, false, positive, and negative.

*Accuracy:* The ratio of accurate forecasts to all alternative guesses is used to compute accuracy, which is one of the most straightforward classification variables.

$$\text{Accuracy} = \frac{\text{Number of correct prediction}}{\text{Total number of prediction}}$$

*Precision-* is a metric that quantifies the degree of correctness of a classification or prediction model. The term "precision" refers to the proportion of properly predicted positive cases, to the overall amount of anticipated positive instances, including comprises both correct and incorrect positives, in the model's output. Put another way, accuracy is a measurement of the ratio of actual positive situations to all of the scenarios that were projected to be positive.

A high level of precision denotes that the layout.exhibits a superior competence to properly determine true cases despite the fact minimizing the occurrence of false

positives in its output. Conversely, a diminished level of precision implies that the model exhibits an elevated frequency of false positives, thereby resulting in erroneous or deceptive outcomes.

*Recall*- The concept of recall pertains to the degree of comprehensiveness exhibited by a classification or prediction model. The term "precision" refers to a statistical metric that calculates the percentage of correctly anticipated positive situations, or "true positives" associated to the entirely number of positive instances that were either correctly identified or missed by the model, which includes both true positives and "false negatives." Stated differently, recall is a performance metric that quantifies the ratio of true cases that are accurately detected by the method.

**The Logistic Regression prediction method**

One of the methods used in the model in the study is the Logistic regression model. Thirty percent of the material set was utilized for testing, while seventy percent was applied for training. Logistic regression method is a popular and simple machine learning approach that works well for classifying data into two groups. It is easy to use and might be the beginning point for any sort of linear problem. Machine learning may benefit from its basic notions as well. A logistic regression model is a statistical technique used to forecast the probability of a discrete occurrence. Features of Logistic Regression:

- In this method, the reliant parameter has a Bernoulli distribution.

- The most remarkable, likelihood approach is used for assessment.

- In fact, there is no coefficient squared for determining demonstrating efficiency; instead, Congruence and KS-Statistics are used.
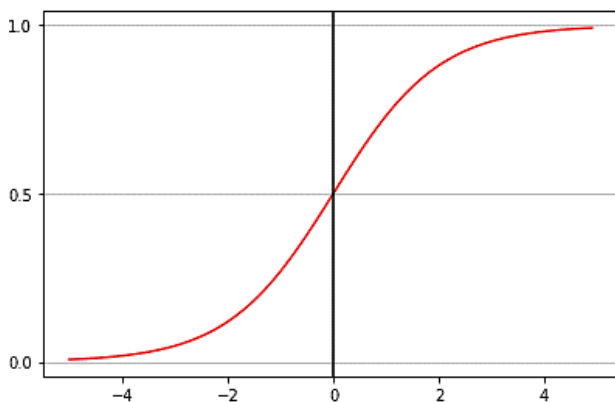


**Figure 2.** Logistic Regression model graph.

## 1.1.  The naive Bayes method

The naive Bayes algorithm aims to detect the new category of the class given to the system through a classification calculation determined according to probability calculations. The naive Bayes method is a classification method that adapts to estimate the relationship between the target label to be achieved and the input parameters applied in the problem. This method uses these probabilities for prediction by calculating the frequency of the combination of independent parameters and dependent variables.

$$P(A|B)=(P(B|A)/P(A))/(P(B))$$

Formula for Bayesian statistical is calculated as above and here: P(A|B) is posterior, the above of the equation is equal to prior x likelihood and P(B) is evidence.

Naive Bayes method was used in the model in the study and 70% of the data was used for training in the model. An attempt was made to predict which class the data would be in by using the probability calculations made with the data in the training set and the 30% of the test data given to the system allocated for prediction.

## Experimental implementation

In this project, the Knime platform was used for the simulation of both prevent models. The interface of Knime is displayed in the Figure below. Knime is an easy, user-friendly, and open-source platform where you can drag and drop the parts you need for modeling into the workspace, create the main interface of the model, and render it visually.



**Figure 3.** Knime software visual

The data were first digitized to be used in the linear regression method and naive Bayes method modeled for the problem. Afterward, all data were normalized to obtain a more efficient running time for both models, as shown in Figure 4.

| Row... | Time Number (dou... | V1 Number (dou... | V2 Number (dou... | V3 Number (dou... | V4 Number (dou... |
|---|---|---|---|---|---|
| Row0 | 0 | 0.935 | 0.766 | 0.881 | 0.313 |
| Row1 | 0 | 0.979 | 0.77 | 0.84 | 0.272 |
| Row2 | 0 | 0.935 | 0.753 | 0.868 | 0.269 |
| Row3 | 0 | 0.942 | 0.765 | 0.868 | 0.214 |
| Row4 | 0 | 0.939 | 0.777 | 0.864 | 0.27 |
| Row5 | 0 | 0.951 | 0.777 | 0.857 | 0.244 |
| Row6 | 0 | 0.979 | 0.769 | 0.838 | 0.305 |
| Row7 | 0 | 0.947 | 0.782 | 0.856 | 0.23 |
| Row8 | 0 | 0.943 | 0.77 | 0.835 | 0.24 |
| Row9 | 0 | 0.953 | 0.779 | 0.856 | 0.242 |

**Figure 4.** A part of the normalizer dataset

In Figure 5 we see the modeling of the Logistic Regression technique. Here, 70 % of the data is used, while the remaining 30 % is reserved for testing. After the training process was completed, system reliability was tested by applying it to the test set using the determined parameters.
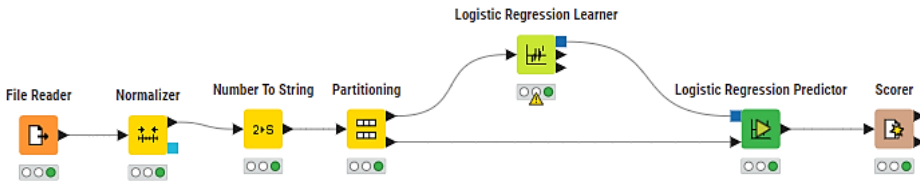


**Figure 5.** Logistic Regression prediction model

For the Naive Bayes model shown in Figure 6, 30 percent of the data set was utilized for testing, while seventy percent were employed for exercising. For Naive Bayes learning, the default probability is 0.0001 and the minimum standard deviation is 0.0001. Then, the Naive Bayes model was tested on the test set.
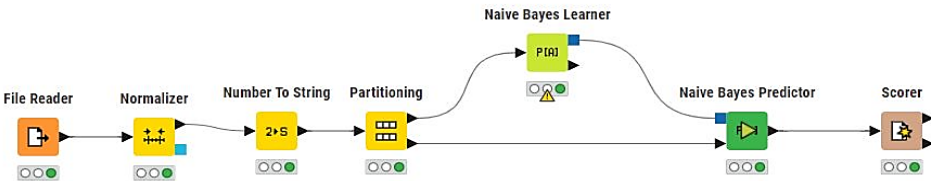
**Figure 6.** Naive Bayes prediction model

## Results

In Logistic Regression modeling, the accuracy rate was 98.83% and the error rate was 1.174%.

As seen in the picture above, in the Logistic regression method model, the quantity of true positives is 125 and the amount of false positives is 25. While the amount of true negatives is 83786, the amount of errors is 1507 in storage and connection tubes.

In Naive Bayes modeling, the accuracy rate was 99.83% and the error rate was 0.169% in this model, the quantity of true positives is 123 and the amount of false positives is 29. However, there are 85271 real negatives, and twenty (20) false negatives are reported.
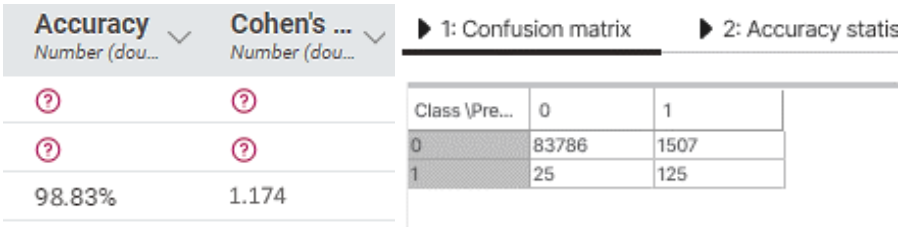


**Figure 7.** Logistic Regression Confusion matrix result
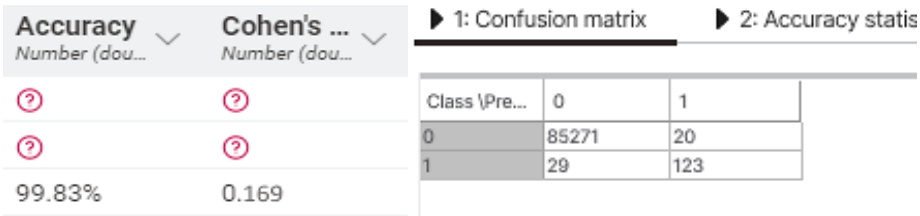


**Figure 8.** Naive Bayes Confusion matrix result

As a result, an analysis was conducted on the Knime platform using the fraudulent circumstances on credit card data set obtained from the Kaggle database. We analyzed two machine learning methods, Logistic regression and Naive Bayes algorithms were used in the analysis. The overall statistics of the two approaches are revealed in Table 1.

**Table 1. Comparative table of the mean-field predictions**

| Prediction method | Accuracy | Error |
|---|---|---|
| Logistic Regression | 98.83 % | 1.174% |
| NaiveBayes | 99.83 % | 0.169% |

## Conclusion

In conclusion, we cannot claim that our algorithm entirely identifies fraud even though there are other fraud detection methodsWe conclude from the results of our evaluation that the precision of both naive Bayes and Logistic Regression is roughly comparable. When it comes to accuracy, recall, F1, and error scores, the Naive Bayes approach performs better than the Logistic regression algorithm. Consequently, we deduce that the Naive Bayes method outperforms the Logistic Regression approach in detecting credit card fraud.

The data above makes it evident that various machine learning algorithms are utilized to recognizing fraud, however, the outcomes are not good enough. Therefore, by using machine learning algorithms to precisely identify credit card fraud, subsequent research may provide more accurate findings.

## References

**Adewumi A. O., Akinyelu A.A.** (2017). A survey of machine-learning and nature-inspired based credit card fraud detection techniques. Int. J. Syst. Assurance Eng. Manage.,8(2): 937-953.

**Awoyemi, John O. et al.** (2017). Credit Card Fraud Detection Using Machine Learning Techniques: A Comparative Analysis. International Conference on Computing Networking and Informatics (ICCNI).

**Behrouz Far et al.** (2018). "Supervised Machine Learning Algorithms for Credit Card Fraudulent Transaction Detection: A Comparative Study." Annals of the History of Computing, 122-125.

**Jiang, Changjun et al**. (2017). Credit Card Fraud Detection: A Novel Approach Using Aggregation Strategy and Feedback Mechanism. IEEE Internet of Things Journal 5, 3637-3647.

**Melo-Acosta, German E., et al.** (2017). Fraud Detection in Big Data Using Supervised and Semi-Supervised Learning Techniques. IEEE Colombian Conference on Communications and Computing (COLCOM).

**Pumsirirat et al.** (2018). Credit Card Fraud Detection using Deep Learning based on Auto-Encoder and Restricted Boltzmann Machine. International Journal of Advanced Computer Science and Applications, 9(1).

**Randhawa, Kuldeep et al.** (2018). Credit Card Fraud Detection Using AdaBoost and Majority Voting. IEEE Access, vol. 6, 14277–14284.

**Roy, Abhimanyu, et al.** (2018). Deep Learning Detecting Fraud in Credit Card Transactions. Systems and Information Engineering Design Symposium (SIEDS).

**Rushin G., Stancil C., Sun M., Adams S., Beling P.** (2017). "Horse race analysis in credit card fraud-deep learning logistic regression and Gradient Boosted Tree", Systems and Information Engineering Design Symposium (SlEDS), 117-121.

**Xuan Shiyang, Guanjun Liu et al.** (2018). Random Forest for Credit Card Fraud Detection. 2018 IEEE 15th International Conference on Networking, Sensing and Control (ICNSC).